~~CONFIDENTIAL~~

Declassified by auth.
ONR Let 8/7/63
Ref: ONR:651:DGR:nbh

Department of the Navy
OFFICE OF NAVAL RESEARCH
Contract N6onr-24428
Project NR 062_087

FREE-BODY MODELING OF THE STABILITY AND CONTROL OF SUBMARINES

Volume I - Text

Joseph Levy
Donald A. Price, Jr.

Hydrodynamics Laboratory
CALIFORNIA INSTITUTE OF TECHNOLOGY
Pasadena, California

Report No. E-27.2
Copy No. 100

May 1956

~~CONFIDENTIAL~~

~~CONFIDENTIAL~~

Department of the Navy
Office of Naval Research
Contract N6onr-24428
Project NR 062-087

FREE-BODY MODELING OF THE STABILITY AND CONTROL OF SUBMARINES

Volume I - Text

Joseph Levy
Donald A. Price, Jr.

Hydrodynamics Laboratory
California Institute of Technology
Pasadena, California

Report No. E-27.2
Copy No. 100

May 1956

~~CONFIDENTIAL~~

CONTENTS*

* Note: All figures for this report will be found in Volume II.

CONTENTS
(cont'd)

Abstract

An experimental study of the dynamic control and stability of submarines has been made by means of small-scale, free-running, powered and controlled models at the California Institute of Technology, Hydrodynamics Laboratory. The experimental and theoretical basis of the modeling of the behavior of fully submerged submarines is discussed. The design and construction of the models are described, and development of experimental techniques is outlined. The experimental program was conducted with models of two full-scale submarines— the U.S.S. Odax and the U.S.S. Albacore— to (1) evaluate the efficacy of small-scale modeling, and (2) to predict control characteristics of a boat of radically new design. Satisfactory agreement between the dynamic behavior in free flight of the small-scale (120:1) model and the Guppy-type submarine Odax is demonstrated for one type of maneuver. Zig-zag maneuvers in the vertical plane were chosen for this purpose because of their simplicity and suitability for comparison with available full-scale data. The model's diving planes were made to reproduce the time-sequence of the diving plane motions of the full-scale submarine and the resulting depth and inclination responses compared to those of the full size vessel. The consistency of the model's behavior was evaluated from repeated tests with each of four selected control programs for which only a single full-scale test was run.

Predictions of the dynamic control and maneuverability characteristics of the U.S.S. Albacore (AGSS 569) Scheme IV submarine, which marks a radical departure in hull design, were made with a 100 to 1 scale model. This model was built at about the same time that the keel was laid for the prototype ship. The studies made with this model were divided into three parts:

(1) Control characteristics in the vertical plane.

(2) Turning characteristics with rudder control alone.

(3) Turning characteristics with depth control, and with combination depth-and-roll control.

The tests under item (1) were made with two sets of appendages (tail structure, bow planes, and bridge fairwater), for which only minor differences in control response were found and no measurable difference noted in directional stability. Items (2) and (3) were made with one set of appendages

(corresponding to those first used on the prototype) and with Froude-scaled model velocity.

Specific maneuvering problems, such as the determination of control plane programs required to execute optimum dives or horizontal turns without changing depth, are solved by successive approximation with the model. The tests show that a high degree of prescience is required and that precise execution of the control program is necessary to successfully accomplish an optimum maneuver.

Comparison of the behavior of the two models shows that the Albacore has a greater degree of directional stability and a faster response to its controls than the Odax. This is certainly due to its better hydrodynamic design. The Albacore model also demonstrated much better consistency in its own behavior than did the Odax model. This is due in part to better design and in part to the improvements made in the techniques of building and operating the models and in processing the model test data.

At the time of this writing, no detailed comparisons have been made between results obtained with the Albacore model and those of the sea trials of the prototype which were made in the fall of 1955. The few spot comparisons which were made (but not included in this report) show good agreement. Detailed comparisons of these two sets of tests will be made at the David Taylor Model Basin (under whose supervision the sea trials were conducted) and will be the subject of a separate report.

CHAPTER 1

INTRODUCTION AND THEORY

This is the final report on an investigation of control and maneuverability of submarines by means of free-flying, powered models which has been in progress for several years. The work was done in the Hydrodynamics Laboratory of the California Institute of Technology, under Office of Naval Research Contract N6onr-24428, as a part of the Bureau of Ships Fundamental Hydromechanics Research program (NS 715-102) which is administered by the David Taylor Model Basin. Most of the results of this study were presented piecemeal in twenty-five progress reports (Ref. 11) and in Refs. 18 and 19.

The objectives of this study may be divided arbitrarily into two parts:

(a) To develop the free-flying model technique and to evaluate it by comparison with full-scale tests.

(b) To use free-flying models to predict the control and maneuverability characteristics of new designs.

The U. S. Submarine Odax (Guppy type) was selected for the first phase of this work because this boat was subjected to an extensive series of sea trials, and good records of its performance were available. The second phase of the study was made with a model of the new high-speed submarine Albacore. The model study was initiated before construction was begun on the Albacore, which was launched in March 1954. Full-scale control and maneuverability tests were made with the Albacore in the fall of 1955, but the records are not yet available for comparison with model results. Both phases of this model study should be viewed as one continuous effort to develop the free-flying-model technique as a research tool, to refine it, and to evaluate it by comparison with full-scale tests.

The problem of control and maneuverability of a submarine is more severe than that of other bodies having six degrees of freedom. The motion of a submarine in the vertical direction is limited to a thin layer of the ocean between the free surface and crushing depth. The thickness of this layer is only about two or three submarine lengths. The disposition of personnel,and the possibility of spilling acid from batteries or of tumbling gyros, set a limit to the allowable inclination of the axis. In addition,

the speed range of a submarine is from reverse, through zero, to full speed ahead, and the boat must be controllable throughout this range. The speed range of an airplane in the air, by comparison, is only between about 70 per cent and 100 per cent of maximum speed forward. When the submarine is operating at or near the free surface the problem is further complicated by wave-making effects.

The submerged speed of submarines was nearly doubled after World War II when the fleet type submarines were converted to Guppies, and since then it was increased again by a factor of over 1-1/2 in the Albacore, which is the forerunner of future hull designs. Further substantial increases in submerged speed appear possible when streamlined hulls will be combined with radically new power plants. These faster submarines will, of course, be capable of executing rapid and daring attack and invasion maneuvers that are completely beyond the range of past experience. This poses the necessary problem of exploring this new potential, of delineating its safe limits, and of determining control programs for optimum maneuvers. The full scale testing, since only a slowly converging asymptotic approach can be made when hampered by the necessity of keeping within safety limitations that are as yet unknown.

The extreme degree of prescience or anticipation required in high-speed maneuvering in the vertical plane may be illustrated by this example taken from an optimum maneuver determined with the model of the Albacore. The problem posed was this: determine the stern plane program which will take the submarine in minimum time from level flight at 25 knots at one depth to level flight 300 feet deeper without exceeding an inclination angle of 30 degrees. It was found that decisive action for recovering from the dive must be taken when the submarine has changed depth by no more than 20 feet, if serious overshooting is to be avoided (see Chapter 5, Figs. 25 and 26). It is obvious that this type of experimentation with a full size submarine can be extremely hazardous. It is imperative, therefore, that other methods be developed for predicting the characteristics of new designs and for exploring the limits of safe performance.

The Free-Flying Model Compared with Other Methods

A great deal of effort has been expended on the theory governing the motion of a free body moving in a fluid medium, and notable progress has

been made, especially in those phases that apply to heavier-than-air craft. The origin of lift on an airplane wing is well understood and its magnitude and line of action are predictable from theory. Nevertheless, model tests are usually resorted to as a final check. On the other hand, the origin of lifts and moments which act on elongated bodies with low-aspect-ratio fins, i.e., on such shapes as submarines, torpedoes, airships and rockets, cannot be predicted from theory with sufficient accuracy. In the case of these shapes, even more than in the case of airplanes, model tests are necessary to evaluate the coefficients of lift and moment. Such tests are usually made with captive models in towing tanks, on rotating arms or in water tunnels, using both stationary and oscillating balances. These tests show that the lifts and moments are nonlinear functions of the instantaneous values of angle of attack, of angular velocity, and of control plane angles. The apparent-mass effects acting on these vehicles (which have an average density approximately equal to that of the surrounding fluid) are nearly as great as the inertia of the vehicle itself, but the magnitude of these effects is difficult to evaluate.

Problems of stability, control and maneuverability may, therefore, be dealt with by one or more of the following methods:

(a) Full-scale tests

(b) Strictly theoretical predictions

(c) A combination of captive model tests to evaluate hydrodynamic coefficients, and the use of these coefficients in the equations of motion to predict free flight behavior.

(d) Free-flying model tests.

Full-scale testing remains the undisputed final arbiter. The function of all the other methods is to make it possible to arrive at a good design before construction of the prototype begins , and to minimize the amount of full-scale testing required to evaluate the design and to determine the limits of its capabilities.

The theoretical approach, especially when modified in the light of existing empirical data, serves well for preliminary design but does not as yet merit full reliance.

Both of the remaining methods make use of model tests and, therefore, rely on the same basic assumption of similarity of the flow patterns about

model and prototype. This question of similarity will be discussed in a following section; here we are interested in a comparison of the two methods with each other and with full-scale testing.

The method employing captive models requires the construction of models, and an exhaustive series of tests to measure eighteen or more coefficients, each under the full range of independent variables. These measurements usually need correction for strut and wall interference. The equations of motion in which these coefficients are used may be linearized only for cases involving small perturbations, such as stability on straight course; the nonlinear terms must be included when dealing with appreciable deviations from linear motion. Modern computing machines do simplify the solution of the equations, and good results have been obtained in cases involving motion in one plane when only three degrees of freedom are involved (see Refs. 2, 3 and 18). The handling of problems with six degrees of freedom becomes quite complex even with modern computing aids.

The free-flying model is a test device which simultaneously measures all the necessary coefficients, solves all the necessary equations, and delivers the solution without resort to any simplifications or assumptions beyond that of similarity of flow. It is free, by its nature, of strut and wall interference. It decides for itself how many degrees of freedom are involved, and deals with any number of them with equal ease.

The free-flying model lends itself to more precise control of initial conditions and of the forcing functions than is possible in full scale, and it yields a more detailed and precise description of the resulting responses. This means that it can be used for more than just solving practical problems of control and maneuverability. It can serve also as the touch-stone against which we may check results obtained by any other method, and thus help clarify our understanding of the theory which governs the free motion of a submerged body.

On Modeling the Motion of a Submerged Body

The term modeling, as used here, has the restricted meaning that the trajectory of the model is geometrically similar to that of the prototype, and the scale ratio between the two trajectories is the same as that of the linear dimensions of the two bodies. In addition, at corresponding pairs of points

on the two trajectories, the two bodies have identical orientations with respect to their trajectories. In other words, we aim to reproduce the geometry of the motion.

It is assumed that the model and prototype are geometrically similar in external shape, and in position within each body of its center of gravity. If the geometry of the bodies is variable (e.g, if there are movable control surfaces) then geometric similarity of the two bodies is satisfied at each pair of corresponding points on the two trajectories. The masses and moments of inertia of the two bodies are also scaled. That is, the masses are in proportion with the third power and moments of inertia with the fifth power of the linear dimensions. If model and prototype operate in different fluids (e.g., model in fresh water and prototype in sea water) then both mass and moment of inertia are scaled in direct proportion with fluid density.

This scaling of the inertial constants of the bodies implies that the motion of the bodies is controlled by the inertial reactions of the fluid medium. However, the forces acting on the body may be affected also by any of the other properties of the fluid and, in addition, both the fluid and the body are acted upon by gravity. The problem of modeling, therefore, is that of determining which types of forces may significantly affect the motion, and of designing the model experiments so that the ratios of the various types of forces to each other are the same in model and prototype. Since inertia is always important in the range of speeds in which we are interested, we compare all other types of forces to the inertial forces. It is possible, in most cases although not in all, to satisfy the demands of two types of forces, say inertia and gravity. As a rule, it is not possible to satisfy more than two, although there are exceptions to this rule. The effect of each class of forces on the required experimental conditions will be discussed briefly below.

Inertial Forces. Where only the inertial reaction of the fluid need be considered, the problem of modeling is quite simple since the motion of the body is independent of the velocity. This can be shown as follows:

If we assume the forward velocity to be constant, then the motion in one plane may be represented by two equations.

$$M_2 \frac{dv}{dt} + M_1 u \frac{d\theta}{dt} = L \qquad (1)$$

$$I \frac{d^2\theta}{dt^2} = M \qquad (2)$$

where M_1 and M_2 are the mass of the body, including apparent mass of the fluid, for motion in the direction of and normal to the axis of the body, respectively; u and v are velocity components in the same two directions; θ is the angle between the body axis and some fixed direction in space; L is a lift acting normal to the body axis; I is the moment of inertia of the body (including apparent mass effects) about a transverse axis through the cg; and M is a hydrodynamic moment. These two equations may be rewritten

$$C_v(1+k_2)\rho\ell^3 \frac{d^2y}{dt^2} + C_v(1+k_1)\rho\ell^3 \frac{dx}{dt}\frac{d\theta}{dt} = C_L \frac{1}{2} \rho \left(\frac{dx}{dt}\right)^2 \ell^2 \qquad (1a)$$

$$C_I(b+k')\rho\ell^5 \frac{d^2\theta}{dt^2} = C_M \frac{1}{2} \left(\frac{dx}{dt}\right)^2 \rho\ell^3 \qquad (2a)$$

where k_1 and k_2 are coefficients of apparent mass, and k' is the coefficient of apparent moment of inertia; ρ is the density of the fluid; ℓ is a characteristic length of the body; $C_v\ell^3$ is the volume of the body; $C_I\ell^5\rho b$ is the moment of inertia of the body; x and y are distances parallel and normal to the body axis; and C_L and C_M are lift and moment coefficients.

Introducing a dimensionless time scale s, of which the unit is "time to travel one ship-length", we have

$$dt = \frac{\ell}{u} ds$$

Substituting for dt in Eqs. (1a) and (2a), and simplifying, we get

$$C_v(1+k_2) \frac{d^2}{ds^2}\left(\frac{y}{\ell}\right) + C_v(1+k_1) \frac{d}{ds}\left(\frac{x}{\ell}\right) \frac{d\theta}{ds} = C_L \frac{1}{2} \left[\frac{d}{ds}\left(\frac{x}{\ell}\right)\right]^2 \qquad (1b)$$

$$C_I(1+k') \frac{d^2\theta}{ds^2} = C_M \frac{1}{2} \left[\frac{d}{ds}\left(\frac{x}{\ell}\right)\right]^2 \qquad (2b)$$

It is seen that x and y appear as ratios to the body length ℓ. If we measure distances in terms of body lengths, so that

$$x' = x/\ell \quad \text{and} \quad y' = y/\ell$$

then the equations reduce to

$$C_v (1+k_2) \frac{d^2y'}{ds^2} + C_v(1+k_1) \left(\frac{d\theta}{ds}\right) = \frac{1}{2} C_L \tag{1c}$$

$$C_I(1+k') \frac{d^2\theta}{ds^2} = \frac{1}{2} C_M \tag{2c}$$

since dx'/ds is identically unity.

The statement that the forces exerted on the body are due to fluid inertia alone implies several additional conditions which will be examined briefly. First, this implies that the apparent mass coefficients k_1, k_2, and k' depend only on the shape of the body. Secondly, the absence of gravitational effects means that the body is adjusted to neutral buoyancy and trim (so that the mass of the body is equal to $C_v \ell^3 \rho$) and the center of gravity and center of buoyancy are coincident. This, of course, means that the average density of the body is equal to that of the fluid. However, this does not necessarily mean that the mass distribution within the body is such that its moment of inertia is equal to that of the displaced fluid. It will be noted that the total moment of inertia was written as $C_I(b + k')\rho \ell^5$ where b is a constant depending on the mass distribution. Lastly, the absence of any but inertial forces implies that the lift coefficient and moment coefficient depend only on the shape of the body and on the instantaneous values of the angle of attack α, the rudder (or other control plane) angle δ, and the dimensionless angular velocity $d\theta/ds$. For geometrically similar bodies

$$C_L = f_1(\alpha, \delta, d\theta/ds) \tag{3}$$

and

$$C_M = f_2(\alpha, \delta, d\theta/ds) \tag{4}$$

Therefore, geometrically similar bodies will describe geometrically similar paths provided their mass distributions are alike (i.e., the constant b is the same) and provided that their control plane actions are the same function of the dimensionless time s. This means that the model may be operated at any convenient speed, since the geometry of the motion is independent of speed.

Effects of Viscosity. It will be convenient, for purposes of this discussion, to distinguish between direct and indirect effects of the viscosity of the fluid medium. Among the direct effects are the presence of a boundary layer and a wake, and the resultant need for a propulsion system to maintain the motion. The indirect effects arise from the fact that the presence of the boundary layer and the wake modifies also the inertial reactions of the fluid. That is, the coefficients of apparent mass and of lift and moment may also be affected by the viscosity.

The Reynolds number is a measure of the relative importance of viscous effects, since it is proportional to the ratio of inertial forces to viscous forces. The Reynolds number is defined as

$$R_e = \frac{u\ell}{\nu} \tag{5}$$

where u and ℓ are the speed and length as defined before, and ν is the kinematic viscosity of the fluid. To be similarly affected by viscosity, a model would have to operate at the same value of R_e as its prototype. That is, a small model should be operated at higher velocity, or in a fluid of lower viscosity than the prototype. This condition can rarely be satisfied, since fluids of appreciably lower viscosity than air or water are scarce, and high velocities are likely to cause other undesirable effects cuch as those due to cavitation in the case of liquids or compressibility in the case of gases. Therefore, it is of interest to examine, at least qualitatively, the effect of a deviation from Reynolds scaling upon the quantities with which we are concerned.

The drag, which is the primary effect of viscosity, varies with Reynolds number throughout the range that is of interest in this work. However, drag itself is not of primary concern in a study of control and maneuverability. It is known that the model will require relatively more power than the prototype. Our concern, in this case, is mainly with the secondary effects of viscosity upon the lift, moment and inertia coefficients. Let us examine briefly the mechanism whereby viscosity affects the lift, as an example.

The lift of an elongated body of revolution with fins is due mainly to the fins. To take the worst case, let us consider fins at the tail end of the body, where boundary layer is thickest. If we compute the over-all thickness of the boundary layer near the tail of a representative streamlined body, we

find that this is approximately as large as the span of a normal fin, so that the fin is nearly all within the boundary layer. However, the effect of the boundary layer upon the lift is measured by the momentum thickness of the boundary layer and not by its over-all thickness. In the range of Reynolds numbers in which submarines operate (up to about 10^9), the momentum thickness is of the order of one-tenth of the over-all thickness. Therefore, the effect of the boundary layer on the fin as a lift-producing element is that its effectiveness is reduced to something of the order of 90 percent of what it would be in a frictionless fluid. Since a small model has a relatively thicker boundary layer than the prototype, this effect on the model is also somewhat greater. However, the ratio of the model fin's effectiveness to that of the prototype is still nearly unity.

Tests made in water tunnels and towing tanks show that the lifts and moments acting on streamlined bodies with fins become independent of the Reynolds number provided this is greater than a critical value which varies somewhat with the shape of the body. For the type of bodies with which we are concerned here, the critical Reynolds number is less than 10^6. Therefore, in experimental studies of control and maneuverability the viscosity effects may be neglected provided the model is operated at a sufficiently high velocity to be above the critical Reynolds number.

Effects of Surface Tension. The surface tension of the liquid may affect the motion of a submerged (or partially submerged) body only when the free surface is disturbed by the motion; that is, only when the body is moving at or near the free surface. The ratio of inertial forces to surface tension forces is proportional to the Weber number, which is defined as

$$W = \frac{V^2 \rho \ell}{\sigma} \qquad (6)$$

where V, ρ and ℓ are velocity, fluid density and length as defined before, and σ is the surface tension of the liquid. As may be seen from Eq. (6), the surface tension forces may become important in experiments using models of small size running at low velocity.

The work reported here was concerned only with operation at deep submergence and, therefore, surface tension forces have no effect on the motion.

Effects of Compressibility. The motion of a submerged body may be affected by the compressibility of both the fluid medium and the body itself. The compressibility of the fluid becomes important when the speed of the motion approaches, or exceeds the velocity of sound in the fluid. Therefore, the motion of a submarine is not affected by the compressibility of the water because its speed is low by comparison with the sonic velocity. Creeping motion of a submarine may, however, be affected by the compressibility of its own hull under the static pressure of the water. That is, a submarine trimmed to neutral buoyancy at one depth tends to sink when creeping or hovering at a greater depth. At speeds above creeping, the effect of hull's compressibility on the motion becomes negligible.

Effects of Cavitation. Cavitation may affect the free-flight behavior of submerged bodies moving at high speed, since the formation of vapor-filled cavities modifies the general flow pattern around the body. The lift and moment coefficients, in the presence of cavitation, are functions of the cavitation parameter, which is defined as

$$K = \frac{p_o - p_v}{1/2\,\rho V^2} \tag{7}$$

where p_o is the static pressure in the undisturbed liquid, and p_v is the vapor pressure. On geometrically similar bodies, cavitation begins at approximately equal values of the cavitation parameter, and the value of K for inception of cavitation depends on the body shape. As K is decreased below the inception value, the intensity of cavitation grows.

When the operating conditions of the prototype are such that cavitation does not develop on it, then the model must be operated at above the inception value of K, but the K values of the two need not be matched. However, when the prototype is cavitating to such an extent that its control characteristics may be affected, then the model must also be operated at the same value of K as the prototype. In those cases in which the model's velocity is dictated by other considerations, the value of K may be adjusted by varying the static pressure in the model system.

Effects of Gravity. Gravitational forces may affect the motion of a submerged body through one or more of the following mechanisms:

(a) By direct action on the body;

(b) By changing the attitude of the body and thus modifying the inertial reactions of the fluid;

(c) By direct action on the fluid which modifies the flow around the body and, in turn, also the inertial reaction.

Direct action on the body occurs when the body is not neutrally buoyant. This superimposes a sinking or rising motion upon any motion which would otherwise exist.

Modification of the body's attitude may result when the center of gravity is displaced from the center of buoyancy. Normally, the cg is below the center of buoyancy for metacentric stability. When the axis of the body is inclined to the horizontal, this results in a static restoring moment. When the body moves on a curved path, this results in a heel angle which, because of the asymmetry of submarine hulls, may appreciably modify the motion.

Modification of the flow about the body by direct action on the fluid occurs when the body moves at or near the free surface, since the wave formation is controlled by the interaction of gravitational forces and the inertial disturbances due to the passage of the body.

In all model experiments in which gravitational forces affect the behavior, it is necessary to maintain in the model system the same ratio of gravity to inertial forces as in the prototype. This means that model and prototype should operate at the same value of the Froude number, which is defined as

$$F = \frac{V^2}{\ell g} \tag{8}$$

where g is the acceleration of gravity. Since g is nearly constant over moderate latitudes, this means that the model's speed should be reduced in proportion with the square root of the linear dimensions.

Froude scaling must be adhered to in all cases in which the inertial reaction of the fluid is affected by gravity. When operating at or near the free surface, the flow around the body is affected by the presence of the free surface, and the lift and moment coefficients become functions of the Froude number, so that

$$C_L = f_1(\alpha, \delta, d\theta/ds, F) \tag{9}$$

$$C_M = f_2(\alpha, \delta, d\theta/ds, F) . \tag{10}$$

When operating at deep submergence, the lift and moment coefficients are not affected directly by the value of the Froude number. However, the attitude of the vessel may be a function of Froude number and, consequently, the inertial reactions also. Here it is necessary to distinguish between motion in the vertical plane and motion in the horizontal plane.

Since submarines are symmetrical about a vertical plane, the equations of motion in the vertical plane are modified to account for gravitational effects by the addition of terms which are independent of velocity or acceleration. Equations (1) and (2) are replaced by

$$M_2 \frac{dv}{dt} + M_1 u \frac{d\theta}{dt} = L \pm (W - B) \tag{11}$$

$$I \frac{d^2\theta}{dt^2} = M \pm B \ell_b \tag{12}$$

where W is the weight of the body, B is its displacement, and ℓ_b is a lever arm which is normally a function of θ. Since these additional terms are independent of speed, it is obvious that their relative importance diminishes as the speed increases, and at high speed their effect becomes negligible. Therefore, in modeling high-speed maneuvers in the vertical plane, Froude scaling may be neglected, and the model's operating speed again becomes a matter of free choice.

In maneuvering in the horizontal plane, the displacement of the center of gravity from the center of buoyancy causes the body to assume an angle of heel, and this, in turn, results in cross-steering effects even in bodies having axial symmetry. When the body is not symmetrical about a horizontal plane, the heel angle is further affected by asymmetry of the lift forces. Since both of these are dynamic effects which are proportional to the velocity squared, their influence on the motion is not negligible even at high speed, and Froude scaling is required.

Selection of the Pertinent Scaling Laws

It is seen that, in studying the free-flight characteristics of submerged bodies by means of small models, it is not possible to satisfy all the scaling laws simultaneously. However, certain regimes allow satisfactory approximation for geometric simulitude of the trajectory, and fortunately these

coincide with the areas of critical control and maneuverability problems.

It is known that for sufficiently deep submergence (greater than three diameters for slender, streamlined bodies) the surface of the water remains undisturbed by the passage of the body, so that free surface effects need not be considered.

Full scale submarines running at full speed may be subject to localized cavitation around small protuberances. Although such cavitation may produce objectionable noise, it is not of sufficient magnitude to affect control and maneuverability characteristics and, therefore, cavitation scaling is not required.

As indicated above (in the discussion of viscosity effects), the model's drag is relatively greater than that of the prototype so that the model requires relatively more power to maintain a given fixed speed on a nearly straight course. However, the variation of the model's speed with angle of attack may be expected to be similar to that of the prototype. Therefore, the percent deceleration of the model when executing tight turns may be expected to be the same as those of the prototype, provided the model's speed is such as to produce a Reynolds number of the order of 10^6 or greater.

Hoyt and Imlay (Ref. 8) have shown that the influence of metacentric stability on the motion of a full size submarine maneuvering in the vertical plane becomes negligible at speeds of nine knots or greater.

Therefore, one may expect geometric similitude of the trajectory for maneuvers in the vertical plane at an arbitrary model speed provided (a) the prototype maneuvers under study are at speeds of nine knots or greater, and (b) the model is operated at a Reynolds number above critical. Thus, for submerged motion in the vertical plane the model is restricted only to the extent that mass and moment of inertia must be properly scaled, and that time be measured in terms of "time to travel one length". This time scale must apply also to the rates at which control planes are moved. For instance, the control planes of a 1:100 scale model running at 10 knots must be moved at 500 degrees per second, if it represents a prototype running at 10 knots in which the plane rate is five degrees per second.

To obtain geometric similitude of the motion when modeling either horizontal maneuvers or any maneuvers at shallow depth, it is necessary,

in addition to the above restrictions, to scale the model's speed in accordance with Froude's law. Since this results in low model speeds, there is the possibility that viscosity or surface tension effects begin to influence the motion.

In the studies reported herein, the models were operated at an arbitrary high speed (14 to 17 fps) in all vertical maneuvers. Therefore, these model results are representative of prototype behavior at speeds of about 10 knots or greater. The horizontal maneuvering tests which were made with the model of the Albacore were scaled for a prototype speed of 25 knots, which resulted in a model speed of 4.25 fps. It was felt that model speeds below this may not be reliable because of Reynolds number effects.

CHAPTER 2

THE FREE RUNNING MODELS

Basic Design Considerations

The entire study, which is reported herein, may be regarded as one continuous effort to develop techniques for building and operating small-scale, self-powered, free running models of submarines, and to evaluate the usefulness of such models for investigating control and maneuverability characteristics by comparing model test results with those obtained with full-scale submarines. Acceptable agreement between model and full-scale behavior has been demonstrated for the case of the U. S. Submarine Odax. The Albacore model may be viewed as serving two purposes: (1) To predict full-scale behavior while the ship was being built, and (2) to provide another measure of the degree of agreement between free-flight characteristics of small models and those of the full size submarines that they represent.

Throughout the several years over which this study extended, efforts were being made to improve and refine all the experimental techniques which are involved in building the models, in operating them, and in reducing the data obtained with the models. The aim was to improve the precision, consistency and reliability of model performance so as to minimize the effect of experimental error and scatter upon the ultimate evaluation of free-flying models for control and maneuverability studies. It is for this reason that the experimental techniques are considered sufficiently important to devote to them two chapters of this report. This chapter describes the design, construction and development of the models, while the experimental techniques will be covered in Chapter 3.

The free-flying tests were made in the Controlled Atmosphere Launching Tank which is described in Appendix B and in Ref. 9 . This tank is approximately 13 feet in diameter and 30 feet long. The useful maneuvering space may be taken as about 23 feet long, 8 feet deep, and about 8 feet wide. It is obvious that models that are to maneuver in this space must be quite small. In the case of the Oxax model, which was to be used mainly in zig-zag tests in the vertical plane, it was decided that the model's length should be limited to about 30 inches, so that a full-scale run about

one-half mile in length could be modeled. This makes the model's displacement only a little over three pounds. Since the model had to be adjusted to neutral buoyancy and trim, it was necessary to hold the total weight of the essential parts of the model to less than three pounds so as to allow for trim-adjusting weights. The maximum allowable weights were, therefore, set as: (1) 1.25 lbs total for the hull, deck plate and conning tower, and (2) 1.25 lbs for the power plant, internal control gear, and any consumables which may be required.

These models were to be used for studying submerged maneuvers only and, therefore, it was necessary to impose the additional basic restriction that the models are not to discharge gases or any other exhaust material during the run, since full-scale submarines have no exhaust when running submerged.

The net water horsepower required to drive the Odax model at the selected speed of 15 fps was estimated to be about 1/8 horsepower at a propeller speed of 23,000 rpm. The mechanical losses in gear trains, bearings and seals were expected to be relatively high in these small sizes and high rotative speeds. In addition to driving the propellers, the prime mover has to drive also some kind of program control device. The basic requirement for the prime mover was, therefore, set as that of developing approximately one-fourth of a horsepower. A high rotative speed at the prime mover appeared desirable in order to avoid the need for gearing up. A nearly constant power output was considered mandatory.

The requirements for the program control device were that it actuate any one (or several) of the control plane sets such as stern planes, bow planes, or rudders, and carry out a predetermined time-sequence of control plane positions with an accuracy of ± 0.1 degree. In addition, it was necessary to provide some means for establishing the phase relation between control plane motions and the motion of the model in its free flight.

The means by which each of these basic requirements was met will be described separately in the remainder of this chapter.

Design and Development of Model Components

Model Shell

The requirements for the shell were as follows:

(1) It must be watertight and light in weight.

Model Shell (cont'd)

(2) It must have maximum usable internal volume for propulsion and control mechanisms.

(3) It must be strong and rigid, yet provide easy access for servicing and repair.

(4) The material used should be dimensionally stable and easily formed into complex shapes accurately.

The method of construction finally selected from among a number of materials and processes considered was that of electroforming dense nickel over a low melting-point alloy form. The form is melted out leaving a thin, impervious, light-weight shell which is rigid and dimensionally stable. The complete model shell is made in three parts: hull, deck and conning tower.

The processes used to produce each one of these parts are as follows: Concave templates of sheet brass are cut to the ship's lines (with allowance for skin thickness). The contour of each template is generated on a pantograph milling machine from 5 to 1 hand cut patterns. These templates are arranged in a dural mold box which has grooves milled on the inside for exact positioning of the templates. The spaces between the templates are then filled with plaster which is hand-finished so that the edges of the templates protrude from the plaster about 1/32 inch. These molds for the hull and conning tower are made in halves (split on the vertical certerline) and for the deck in one piece. Low melting-point allow (Cerrobase) castings are obtained from these molds , which are slightly over sized but with the exact contour lines (as formed by the templates) cast into them. The castings are then hand finished down to these lines and mounted on hangers for plating. The above sequence is illustrated in Fig. 2-1

The electroforming process is carried out in two steps. The cerrobase forms are suspended first in a cold bath and plated with soft nickel to about 0.005 inch thickness. During this period the forms are removed from the bath several times and the thickness of the nickel plate is measured at several selected control points. The distribution of electrodes and of so-called "roller wires" are adjusted each time to minimize the tendency of the plating material to form excessive deposits on relatively sharp edges and to avoid plating in concave areas. The remaining 0.005 inch of the shell is plated with hard nickel in a hot bath held at 160° F. This process results in a fairly uniform shell thickness of 0.008 to 0.010 inch.

This thin shell remains true to form and surprisingly rigid even after the cerrobase is melted out. The hull shell is cut into two parts, at the maximum diameter, to facilitate installation of the power plant. A brass stiffening ring is inserted at this parting section to increase the rigidity and to facilitate reassembly.

Power Plant

The basic requirements for the power plant are:

(1) To drive the model a distance of 30 to 50 feet at a nearly constant speed of about 10 knots (17 fps);

(2) To fit the narrow, long space within the hull and be light in weight (about 1-1/4 lbs) including expendable;

(3) All expendables must be accommodated and retained within the hull, without appreciable shift of the C.G. during the run.

Several types of power plants were considered. A d.c. electric motor drive with its easy speed regulation and simplicity was impractical because the large power source required (batteries) could not be fitted into the hull. A compressed gas turbine-type drive was unsatisfactory because the hull volume was not sufficient to accommodate the expanded gas. Clock-spring type motors did not appear feasible because of high weight to power ratio and gearing problems. Considerations of this kind led to design of two types of motors, and test setups for both were begun simultaneously.

A rubber-band motor was considered first because of the high capacity of rubber for storing energy and because of the absence of expendables of any kind. However, no information was available on the hysteresis losses in rubber when releasing energy at the rate required in this case. A mock-up motor was designed and built in which six 1/4-inch diameter rudder cords were used to store the energy, and a tapered drum and gear train were designed to produce constant torque at the propeller shafts. Tests showed that such motors have a high peak output at the beginning and an extreme drop-off immediately thereafter, and that, in general, the performance depended very much on the recent history of the rubber, e.g., the number of load repitions and the duration of the stress. This type of motor had to be abandoned because of the low ratio of energy output to energy input and the unpredictability of the behavior.

A terry type turbine motor was started parallel with the rubber-band motor, and this power plant proved most practical and was used in the models.

The turbine wheel is driven by a water jet which, in turn, is driven by a compressed gas. The energy is stored in an aircraft-type pressure accumulator containing nitrogen at high pressure (2200 psi). The water charge is forced into the accumulator through a special check and trigger valve, extending a diaphragm (which separates the water and gas) and compressing the nitrogen to about 2400 psi. A trip lever operated through the model hull triggers the valve and admits water to the turbine nozzle. Figure 2-3 shows the water jet issuing from the nozzle in air. The turbine wheel is also shown. Using water for the jet fluid, instead of gas, makes it possible to run the turbine wheel at a reasonable peripheral speed and still obtain fairly good efficiency and with only a small pressure drop during the run. Also, it eliminates the problem of exhausting the gas into the interior of the hull.

Program Control System

The requirements for the program control system are as follows:

(1) Control surface angles must be adjusted and controlled to $\pm 0.1^{\circ}$.

(2) The control program must be consistent and repeatable.

(3) The control programs must be easily interchanged.

(4) The phase relation between the control plane motions and motion of the model as a whole during the free-running test must be known precisely.

These requirements led immediately to a completely mechanical system for the sake of simplicity, ease of construction and reliability. The fourth requirement evolved to a flashing bulb technique. The programming device consists of a very accurately cut flat-plate cam sliding in a grooved track and driven by the turbine through a reducing gear and lead-screw drive. A bell-crank type follower rolls along the contours of the cam and transmits the motion to the control plane through a connecting rod. The linkage is spring-loaded against the cam to take up necessary pivot slack and provide exact tracing of the control program. The program may be cut to a high degree of precision (elevation tolerance is ± 0.0002 inch) rather easily but requirement (1) posed some ticklish problems. The system and supports must be very rigid to prevent elastic deflections, yet it must remain extremely light in weight. The pivot clearances must be very close (0.0005 in. max. diametral clearance) yet keep friction to a minimum; and, in addition, the spring loading of the system must be sufficient to overcome the external

forces on the planes as well as take up slack and provide good cam follow without introducing excessive friction and resulting hysteresis in control plane moments.

Requirement (4) is necessary in order to prove similarity between model and prototype motions for a given control program. The images of the model on the 35 mm film used to record the trajectory are too small to ascertain from them the position of the control planes in each frame. The motion of the model as a whole may be determined quite precisely from these films, while the motion of the control planes may be determined by a separate test (in air or in a water tunnel) but to establish the phase relation between these two motions required a special signalling device that could be recorded during the test run. The use of a sound signal, generated by a spring leaf snapping against the model hull, to be picked by a hydrophone suspended in the water was tried. The hydrophone picked up sounds from many sources, such as the propeller, launcher, and the "singing" of the high-speed flash lamps. The problems of identifying each sound and its reverberations in the tank, and of tying-in the sound record with the photographic record proved too difficult, and this approach was abandoned.

A flashing light signal was then considered. There were no known flash lamps of high intensity and sufficiently short duration which could be carried in the small model together with the necessary power supply and switching equipment. However, a successful arrangement was developed by using parts of a readily available bulb, as shown in Fig. 2-4. The bulb of a photo-flash lamp (No. 5) is broken off, the metallic wire filling is removed, and the base also broken off. This leaves only the ignition squib consisting of a glass support, two wire leads with a filament between them, and a dab of what appears to be some explosive material at the junction of each wire with the filament. This is enclosed in a small lucite tube and sealed with wax. Two of these lamps mounted in a larger tube flash through a window in the conning tower. Two silver contacts attached to the program cam close separate circuits near the beginning and near the end of the run to fire the bulbs. Small dry cells inside the model hull provide the necessary current.

These lamps produce enough light to leave an unmistakable mark on the film. The total duration of the flash is about 0.006 sec. and the position of the maximum intensity can be estimated to ± 0.0005 sec. The delay time

between closing of the cam contact and the appearance of the maximum intensity on the film is known also to the same precision. This light signal device allows alignment of the control program to within ±0.05 second prototype time.

This discussion has outlined the development of the main components of the models used in the study. Although many refinements in construction and design evolved, both the Odax and Albacore models utilized the basic techniques described here. Further details of construction and the improvements thereupon are given under the description of each model.

Description of the U.S.S. Odax Model

The free-running model of the U.S. Submarine Odax (SS 484) as shown in Fig. 2-5 represents a 120:1 scale reproduction of the "Guppy" type conversion with horizontal stabilizers. The model is 30.63 inches long and displaces 3.15 lbs in fresh water. Table 2-1 lists a comparison of other pertinent model and prototype dimensions.

The electroformed nickel shell is shown in Fig. 2-5 in completed form. The three hull components (see Fig. 2-6) weigh a total of 0.93 lbs. The hull was cut circumferentially to melt out the cerrobase form and to provide access for installation and servicing of the model propulsion and control mechanism. The two hull sections are soldered together with a joining ring while aligned in the assembly jig shown. This simple jig lines up the centerline of the model with an accuracy of five minutes of arc in both horizontal and vertical planes, and with an accuracy of about fifteen minutes in twist. The program cam is changed by disassembling the model hull at this takedown joint. The water charge for the turbine is loaded through the circular hatch in the deck, which also contains the starting valve trigger button.

Figure 2-7 shows closeup views of the control surfaces, propellers and stabilizers. The rudder and stern planes were first made of lucite but later remade in brass. The positions of the pivot shafts are clearly shown. Inside the hollow vertical stabilizer, which is formed integral with the hull (as is the horizontal stabilizer), a horn connects to the control linkage. The bow planes are mounted in the rigged-out position and may be preset to a given angle.

Some details of the power plant are shown in Fig. 2-8. The exploded

TABLE 2-1

U.S.S. ODAX SS 484

PROTOTYPE AND MODEL DIMENSIONS

Quantity	Prototype	Model	
		Scaled	Measured
Scale	120	1	1
Length	306.3 ft	30.63 in.	30.63 in.
Beam	26.0 ft	2.60 in.	2.60 in.
Displacement	2813 tons*	3.65 lbs*	3.154 lbs
Longitudinal C.G. and C.B.	152.5 ft	15.25 in.	15.32 in.
Vertical C.B. above base line	11.01 ft	1.101 in.	1.00 in.
Vertical C.G. above base line	10.25 ft	1.025 in.	0.91 in.
Metacentric Height	0.76 ft	0.076 in.	0.090 in.
Radius of Gyration	70.5 ft	7.05 in.	6.90 in.
Propellers (2) dia.	8.0 ft	0.8 in.	
pitch	5.667 ft	0.567 in.	

*Including free flooding volume.

view shows the relative position of the diaphragm which separates the water from the nitrogen. During charging and discharging, the diaphragm actually turns inside out. The small metal button seals off the outlet, preventing extrusion of the plastic into the control valve under the nitrogen pressure. The nitrogen is charged through a check valve at the right end of the accumulator in Part(c) of the figure. The charging and starting valve is shown at the left end of the accumulator. The water discharges from the valve through the small tube to the 0.013"diameter nozzle in the turbine frame.

The nozzle fits into the socket directly above the turbine wheel shown in Fig. 2-9a. The 1-1/2-in. diameter wheel develops about 1/4 horsepower at 28,000 rpm for 2 seconds. The turbine shaft extends to the gear box in the center of the support boom (Part b) driving the two propellers and program cam lead screw through reduction gears. The 0.8-in. diameter counter-rotating propellers turn at about 22,000 rps and propell the submarine for 2 seconds at 15-16 fps.

At the left end of the support boom above the propellers is seen a sawtooth program cam. The cam moves forward from the position shown about 3-1/2 inches during a run and counter-balances the movement of the water charge aft from the accumulator through the turbine. Three program cams representing full-scale run numbers 194, 86 and 84, respectively, are shown in Part(c). The silver cam light contact is seen to the left of the mounting holes on each cam. A fiber ramp deflects the two spring leaves mounted on the frame so that they snap down on the contact quickly and consistently. The ramp (see Fig. 2-9d) is so contoured that, on returning the cam to the starting position, the spring leaves are deflected to the opposite side to prevent fouling with the vertical drop-off of the ramp.

Figure 2-10 shows the arrangement of the protective fenders that were added to the horizontal stabilizer to prevent fouling of the propeller with the launcher guide rails. These fenders were later removed after the launcher and model pusher were revised and a series of test runs made to determine any effects upon the model behavior.

Description of Albacore Model for Vertical Maneuvers

The free-running model used in this part of the investigation was a 100 to 1 scaled reproduction of the submarine U.S.S. Albacore AGSS 569 (SST Scheme IV) with two control surface configurations. Figure 2-11

shows the model with the "original" and "revised" control surfaces, respectively, mounted on the same hull. The model, as shown, is 24 inches long, 3.27 inches maximum diameter and displaces 4.5 lbs (original) and 4.52 lbs (revised), representing the full-scale 200-foot, 2061-ton (original) and 2071 ton (revised) displacement submarine. Table 2-2 lists comparisons of other pertinent dimensions. The two configurations of control surfaces and appendages used for the model tests were designated "original" and "revised" since several sources exist for each configuration as listed in Table 2-3. Figure 2-12 shows a relative comparison of the various surfaces while the locations are illustrated in Fig. 2-11. There is relatively little difference in the projected areas except for the vertical stabilizers and the bow planes. The location of the revised bow planes is considerably altered, and the type of motion is unique. The operating shaft is inclined down at 45 degrees from a point 75 degrees below the vertical plane of symmetry while the plane axis extends horizontally. This causes a wobbling motion of the planes during deflection, whereas the original planes pivoted around an operating shaft inclined 30 degrees downward from the hull centerline. The major difference in the tail assembly is in the reduced area of the vertical stabilizers for the revised version. The revised bridge fairwater and dorsal fin arrangement is slightly larger than the original version but of the same configuration and location.

The shape of the Albacore by comparison with the Odax is seen to be shorter and fatter and to consist of a body of revolution with the mere suggestion of a deck and an airfoil-type bridge fairwater (or conning tower). The body of revolution is defined by a 6th-degree polynomial equation formulated in Ref. (13) with parameters selected on the basis of a series of resistance tests (Ref. 14).

The technique of construction of the cerrobase forms was altered slightly, therefore. The circular cross section portion of the hull was turned on a lathe with a contour attachment, while the forward deck was cast in a template mold. The deck was then recessed into the turned hull form after hand finishing to the contour lines. A close examination of Fig. 2-13a will reveal the matching line along the tangency contour between the hull and forward deck. The electroformed hull before melting out of the cerrobase form is shown in Part (b), while the complete nickel shell is seen

TABLE 2-2

U.S.S. ALBACORE AGSS 569 (Scheme IV Submarine)

PROTOTYPE AND MODEL DIMENSIONS

Quantity	Prototype		Model	
	Original	Revised	Original	Revised
Scale	100	100	1	1
Length between perpendiculars	200 ft	200 ft	24.00 in.	24.00 in.
Length over-all	203 ft-7 in.	203 ft-7 in.	24.43 in.	24.43 in.
Displacement	2061 tons	2071 tons	4.53 lbs (4.505 lbs)*	4.55 lbs (4.515 lbs)*
Beam	27 ft-3 in.	27 ft-3 in.	3.27 in.	3.27 in.
Longitudinal C.B. and C.G. aft or bow	89.16 ft	89.95 ft	10.699 in. (10.680 in.)*	10.794 in.
Vertical C.B. above base line	13.90 ft	14.00 ft	1.668 in. (1.667 in.)*	1.680 in.
Vertical C.G. above base line	13.09 ft	13.18 ft	1.571 in. (1.566 in.)*	1.582 in.
Metacentric height	0.81 ft	0.82 ft	0.097 in. (0.081 in.)*	0.098 in. (0.091 in.)*
Radius of gyration	46 ft	45.80 ft	5.52 in. (5.47 in.)*	5.496 in. (5.68 in.)*
Propeller diam.	10 ft-2 in.	10 ft-2 in.	1.22 in.	1.22 in.
Propeller pitch	9 ft-3 in.	9 ft-3 in.	1.11 in. (1.02 in.)*	1.11 in. (1.06 in.)*
Projected areas of appendages				
Stabilizers:				
- Horizontal	230 ft^2	213 ft^2	3.31 $in.^2$	3.07 $in.^2$
- Vertical	230 ft^2	159 ft^2	3.31 $in.^2$	2.29 $in.^2$
Elevators	104 ft^2	107 ft^2	1.50 $in.^2$	1.54 $in.^2$
Rudders	103 ft^2	107 ft^2	1.48 $in.^2$	1.54 $in.^2$
Bow Planes	54 ft^2	32 ft^2	0.78 $in.^2$	0.46 $in.^2$
Conning Tower	239 ft^2	277 ft^2	3.44 $in.^2$	3.99 $in.^2$
Dorsal Fin	27 ft^2	24 ft^2	0.39 $in.^2$	0.35 $in.^2$
Bow Plane Stock ℄ aft of bow	15 ft	20.75 ft	1.80 in.	2.49 in.

* Values measured during test program.

TABLE 2-3

REFERENCE DRAWINGS FOR CONTROL SURFACES AND APPENDAGES OF THE U.S.S. ALBACORE USED IN MODEL TESTS

Appendage or Control Surface	BuShips Drawing Number	
	Original	Revised
Stern Stabilizers:		
Horizontal	1189546 Alt. 0	1190882 Alt. 0
Vertical	1189546 Alt. 0	1190888 Alt. 0
Elevators	1189546 Alt. 0	1190882 Alt. 0
Rudders	1189546 Alt. 0	1190888 Alt. 0
Bow Planes	P. D. 1663 Alt. 2	1190328 Alt. A
Bridge Fairwater and Dorsal Fin	P. D. 1663 Alt. 2	1190328 Alt. A

in Part (c), with afterdeck, bridge fairwater and joining ring in place.

This hull take-down joint provides access for installation and removal of the propulsion and control mechanism during major repairs and alterations. Access for adjustments and minor repairs is provided by hatches in the deck and a large opening in the hull underneath the deck. The two hull sections are aligned to within ±0.05 degree axially and ±0.2 degree in roll in the jig shown in Fig. 2-14. The transverse supports were cast to the hull contours before cutting of the shell and scavenging of the cerrobase. The contours of the nickel shell were found to be accurate within ±0.001 inch at the center of the hull and within ±0.005 inch near the ends on the smaller diameters. This corresponds to ±0.1 inch and ±0.5 inch, respectively, full scale.

The stabilizer fins were first plated from nickel in the same manner as the hull shell. These proved to be unsatisfactory in use because of their low rigidity due to small wall thickness (0.010 inch) and relatively large load applied for deflecting the control surfaces. The stabilizer fins finally used for these tests were machined from solid brass on the pantograph milling machine. A comparison of the plated and machined stabilizer fin values is shown in Fig. 2-15. The wall thickness of the machined fins is 0.025 - 0.030 inch, giving a strong, rigid and yet sufficiently light assembly. The control planes were machined from solid brass also.

Model Trim Adjustments: The greater displacement of the Albacore model and the light weight nickel shell allow a wider latitude in weight distribution and adjustment in addition to more substantial and rigid machinery than was possible for the Odax model. The location of the center of buoyancy is fixed, of course, by the hull shape and free-flooding volume. The means of controlling buoyancy, metacentric height, trim and radius of gyration are shown in Fig. 2-16 for the forward hull section. Mounted on the joining ring are three movable main ballast weights, two telescoping horseshoe weights for raising or lowering the center of gravity (metacentric height) and a single crescent for adjusting the roll trim. The radius of gyration and buoyancy are adjusted by altering the magnitude of these main ballast weights and the ballast pellets in the bow and stern tanks. Inclination trim is adjusted by shifting the pellet ballast between stern and bow tanks. The range of adjustment for these weights is small but sufficient to control the metacentric height, moment of inertia and trim within acceptable limits for the high

model-speed runs. Table 2-2 shows some measured values for the above dimensions.

The free-flooding volume of the model is different from the full scale, as shown by Fig. 2-17. On the model only the tail assembly is free-flooding, whereas on the full scale submarine the bridge fairwater, deck and upper portions of the hull free-flood in addition to the tail assembly. The effect of this difference in free-flooding volume is to raise and move forward the center of buoyancy in the model compared to the prototype (see Table 2-2).

Power Plant: The power plant of the Albacore model is an enlarged (about 20 percent) and improved version of the Odax model power plant. The accumulator and trigger valve are shown in Fig. 2-18. The sliding piston (with an "O" ring seal) and cylinder arrangement, replaces the plastic diaphragm. During loading, the water charge displaces the piston which compresses the nitrogen from 2200 to 2400 psi. During discharge the trip-lever (operated by a plunger through the hull) releases the valve piston which is forced up by the water pressure to uncover the nozzle-tube part. The water then issues from the 0.015-inch diameter nozzle at about 410 fps for 2-1/2 sec. and drives the Terry-type turbine at about 30,000 rpm.

The turbine drives the propulsion and control machinery pictured in Fig. 2-19 through a reduction gear train. The 1.22-inch diameter five-bladed propeller rotates at about 11,000 rpm with a 1.06-inch advance of the model per revolution. The propeller shaft is sealed against leakage by an "O" ring at the tail assembly bulkhead.

Control Mechanism: The control mechanism for the Albacore model is heavier and more rugged, as seen in Fig. 2-19. Two control program cams are provided for simultaneous operation of two or more control surfaces although one only was utilized for the vertical maneuvers. A 2 to 1 gear reduction from the propeller shaft drives the cam lead screw, advancing the cam bridge to which the cams are fastened at a rate of 0.0125 inch per revolution of the propeller. A sliding drive nut fits into a vertical slot in the bridge, allowing transverse movement of the nut without disturbing the cams. A small tab on the bottom of the nut fits into a hole below the bridge slot and takes up the nut torque. The cams are shown about half way through their travel with the stern plane deflected to about 12 degrees climb. A 1/8-inch diameter roller follows the cam contour and transmits the motion

to the planes through the follower bell crank and connecting rod. The initial plane angle is adjusted by changing the connecting rod length with the differential turnbuckle. One revolution of the turnbuckle deflects the stern plane by 0.5 degree. A "dog-leg" shaped extension of the connecting rod operates the stern plane horn through the hollow horizontal stabilizer fin. A neoprene bellows seals the tail cone bulkhead where the rod passes through yet allows free movement of the rod. A coil spring attached to the bulkhead loads the linkage against the cam and takes up slack in all pivots except the stern plane pivots which have a maximum play of ± 0.05 degree. The program cam has a deflection ratio of 0.0084-inch elevation per degree of stern-plane rotation which is linear over a range of ± 18 degrees. The cams are contoured to within ± 0.0002 inch (± 0.02 degree) while the linkage is maintained to give a maximum plane deviation of ± 0.1 degree. The slope of the contour shown in Fig. 2-19 represents a full-scale plane deflection rate of 5 deg/sec. The small notch at the left end of the cam is a reference for positioning the cams in the model before each test run.

A silver contact for operating the cam lights (program cam position indicators) is mounted on the underside of the cam bridge and makes contact with six phosphor bronze spring leaves mounted inside the machinery boom (see Fig. 2-19). Three minature pen-light bulbs mounted in the bridge fairwater (Fig. 2-20a) are flashed successively by alternate contacts to produce the streak on the recording film shown in Part (b). The circuit shown in Part (c) allows multiple flashing of the bulbs, replacing the one-shot flash bulb used in the Odax model. Four small pen cell batteries charge up the condenser through the resistor before and between contacts. When a contact is grounded the condenser discharges, bringing the light up to brilliance quickly while the batteries maintain the current for the duration of the contact. Use of the condenser reduces the delay between contact and appearance of the streak on the film to 0.005 second, which represents 7.5 feet full scale at 25 knots.

Description of Albacore Model for Horizontal Maneuvers

The Albacore model as used for the horizontal maneuvering at Froude-scaled speed represented the "revised" configuration of control surfaces and appendages only. Figure 2-21 shows several views of the model ready to run and also disassembled. Major modifications were required in the power plant

for reducing speed from 15 to 4.2 fps and in the control mechanism for addition of rudder and dorsal rudder control. Improvements in the static trim adjustments were also required for more precise control of weight distribution.

Hull: A new hull and main afterdeck were electroformed for the horizontal turning maneuvers incorporating several improvements. Recesses, such as shown in Fig. 2-22 were formed in the hull during plating for the main hatch and two afterbody access hatches. The main deck fits into the hull recess and is held by the fastening screw. The joints are sealed watertight with rosin wax which requires little heat and minimizes distortion of the hull from repeated heating and cooling. The bridge fairwater is likewise held with a screw and wax sealed while the afterbody access hatches are sealed and held by wax.

The hull take-down joint is a bayonet sleeve-type joint allowing faster disassembly and more accurate assembly and alignment. Three radial pins (shown in Fig. 2-23) in the forward section engage the axial slots in the aft section and lock in place with a 7-degree rotation. The nozzle tube outlet on the trigger valve was shifted to a position coaxial with the hull longitudinal axis with an "O" ring seal to allow rotation of the tube relative to the valve during locking of the bayonet joint. This joint is sealed with wax also.

Propulsion System: The propulsion system remains the same as used for the vertical maneuvers with appropriate modification for reducing the model velocity from about 16 fps to 4.2 fps, and for extending the run time from 2.0 seconds to 10 seconds. This was accomplished by reducing the turbine jet diameter from 0.015 inch to 0.008 inch, increasing the gear ratio from 3:1 to 9.36:1 (turbine speed to propeller speed), and reducing the initial accumulator pressure from 2200 psi to 1850 psi. The resulting propeller speed was then about 3300 rpm compared to 11,000 rpm previously. The turbine wheel speed remained about the same (30,000 - 33,000 rpm). The power output was reduced from about 0.25 hp to 0.04 hp, of which 0.03 hp is absorbed by the mechanism leaving 0.01 hp to propel the model. Due to the large effective inertia of the double reduction gear train and program cam drive compared to the small jet size, about one second is required to accelerate the mechanism up to running speed. Minor variations of velocity are made by means of a pressure bleed valve on the accumulator which allows

control of pressure within ±10 psig. The value consists of a vented hollow needle pin-sealed with an "O" ring. The vent port is screwed in past the "O" ring, allowing the gas to leak out slowly.

The speed regulation of the mechanism proved quite good, while the travel of the model per revolution of the propeller was approximately 1.00 in/rev. This corresponds to a slip of 11 percent on a straight course.

Control Mechanism: A general view of the machinery boom, linkage and drive shaft connected to the tail section is shown in Fig. 2-24a, as seen from the port side, while Part (b) shows a closeup of the linkage viewed from the starboard side. The stern plane linkage is essentially unchanged except for the zero adjusting mechanism. The differential turnbuckle is replaced by a two-piece follower bell-crank mounted on common pivots. A set-screw adjustment varies the angle between the follower arm and the linkage arm to provide zero linkage positioning over a ±1 degree plane angle range. Large changes are made by slipping the rod in the clamp. The long coil spring provides adequate loading to take up slack in the linkage and load against the program. The tail section linkage and stern plane horn remain unchanged.

The rudder control programming makes use of the space cam mechanism originally intended for control of the bow planes. Two follower assemblies were used during the horizontal turning maneuvers, the one shown in Fig. 2-24b being used for all except the roll control tests (Phases 3 and 4). The follower-crank shown here is similar to the stern-plane assembly. The transverse shaft of the rudder push rod pivots in the horizontal bearing on top of the bell-crank, while the opposite end pivots on the vertical shaft of the rudder horn (see Fig. 2-25). The unavoidable misalignments due to movements of the ends in perpendicular planes is accounted for by allowing side play in the horizontal bearing. The follower assembly is spring-loaded against the program cam by the arched leaf spring shown. Play in the remaining linkage pivots is controlled closely enough by nickel plating of the pivot shafts to preserve the ±0.1 degree over-all play. Two neoprene bellows seal the rudder and stern plane control rods at the tail bulkhead. A telescoping clamp on each rod provides for large zero shifts and for removal of the tail section.

The rudder and stern plane pivot arrangement is shown in Fig. 2-25a and 2-25b. A hollow vertical post between the vertical stabilizer fins supports

the center bearing cross and provides a bearing for the rudder pivot shaft. The rudder planes are soldered to the shaft extension while the inboard ends pivot on the post. The fixed mounting of the center cross provides an inboard bearing for the stern planes. The stern plane shaft is carried around the vertical post by a "yoke" inside the center cross which is relieved to allow ±20 degrees stern plane angles. The control rods may be seen protruding from the stabilizer fins.

The dorsal rudder control linkage (added for Phases 3 and 4 only) is operated simultaneously by a common cam follower from the rudder program cam. Partially assembled views of the model with the dorsal rudder linkage are seen in Fig. 2-26. The two-piece rudder follower assembly is replaced with a single spring steel piece. The rudder and dorsal rudder yokes pivot on a common shaft with provision for separate pivots to change the dorsal rudder ratio. The neutral angle of the rudder is changed by flexing of the follower while the dorsal rudder neutral angle is changed by altering the length of the control rod at the telescoping joint. The dorsal rudder is pivoted in the existing bearings of the bridge fairwater by the operating tab, which allows removal of the bridge fairwater as a unit for servicing of the cam light bulb. The operating shaft is sealed at the deck by an "O" ring to prevent leakage into the hull, while a chamber around the pivot horn and shaft drains any possible leakage into the turbine compartment. A neoprene bellows on the control rod, where it pierces the turbine bulkhead, prevents spray from the turbine collecting in the afterhull. This linkage provides 37.5 degrees and 22.5 degrees dorsal rudder deflections for port roll for 35-degree and 18-degree starboard rudder throw angles, respectively, with an accuracy of ± 1/2 degree.

For preliminary roll control tests, a reduced height bridge fairwater was cast in wax, duplicating the top third of the electroformed unit. Figure 2-27 shows the wax mold in place over the base with the full height bridge fairwater for comparison.

Model Trim Adjustments: The trim of the model was adjusted to the values shown in Table 2-4 as compared to the scaled values listed. The range of adjustment available and the change during the test run is shown also. The mechanism for independent adjustment of the C.G. in three directions is shown in Fig. 2-28. Vertical trim weights mounted on the take-down joint bulkhead are moved around the circumference with about 2-1/2 inches vertical travel

TABLE 2-4

MODEL STATIC TRIM CONDITIONS AND ADJUSTMENTS
FOR THE HORIZONTAL TURNING MANEUVERS

Quantity	Scaled	Measured	Range of Adjustment	Change During Run
Center of buoyancy:				
in. above baseline	1.680	1.686	0	0
in. aft of bow	10.794	10.662	0	0
Center of gravity:				
in. above baseline	1.582	1.588	+0.016 to - 0.051	-0.010 (est)
in. aft of bow	10.794	10.662	±0.012	0
Metacentric height in.	0.098	0.098	+0.016 to - 0.051	+0.010 (est)
Radius of gyration in.	5.496	5.496	±0.160	+0.082 to -0.122
Displacement lbs.	4.639 (sea water)	4.498 (fresh water)	±0.100	0
Static Inclination deg.	–	0	± 15	± 0.2
Static Roll deg.	–	0	± 3	–

through the hatch with the wrench shown. The longitudinal trim weight slides on rails along the bottom of the turbine compartment behind the vertical trim weights. The longitudinal trim may be adjusted externally with the model submerged by means of the slotted arm and shaft which is sealed at the deck by the "O" ring, as shown in Part (a). No provision is made for counteracting the 0.010-inch change in vertical C.G. due to water discharging into the bottom of the turbine compartment from its initially higher position in the accumulator. Longitudinal sloshing of the water is limited by the baffling effect of the trim weight assembly, and has no measurable effect upon the static trim of the model. The longitudinal weight transfer due to the water movement aft is counterbalanced by the forward travel of the program cam and yoke assembly. Individual cam weight differences are accounted for by adding proper ballast at the cam yoke. Although static trim is controlled within ± 0.2 degree, this weight transfer causes a 7 percent reduction of moment of inertia of the model during the run. The radius of gyration was adjusted initially high so that approximately the scaled value is attained when the control action is initiated. The static roll trim is adjusted by the transverse movement of a weight sliding in a tube fixed to the trigger valve, as shown in Part (b). Adjustments are made through the hatch.

CHAPTER 3

EXPERIMENTAL TECHNIQUES

The development of the small scale free-running submarine models required a parallel development of experimental techniques and procedures in order to assure consistent and reliable test results. This chapter describes some of the test procedures used and the auxiliary equipment developed to meet the tolerance requirements.

Model Performance

In addition to extensive testing of the various components of the model mechanisms, the performance of each model as a unit was tested for running speed and control programming. The test setup with the Odax model in the Free Surface Water Tunnel is shown in Fig. 3-1. A modified G.E. magnetic phonograph pickup is attached to the stabilizer fin so that it will generate pulses due to the passage of the propeller blades. These pulses, together with a timing signal, are recorded on an oscillograph. A propeller release wire prevents freewheeling of the propellers in the stream and thus starting of the program cam on its way prematurely. The model is mounted on a swinging parallogram suspension. The operator is seen holding a rod against the starting button of the model ready to tap the rod with a hammer. A wire connecting the rod and hammer with the oscillograph puts a pip on the oscillogram to indicate the instant the turbine is started. A moving picture of the stern plane motions is taken simultaneously with the oscillogram to determine how well the cam program is followed. For later test setups the cam lights were included in the field of view of the camera.

During such a test the water is run past the stationary model at about the free-running speed of the model, the model's power plant is started and a time history of the propeller speed and plane motions is obtained. With the magnetic pickup mounted close to one of the propellers, the propeller speed and thrust are not exactly the same as in a free run. However, the relative magnitude of the variation in speed is indicated quite precisely. The thrust of the propellers is indicated roughly by the relaxation of the spring at the top of the suspension bar as the model swings forward against the stream when the turbine is started. Various alterations to the power plant and control system were made on the basis of these tests until satisfactory

performance was obtained. Figure 3-2 shows typical propeller speed histories for the Odax and Albacore models at a tunnel speed of about 15 fps. It is seen that the propellers come up to speed very rapidly (full speed is about 0.2 sec.). The drop in speed after 1.0 sec. for the Odax model (2.0 sec. for the Albacore) is felt to be due to the accumulation of enough water mist in the turbine compartment to slow the wheel. The curve for the Odax with cams shows little difference due to the programming of the planes.

Tests of the Albacore model for horizontal maneuvers were made first on a bench mockup similar to Fig. 2-8 using a prony brake on the propeller shaft. Propeller acceleration and running speed were measured with a free shaft with a history similar to Fig. 3-2. The larger effective inertia of the higher ratio gear system and the smaller jet size (0.008-in. dia.) resulted in a longer acceleration time (about 1.0 sec.). A time delay was incorporated in the launcher circuit to allow the model motor to accelerate to speed before ejecting the model from the launcher.

Measuring Fixtures

Control Plane Angles: In order to measure and control the physical constants and control surface's angle and motions, a number of fixtures and jigs were developed. The device for measuring the Odax model plane angles is shown in Fig. 3-3a. It was assembled from existing parts and consists of a telescope with cross hairs, parts of a drafting machine and adjustable stand. The device measures the angle between the stern plane chord line and a horizontal line scribed on the edge of the fixed stabilizer to an accuracy of $\pm$ 5 minutes of arc. The bow plane angles are compared to a horizontal reference line on the measuring stand. The stern plane motions are checked point by point as the program cam is advanced by turning the propellers by hand.

Pointers were attached directly to the control surfaces and protractor scales mounted on the jig for determining plane angles on the Albacore model. Figure 3-3b shows the arrangement used for calibrating the control programs for the vertical and horizontal maneuvers. The planes are held at the zero angle by contoured "zero" blocks while the pointers are adjusted to the scale zero index as illustrated in Parts (c) and (d). With zero blocks removed, the planes are set at the desired neutral angle by means of the appropriate

linkage adjustments. The program cams are advanced by turning the propeller with the hand crank and revolution counter. The operator reads the plane angles on the scales as a function of propeller revolutions, while the meter indicates the position of the six cam light contacts. This position history of control planes versus propeller revolution is correlated with the model position in the tank by means of the cam light flashes. (See Appendix C). Similar fixtures for the dorsal rudder and bow planes mount at appropriate positions on the measuring jig.

Propeller Gage: A gage was developed for checking the propeller blade's angle and straightness for the horizontal maneuvering tests. For the high model speed tests, the propeller condition was not critical as long as constant speed was maintained. But at Froude scaled speeds, small differences in the propeller had a noticeable effect upon the model behavior. The gage (Fig. 3-3d) consists of a two-pronged pointer mounted on a sliding bar with an adjustable point beneath. With the bar extended against the stop, the lower point indexes the blade to a vertical position while contact with both prongs of the pointer indicates blade straightness to within one-half (1/2) degree. The pointer angular position then measures the blade pitch angle to within one-half (1/2) degree.

Static Trim Constants: The static trim constants (buoyancy, longitudinal trim angle, moment of inertia) for the Odax model and the Albacore model for vertical maneuvers were adjusted and measured only once prior to the test program. The method employed was to suspend the model from a knife edge at different attitudes and determine C.G. location by the intersection of the respective vertical lines from the knife edge. The center of buoyancy was determined by suspending the model under water and measuring the moment required to pull the vertical plane of symmetry to horizontal. Moment of inertia was measured on a torsion balance by comparing the period of oscillation of the model to that of a calibrated rod. Static trim and buoyancy were checked visually prior to each run by releasing the model while submerged.

C.G. - I Balance: For the horizontal maneuvers with the Albacore model at 4.2 fps, buoyancy and static trim were measured and adjusted before each test run while metacentric height and moment of inertia were measured for each control program series These static constants of the

model were measured and adjusted using the device shown in Fig. 3-4. The "C.G. -I Balance" consists of a clamping ring with transverse stub shafts supported by precision micro ball bearings with a torsion wire clamped at a third support. The balance frame is doweled to the model measuring jig so that the ring is clamped on the model at the scaled longitudinal C.G. location on the hull axis. With model adjusted to neutral buoyancy, the longitudinal trim is adjusted in the flotation tank as illustrated in Part (b). With the outboard bearing removed, the roll trim is measured (still submerged) with the attachment shown in Part (c). The buoyancy tank accounts for the tare weight of the ring and attachment with the balance weight in the center position. With the model clamped in the ring, the displacement of the weight required to recenter the pointer is a measure of the static roll trim. With the balance in the vertical position, as shown in Part (d) and with the outboard bearing removed, the model and ring pivot around the inboard spherical bearing, the weight being supported by the torsion wire. The balance is recentered by moving the weight along the calibrated rods to determine metacentric height while submerged and vertical C.G. location in air. With the outboard bearing replaced and balance rods removed, the frequency of oscillation (in air) is compared to that of the calibrating rod to determine moment of inertia. The longitudinal C.G. location is measured in air with the model and balance in a horizontal position by adjusting the weight on the longitudinal rods. This device allows measurement of C.G. and metacentric height to within 0.001 inch, radius of gyration to within 0.002 inch, static roll angle to within $\pm$ 0.2 degree and adjustment of longitudinal trim to within $\pm$ 0.2 degree.

Metering Pump: The models require only a small amount of water charge to operate the turbine, but it must be loaded against the high pressure (2200 psi) of the accumulator. Figure 3-5 shows the Albacore model being charged with a special metering pump built to fulfill these needs. A nozzle at the bottom screws into the model trigger valve. The hand-operated screw pushes a 3/4-inch diameter piston in the pump body and forces the water charge into the accumulator against the gas pressure. The gage indicates the water pressure while the quantity is metered by counting revolutions

Test Procedure

The procedure for conducting a model test was essentially the same for the Odax and Albacore models. Refinements evolved only in the manner of performing individual measurements with the auxiliary equipment described above.

The launching tank is prepared for a test run simultaneously with the model, as described in Appendix B. The model is prepared and the test run made in the following sequence:

(1) Fresh batteries and the proper program cam are installed. The mechanical operation of the model machinery and control linkage is checked by running the turbine with an air jet.

(2) The model is placed in the measuring jig; alignment of hull, control surfaces and propeller is checked and adjusted, and the program cam is calibrated.

(3) After calibration, the program cam cams are returned to the starting position, the deck and bridge fairwater are mounted in place and the model checked for leaks by applying a slight internal air pressure with the model submerged in a small flotation tank.

(4) The model accumulator is charged with 0.08 lb water with the metering pump. The weight before and after loading is recorded.

(5) The static trim constants are measured and adjusted as necessary.

(6) The accumulation of dirt and oil from handling is washed off and the model checked again visually while being carried to the launching tank.

(7) A final check of buoyancy and trim in the tank is made after flooding the free-flooding spaces by releasing the model when completely submerged.

(8) The model is slid into the launcher guide rails, seated against the model pusher, and the turbine trigger adjusted.

(9) The tank is darkened, the model is launched and the trajectory recorded as described in Appendix B.

(10) After the run, the model is retrieved with an adjustable claw device, and the buoyancy and trim checked.

(11) Visual observations are compared and necessary corrections decided upon for succeeding runs.

(12) The water charge is drained, the model dried with air, the cams returned to the starting point, and the above procedure repeated for succeeding runs.

CHAPTER 4

TEST RESULTS AND DISCUSSION - U.S.S. ODAX

Purpose

The purpose of Part 1 of the investigation of the dynamic control characteristics of submarines by means of free-running models was to determine whether the small-scale model will duplicate the dynamic behavior of the full-scale vessel. The U.S. Submarine Odax was selected for this part of the study because this boat was subjected to an extensive series of sea trials, and good records of its performance over a wide range of test conditions and a variety of maneuvers were available. The sea trials (Ref. 17) included meander tests, zig-zags in the vertical plane, dive-and-pullouts, and horizontal maneuvering tests. The parallel purpose of developing the free-flying model technique is implicit here as well as in the remainder of this work. The results presented in this chapter represent the first step in proving and evaluating the model technique. As was pointed out in Chapters 1, 2 and 3, the precision used in building and operating the model and in making the measurements must be of sufficiently high order so as to eliminate this consideration in the evaluation of the efficacy of the method. Throughout the study, efforts were being made to improve and refine the experimental techniques. The test results are presented in chronological order (Chapters 4, 5 and 6) and give an indication of the improvements that have been achieved.

Model Test Program

The model test program consisted of determining the response of model to four control programs selected for reproducibility of control action and type of response. The first type of program considered was the pull-out maneuver which appeared simple at first since it consists of only one dive or rise and one pull-out. However, this very simplicity makes it a difficult maneuver to reproduce because, in reality, it is not a well defined one in itself, but consists of two transitions, first from a level path to an inclined path and then back to a level path. Also the motion of the vessel during this transitional type maneuver is particularly affected by the recent history of the motion, that is, by any angular displacements or angular velocities that may have existed just prior to the beginning of the maneuver. Since the records of the prototype maneuvers did not include the motion covering a

sufficient time interval before the maneuver was entered into, it would not be possible to reproduce the minor events preceding the main maneuver.

The zig-zag tests appeared easier to carry out with the model since the motion eventually settles down into a repetition of cycles that are similar to each other. The zig-zag test records of the Odax also start at the instant the maneuver is entered into, but the motion appears to be only slightly affected by prior events of minor magnitude. For some of the runs, the record actually begins with the submarine already in the maneuver, so that a definite and large motion already exists and would provide a measure of this effect on the model trajectory.

This type of control program was selected, therefore, as being most suitable for reproducing with the model. If period and amplitude of oscillation of the model about a median line were similar to the prototype, then it was felt that a suitable modification of the diving plane motion prior to the main maneuver or during the first half cycle only would provide over-all agreement. Four full-scale runs of the zig-zag type were selected from the sea trials on the basis of (1) period of the cycle, (2) regularity of control plane program, i.e., absence of "hash", (3) full-scale speed of nine knots or more for the reasons outlined in Chapter 1, and (4) use of active stern plane control only.

Prototype and Model Test Procedures

The procedure for the full-scale test was as follows:

(1) With the ship in neutral trim and buoyancy, and with bow planes set at zero, the ship was run at the desired speed and at a depth of 175 feet for a long enough time to obtain steady trim and diving plane angles.

(2) The stern planes were then moved quickly to a dive angle of $+\delta_s$ and held until the trim angle reached $-\theta$, then moved quickly to a rise angle of $-\delta_s$ and held until the trim angle reached $+\theta$; then moved quickly to a dive angle of $+\delta_s$ and this cyclic pattern continued.

For an initial rise in the first cycle, the above signs are reversed. Table 4-1, below, gives the schedule for the full-scale trials which were tested with the model.

TABLE 4-1 - ZIG-ZAG TEST SCHEDULE (Excerpts)

Test No.	Speed knots	Execute angle - θ degrees	Stern plane angle degrees
84	10	8	10
86	14	use 3^{o} first reversal then 0^{o}	10
87	14	2	10
194	10	use 3^{o} first reversal then 0^{o}	15

The records of these full-scale tests, made by automatic recording instruments, showed continuous plots of the angular positions of stern planes, bow planes, and rudder, as well as speed, depth, inclination (a pitch), roll and heading, all plotted against time. In all the tests listed in Table 4-1, the bow planes and rudder were held in neutral position throughout each run.

Since the model contains neither pilot nor any instrumentation which senses depth or inclination, it was not possible to present instructions to the model in the same form as given for the full-scale trials. The model was instructed, by means of the mechanical cams described in Chapters 2 and 3, to reproduce the same time-sequence of stern plane motions as were carried out in the full-scale sea trials. The unit of time that was used in going from full scale to model was not the arbitrary unit of "seconds", but the dimensionless unit "time to run one ship-length".

The model test runs were made in two steps, as follows:

(a) The model was run with pre-set control planes, i.e., no control programming, and the angles changed until a nearly straight and level run was obtained. The model buoyancy and trim were adjusted to neutral before each run.

(b) The test run was then made with the control program superimposed upon the control plane "neutral" angles of (a). A short neutral run of about two shiplengths is provided before start of the control program for the purpose of evaluating the initial conditions and their effect upon the subsequent trajectory. The control program is determined and correlated with the resulting trajectory as described in Chapter 3.

Presentation of the Test Results

The model test results are presented in Figs. 4-1 to 4-5. Three curves are shown for each test made: (1) the stern plane action, (2) an elevation view of the trajectory, and (3) pitch angle, all plotted against either horizontal distance or time in prototype scale. Two modes of presentation are used in order to show the entire process used in handling the data and at the same time avoid tedius repetition:

(a) Two individual tests are used as samples to show, step-by-step, the processes involved in going from raw model test data, to conversion to prototype time and distance scales, to comparison of model and prototype test results, and the two simple corrections applied to the model data. These two tests are presented in Figs. 4-1a to 4-1c and Figs. 4-2a to 4-2e.

(b) For the remainder of the tests the results are presented in groups of repeat tests, each group made with one stern plane program to indicate the degree of consistency of the model's own behavior. These are shown after having been corrected in the same manner as in the two preceding examples, and the magnitude of the two corrections are indicated on each individual curve.

An average is obtained from each group or family of model curves, and the average model behavior is compared with that of the prototype.

These groups of tests are presented in Figs. 4-2f through 4-5d.

Adjustment of the Model Data

Although no records were made prior to each maneuver, an attempt was made to control the initial conditions of the prototype by running long enough to obtain steady trim and diving plane angles. (See Test Procedure (1)). That is, some measure of continuous control was exercised. However, for the model tests, no such continuous control was possible and the initial conditions depended upon the manner in which the launching mechanism releases the model after accelerating it up to its constant running speed and the behavior of the model during the neutral portion of the test run. A tight rail or launcher could not be used for fear of damaging the model, and some looseness existed in the device. The model, therefore, did not always start out level or with zero angular velocity.

Two separate adjustments of the model data were made, as illustrated in Fig. 4-1, for a typical model test run. The response of the model to

Program Cam No. 7, representing prototype run No. 84, is shown in Fig. 4-1a as received from the analyzer (see Appendices B and C). The data points shown represent the position and attitudes of the model at each frame recorded (0.05 second intervals) as indicated by the counter readings. The distance scale in the launching tank is also shown. The short, heavy lines denote the position of the model at which the cam lights flash after being triggered by the contacts on the program cam. The depth trajectory is seen to be starting slightly downward due to the action of the launcher.

This model test data is expanded to full-scale dimensions as described in Appendix C and compared to the prototype behavior for the corresponding control program in Fig. 4-1b. The stern plane action shown reproduces that of the prototype very closely. The positions of the cam light signal are seen near the beginning and about half way through the program. The slopes of this curve represent a plane movement rate of 5 deg/sec.

The inclination and depth curves are shown to a distorted scale since they are plotted against time instead of horizontal distance. The discrepancy between model and prototype curve is therefore very much exaggerated. The peaks of the model curves are seen to be below those of the prototype, and the model trajectory generally slopes downward. These curves are aligned horizontally by the first cam light position as determined from the bench calibration of the control program. The interval between the cam light positions is seen to compare closely.

Figure 4-1c shows the comparison of the model and prototype curves after applying the corrections in two steps. The first correction consists of a change in the inclination of the average path of the model's trajectory based on the slope of the neutral portion of the trajectory. That is, the trajectory is rotated in the plane of the paper to make the neutral portion horizontal. It will be noted that the relation of the model trajectory amounted to only 0.35 degree in the case shown here. In none of the runs was this correction more than 2 degrees. This correction when applied to the inclination curve consists of the addition of a constant angle equal to the rotation of the trajectory.

Now, it will be noted that although the amplitudes agree, there is a phase difference between the model and prototype curve. The second correction accounts for this difference by a shift in the time scale of the model

curves as shown in Part (2) of Fig. 4-1c. This amounts to a few seconds on the prototype time scale or a few hundredths (0.06 sec) on the model's time scale. Both corrections are made on the basis of the depth trajectory curve, and the inclination curve is adjusted by the same amount. These corrections are made arbitrarily to show the small magnitude of correction required to obtain good agreement between model test results and the full-scale runs. It is believed that these differences are due primarily to the manner in which the launcher mechanism starts the model on its way.

Although the model generally started off slightly downward, in some cases the launcher caused it to slope upwards. Such a case is shown in Fig. 4-2 for test run No. 446 with program cam No. 8 representing prototype run No. 87. Figure 4-2a shows the model trajectory with data points as it appeared in the tank. Part (b) shows the depth trajectory of the model compared to the prototype plotted again to an exaggerated scale. On rotation through an angle of 1.51 degrees clockwise, as in Part (c), quite good agreement is obtained except for a phase difference. After a shift of 2.5 seconds, the agreement is good until toward the end of the trajectory. The corresponding inclination curves showing the successive corrections are seen in Fig. 4-2e.

A comparison of four model curves after applying the above corrections is shown in Fig. 4-2f. The repeated model trajectories indicate a consistent model response to the program and give a measure of the effect of the initial conditions upon the reproducibility of the dynamic response. It may be noted that the deviation increases rapidly, particularly in depth, toward the end of the run. This is due to the exhaustion of the water supply in the model's power plant. Power cutoff always causes this model to dive.

Figure 4-2g shows a comparison of the average response of the model, taken from the four tests of Fig. 4-2f, with that of the prototype. The agreement, although not perfect, was considered remarkably good at the time of these tests. If the tests were done again at present it is felt that the results would be at least more consistent and a better measure of the degree of agreement could be obtained.

A number of comparisons with other prototype tests gave similar results. Figure 4-3 shows the results obtained with program cam No. 6, representing prototype run No. 86. For this run, the submarine had already

begun the maneuver before the record started. Estimated control program and response were obtained and the initial plane motion designed therefrom. Figure 4-3a shows the relative response of eight model runs after applying corrections. The initial conditions are seen to vary considerably but the general response is consistent in form. The four runs with the larger initial slope of the trajectory are seen to oscillate with a larger amplitude, also. However, the average response of the model (Fig. 4-3b) is seen to compare quite well with the prototype response. The amplitude of the depth response of the model is seen to be slightly greater than the prototype. The deviation again grows larger toward the end of the trajectory.

A comparison with prototype run No. 194 of six model tests run with program cam No. 5 is shown in Fig. 4-4. Part (a) shows the relative response and consistency of the model after applying corrections, while Part (b) shows the comparison of average model and prototype response. It may be noted that this series had stern planes deflection angles of $\pm$ 15 degrees whereas the other programs tested had $\pm$ 10 degrees. Also, the prototype speed is 10 knots compared to 14 knots for Fig. 4-2 and 4-3 while the model speed remains constant. This means that for the length of the model's trajectory a larger number of cycles is possible before power cutoff. The six model tests still show quite good consistency over almost one additional cycle, while the relative differences remain about the same. The average response of the model appears to compare with that of the prototype somewhat better than with runs Nos. 86 and 87 as shown in Fig. 4-4b.

As has been pointed out previously, it was felt that the launcher released the model in such a manner that the model started downward. This was found to be the case when the launcher rails were removed. The model fitted in the rails with the axis inclined downward with respect to the line of motion, and consequently when ejected by the launcher the model started on an initial trajectory that was inclined downward in most cases. Therefore, the launcher was suitably modified and a few model test runs were repeated.

Another factor entered into repeating some tests also. Most of the preceding tests were made with small fenders added to the fins on the model which were necessary to prevent damage to the propellers during launching. It was found that at the end of the acceleration period, when the stern of the model left the pusher, the stern dropped and the propeller tips were damaged

by contact with the lower rails. A temporary cure was effected by soldering small vertical plates along the edges of the fins (see Fig. 2-10). To eliminate the need for fender plates, a fifth rail was added along the bottom of the launcher rails under the vertical rudder.

Figure 4-5 shows a comparison of model test runs, (a) before the above modifications were made, and (b) after the modification. A comparison of the average model trajectory for each series of tests with the prototype run No. 84 is seen in Fig. 4-5c. The first series of test runs exhibited the usual initial downward slope, while the second series of runs showed that the model left the launcher on a trajectory that was very nearly horizontal. Nevertheless, the subsequent model trajectories had to be rotated slightly in either case. It may be noted in Fig. 4-5a that most of the curves had to be rotated up, or counterclockwise, for the first series, while for the second series all were rotated down, or clockwise.

The comparison of average model runs and prototype trajectory in Fig. 4-5c indicate that the modifications to the launcher and removal of the fenders did not alter the behavior of the model by very much. If we take the amplitudes of oscillation of the full-scale submarine as 100 percent, then in the first series of model tests the amplitude in depth was 98.8% and in pitch 90.3 percent, while in the second series the amplitude in depth was 104.3 percent and in pitch 92.5 percent.

The trend of the variation of amplitudes of oscillation of the model as a function of the inclination of the neutral portion of the model trajectory is shown in Fig. 4-5d. The abscissa shows the angle through which the model trajectory had to be rotated for comparison with the prototype trajectory, and the ordinates give the resulting amplitude of oscillation in depth and in pitch. The curves show that the resulting amplitude in depth is a linear function of the inclination of the model trajectory and that two lines may be drawn through the points, one for the first series of runs and another for the second series. The distinction between the two series of runs is not as clear in the case of pitch amplitude, since one curve can be drawn through all the points. It is not known whether the differences exhibited by the two series of tests are due to the modification of the launcher and removal of fenders from the fins or, perhaps, due to the fact that the model mechanism as a whole had taken considerable wear in the intervening test runs. Figure 4-5c does seem

to indicate that correction by rotation of the model trajectory is not the best possible method. This would be true if the deviation were due to an inclination of the average path of the model rather than a bending of the average path, which appears to be the case. The Guppy type submarine appears to be sufficiently unstable to make it impossible to maintain a straight course for any length of time without steering. However, a better method of correction has not been devised since it is not known what the curvature of the path would have been for any given run if the diving planes were held in a fixed position.

Summary and Conclusions

Comparisons of the dynamic behavior of a free-running model with that of the prototype for a zig-zag type of maneuver have been presented. A small scale model of a Guppy type submarine, the U.S.S. Odax, was used because good records of its performance were available. The zig-zag maneuver was selected for the purpose of comparison of the dynamic behavior of model with prototype as being the most suitable for reproducing with the model. Differences between model and prototype test procedure and effects upon the model behavior have been pointed out. Samples of model experimental results indicating measuring accuracy and data consistency have been shown. Corrections of minor magnitude to the model curves for comparison with prototype trajectories have been described and the reasons for them explained. Test results showing the dynamic response of the model with four stern plane control programs and comparison with the prototype response have been presented. The model was seen to demonstrate quite consistent behavior and reproducibility for successive test runs with each control program. The consistency and reproducibility of the prototype runs is not known and no comparison in this respect was made. Quite good agreement between the average response of the model and that of the prototype for a single run has been demonstrated.

From the results presented in this chapter we may draw the following conclusions:

(1) The small-scale, free-running model can duplicate the dynamic behavior of full size submarine with satisfactory precision for zig-zag type maneuvers.

(2) The model exhibits consistent and reproducible dynamic response for a given control program.

(3) The model of the Guppy type submarine exhibits known unstable control and stability characteristics of the full-scale boat.

(4) The modeling technique by means of free-flying, powered and controlled models has been successfully developed for model dynamic behavior in the vertical plane.

CHAPTER 5

TEST RESULTS AND DISCUSSION - U.S.S. ALBACORE MODEL IN VERTICAL MANEUVERING

Purpose

The purpose of Part 2 of the study of submarine control by means of small scale, free-running models was to determine the dynamic control characteristics of the U.S.S. Albacore AGSS 569 (SST Scheme IV) submarine for maneuvers in the vertical plane. More specifically, the test program was designed to determine:

1. The transient behavior on entering a dive or a rise, on settling down to an inclined path, and on leveling off.
2. Equilibrium turning conditions in rise and dive as a function of stern plane angle.
3. Precise control programs for executing optimum depth changing maneuvers.

Model Test Program

The model test program was conducted in seven general phases as listed below:

Original Configuration:

Phase 1 - Determination of the directional stability of the model for variation in initial angular velocity and trajectory angle, longitudinal velocity and acceleration, metacentric height, and for small control surface angle changes.

Phase 2 - Determination of the control characteristics of the model on entering a rise or dive for various stern plane angles at two plane rates.

Phase 3 - Determination of the damping response of the model in dive and inclined path type of maneuver for one stern plane angle with various holding times.

Phase 4 - Determination of the control program for an optimum dive and pullout trajectory for a 300-foot depth change with a 30° maximum inclination.

Revised Configuration

Phase 5 - Determination of the directional stability of the model for variations in static longitudinal trim and buoyancy.

Phase 6 - Determination of the control and damping characteristics of the model in (a) rise and dive for various stern- and bow-plane angles and (b) turning for small rudder angles.

Phase 7 - Determination of the control program for an optimum dive and pullout trajectory for a 300-foot depth change with (a) 30° maximum inclination and (b) 15° maximum inclination; also comparison of experimental and computed trajectories for a given control program.

The test conditions showing the range of variables are shown in Table 5-1a for each phase of the model test program. The order of tests shown does not correspond to the actual experimental sequence (which depended upon development of experimental techniques) and evolution of the test program with growing knowledge of and familiarity with the behavior of the model.

TABLE 5-1a

MODEL TEST PROGRAM - PART I

Phase	Configuration	Type of Maneuver	Velocity Linear ft/sec	Velocity Angular deg/sec	Metacentric Height ft	Response Characteristic Determined
1	original	neutral	15	± 0.3	0.8	directional stability
1	original	neutral	13-16	0	0.8	directional stability
1	original	neutral	15	0	0.7-1.0	directional stability
			Stern plane throw angle deg.	Plane throw rate deg/sec	Holding time at throw angle sec.	
2	original	dive	3-18	5	∞	transient and equilibrium turning conditions
2	original	dive	18	10	∞	
2	original	rise	3-18	5	∞	
3	original	dive incline	18	5	1-8	damping
4	original	depth changing	18 dive and rise	5	4-6 dive 7-9 rise	optimum pullout trajectory

TABLE 5-1b

MODEL TEST PROGRAM - PART 2

Phase	Configuration	Type of maneuver	Buoyancy lbs.	Static Trim deg.	Response characteristic determined
5	revised	neutral	+10,000 to -25,000	0	directional stability
5	revised	neutral	0	+18 to -20	directional stability

Phase	Configuration	Type of maneuver	Plane Throw Angles			Holding time at throw angle - sec.	Response characteristic determined
			Stern deg.	Bow deg.	Rudder deg.		
6	revised	dive	+18	0	0	-	
	revised	dive incline	+18	0	0	5	
	revised	rise and dive	-3 to +3	0	0	-	Transient and equilibrium turning conditions.
	revised	rise and dive	0	-3 to +3	0	-	
	revised	horizontal turning	0	0	0 to -1	-	

Phase	Configuration	Type of maneuver	Stern Plane Throw Angle deg.	Maximum Inclination deg.	Scaled Velocity knots	Response characteristic determined
7	revised	depth changing	± 18	+ 30	25	Optimum pull-out trajectory
7	revised	depth changing	± 12	+15	25	Optimum pull-out trajectory
7	revised	depth changing	± 18 max.	+30	95	Computed vs experimental trajectory comparison.

Presentation of Results

The results are presented in a series of tables and curves (see Vol. II) showing the dynamic response of the model to various static stimuli and dynamic control programs. The sequence of figures follows the test program outline of Table 5-1 with the exception of Phases 1 and 5 which are discussed simultaneously. Table 5-1 will also serve as a general index for the figures for Chapter 5.

Four principal types of curves are utilized to illustrate the trajectory response of the model; (a) trajectory history, (b) curvature history and (c) transient and equilibrium conditions:

(a) The "trajectory" history curves present the linear and angular position data as expanded to full scale and plotted against the distance along the trajectory. The linear position data (depth or lateral) is plotted to a one to one scale to give a graphic picture of the position data. The angular position (inclination, roll or azimuth) data is plotted to an arbitrary scale. The time scale is computed on the basis of a constant full-scale speed of 25 knots. The control programs are computed from the bench calibration and aligned by means of the cam lights.

(b) The "curvature" history curves give the rates of change of the linear and angular position data of curve type (a) expanded to full scale and plotted against the distance along the trajectory. The control program is generally not shown, being identical to that on the trajectory history.

(c) The "transient and equilibrium conditions" curves show characteristic response (usually turning rates, angle of attack) as functions of a common parameter (usually control deflection angles) for a family or group of tests with similar control programs.

Curve types (a) and (b) may be presented in three classes of plots; (1) individual run, (2) composite and (3) family:

(1) The "individual run" curve shows the model response for a single test run as it occurred in the tank with the control program aligned by means of the cam lights or static test conditions indicated.

(2) The "composite" curves compare individual runs made under identical conditions of control program or static stimuli after aligning by a common index (cam light position or start of control action). Initial trajectory conditions may or may not be reconciled to indicate total or relative effects, respectively, of variations of launching speed and attitudes, and control actions upon the consistency and performance of the model.

(3) The "family" curves compare average composite curves aligned by the start of control action for control programs of the same general type. Each average curve is determined from a point by point averaging of the composite curves. Data points are usually omitted on the family curves.

Other curves, as needed, are explained in the discussion. For the most part, the results are presented in a series of family curves for each curve type.

Correction for Initial Conditions

The initial conditions of the trajectory depend upon the manner in which the launcher releases the model. In extreme cases, the attitude of the model was found to vary from 1 degree nose down to 3 degree nose up with angular velocities of up to 26 deg/sec (0.7 deg/sec full scale). Normally, the model left the launcher at about 1 degree nose up and maintained a straight trajectory. For the purpose of comparing the relative response of individual test runs in composite curves, these initial conditions are reconciled as shown in Fig. 5-1a and b. The depth trajectory is "rotated" to make the initial (or neutral) portion of the trajectory level, and the inclination curve is shifted correspondingly. The rate of change of depth also is shifted by the sine of the rotation angle.

The validity of this technique of comparison is shown in Fig. 5-2 where three successive runs with the same control program are compared. Figure 5-2a shows the runs as aligned by means of the cam lights. Note that all runs reach the same final curvature as indicated by the parallel plots of the inclination curves regardless of the initial attitude or angular velocity. Figure 5-2b shows the curves after rotation where the effect of large initial angular velocity is shown in reducing time to reach final curvature. Test run No. S-99 has an initial angular velocity that is considered excessive because it affects the transient response appreciably. Therefore,

for determining the "average" curve for this particular control program, test run S-99 was discarded and only run S-100 and S-101 were used.

Determination of Control Program

The correlation of the stern plane control program with the trajectory is of critical importance in comparing the response of the model for different configurations of control surfaces for the same program. It is also important in determining the time required to reach a given change in position or attitude, such as the time to attain a 10-degree inclination after the dive planes have been moved.

The time delay between contact and brilliance of the cam light was measured electronically and photographically as described in Chapter 3. An additional check was made during a normal sequence of test runs by measuring the stern plane angle with respect to the hull axis as well as inclination and depth. A special tab was attached to the stern plane and these measurements compared to a previous test run. Fig. 5-2c indicates no significant difference between the stern plane action measured in the analyzer and that measured during the bench calibration and aligned with the predetermined cam light delay.

Discussion of Results

The over-all performance of the model of the SST U.S.S. Albacore (SS569) indicates exceptional directional stability and maneuverability characteristics for both configurations of control surfaces used in the free-running tests in the Controlled Atmosphere Launching Tank. Indeed, the directional stability of the model was such that the behavior in the tank soon became an indicator of the performance of the model mechanism, the consistency of the launching gear and the quality of the trajectory analyzer continuity and consistency.

Phases 1 and 5: Directional Stability

The series of tests shown in Figs. 5-3 through 5-10 were made primarily for determining the behavior of the model in order to (1) establish experimental operating limits of the physical characteristics within the control of the experimenter, and (2) to evaluate the effect of spurious and erratic forces beyond the control of the operators. In addition, the information

derived from these tests is of value as an indication of the dynamic stability of the full scale submarine in at least a qualitative manner, and also as a comparison with the behavior of the U.S.S. Odax model.

These test runs were made with "neutral" control angles, i.e., those control surface settings for which the model would maintain a straight trajectory with zero angular velocity of inclination, azimuth and roll - and with the physical characteristics (buoyancy, static inclination and roll trim, hull and propeller alignment, surface contours and roughness) of the model controlled as precisely as possible. No distinction is made between configurations of the control surfaces as regards directional stability, except as noted on the curves and in the text. In general, significant differences in directional stability between the two configurations used with neutral control settings were not detectable in the tank or measurable from the data.

The consistency and directional stability of the model is illustrated in Fig. 5-3 for three test runs made under as nearly identical conditions as possible. The buoyancy was controlled to within $\pm$ 0.00025 lb., the static inclination trim to within $\pm$ 0.5 degree and the control surface angles to within $\pm$ 0.1 degree. Figure 5-3a shows a comparison of the trajectories as they occurred in the tank, while Fig. 5-3b shows the comparison when the initial conditions are reconciled. These trajectories are typical of the behavior of the model whether with the original or the revised control surface configuration. The neutral angles were determined from visual observation of the trajectory in the tank by trial and error, i.e., the control surface angles are altered on the basis of the observed trajectory for the previous run until a straight run was obtained. As indicated in Fig. 5-3a a "level" run is difficult to achieve because of variations in initial launching conditions.

The variations of initial velocity, angular velocity in inclination, yaw and roll indicated are within the normal range for the launcher arrangement used for these tests and are inherent in the design. The four-pronged pusher shrouds the propeller and control surfaces quite effectively (see Fig. B-5) during acceleration and inhibits establishment of full flow over the tail assembly until the tail clears the launcher guide rails. This generally results in a nosing up impulse due to the lift on the hull before the stern planes take hold, and causes the upward inclined trajectory. Necessary clearances

between the model and guide rails contribute also by allowing slight misalignments, variable friction and initial angles of attack.

One may consider these initial conditions as disturbances imparted to the model originally traveling along a trajectory defined by the centerline of the launcher guide rails. The divergence of the subsequent trajectory would then be a measure of the dynamic (directional) stability of the model. Quite good stability in the vertical plane is indicated since the model settles down to a new, essentially straight course in 1-1/2 to 2 ship lengths. The small, constant angular velocity(which is of the opposite sign as the disturbance) is felt to be due to variation from run to run of the neutral angle within the $\pm$ 0.1 degree tolerance. When compared to response of the U.S.S. Odax model (a submarine with known dynamic instability) for similar disturbances, the Albacore model appears to possess almost exceptional directional stability. The same launching mechanism with similar guide rails was used for both models, so that disturbances of a similar nature and magnitude occurred. Figure 5-4a compares the envelopes of repeat test runs of the Odax and Albacore models as the trajectories appeared in the launching tank, while Fig. 5-4b shows the trajectories rotated to reconcile the initial conditions. The trajectories for the Odax model exhibit an increasing divergence which is typical of dynamic instability, whereas the trajectories for the Albacore model indicate a much smaller constant divergence. The behavior shown here is typical of that observed for a large number of test runs made with both models. For the Odax model, it was always difficult to determine neutral control angles,and repetition of a neutral trajectory was unreliable due to the growth of the initial "disturbances". On the other hand, the excellent stability of the Albacore model allowed easy and quick determination of neutral settings (from a few runs) that could be relied upon for the entire duration of the test program.

Sensitivity of Model Response - Static Trim.

Figures 5-5 through 5-10 show the sensitivity of the model response to a variety of static, dynamic and physical parameters. The effects of changes in static trim and buoyancy upon the neutral trajectory of the model at a constant model speed of 15.5 fps are shown in Figs. 5-5a and 5-5b. The technique was to compare the trajectories for large variations of ballast shifts and changes to those obtained for zero static trim and neutral buoyancy.

The datum trajectories are those shown in Fig. 5-3, for which the static trim buoyancy was adjusted very precisely prior to each test run. (The metacentric height of the model was 0.091 in. - 0.76 ft full scale.) The range of applied moments and loads, and resultant static conditions is shown in Table 5-2. The static force and moment coefficients ($Z'_B = Z_B / \frac{1}{2}\rho \ell V^2$ and $M'_\theta = M_\theta / \frac{1}{2}\rho \ell^2 V^2$) listed for each condition show the magnitude of the applied static forces and moments relative to the dynamic control forces available (M'_δ, M'_α, Z'_δ and Z'_α) at <u>model</u> and <u>full-scale</u> velocities. The applied static forces are seen to be actually quite small compared to the dynamic control forces available at model speed, so that one would expect little effect upon the trajectory. At full-scale speed of 25 knots, the static and dynamic forces are of the same order of magnitude, requiring an angle of attack of up to 1.0^o and stern plane deflection of about 1.0^o, whereas at model speed control and attack angles less than the experimental error are involved. This, in essence, is the basis for neglecting metacentric stability for the model speed used. The curves of Fig. 5-5a and b show that the variation of the trajectories is within the normal range of scatter for neutral runs with zero static trim and buoyancy. The values of average angular velocity and vertical rate in Table 5-2 also indicate little effect upon the response of the model and exhibit no trend with variation of static trim and buoyancy. These tests proved to be of great value as far as operation of the model was concerned for the speed range used (15 – 16 fps). The static trim and buoyancy, having negligible effect upon the response of the model, did not need to be adjusted extremely close to zero conditions, thereby eliminating much tedious and time-consuming work of adjusting the model for each test run. The results also indicate an interesting and valuable property of high-speed submarines; namely, large changes of trim and buoyancy may be rather easily overcome by maintaining speed and "flying" the ship in a planing attitude. A comparison of the stern plane rates, M'_{δ_s} and Z'_{δ_s} to the static moment and force coefficients M'_θ and Z'_B, shown in Table 5-2 indicates only small plane deflections are required to balance the static conditions and yet leave adequate deflection for maneuvering.

TABLE 5-2a

STATIC TRIM EFFECTS

Applied Moment, M_θ		Static Trim	Moment Coefficient, M'_θ *		Avg. Angular Velocity
Model lb-in.	Full Scale lb-ft x 10^{+6}	deg.	Model at 15 fps x 10^{-4}	Full Scale at 25 knots x 10^{-4}	rad/sec
0	0	0	0	0	+ 0.00033
+ 0.028	+ 0.233	+ 3.9	+ 0.013	+ 0.16	+ 0.00024
+ 0.056	+ 0.467	+ 7.8	+ 0.027	+ 0.33	- 0.00013
+ 0.084	+ 0.700	+ 11.8	+ 0.040	+ 0.49	+ 0.00053
+ 0.112	+ 0.933	+ 15.8	+ 0.054	+ 0.66	+ 0.00063
- 0.140	- 1.168	- 20.0	- 0.067	- 0.82	+ 0.00018

$M'_{\delta_s} = -0.87 \times 10^{-4}$/deg. **

$M'_\alpha = -1.7 \times 10^{-4}$/deg. **

* $M'_\theta = M_\theta / \frac{1}{2}\rho \ell^3 V^2$

** Taken from Ref. 12.

TABLE 5-2b

BUOYANCY EFFECTS

Applied Load		Force Coefficient, Z'_B *		Avg. Vertical
Model lb	Full Scale lb	Model at 15 fps x 10^{-4}	Full Scale at 25 knots x 10^{-4}	Rate ft/ft
0	0	0	0	- 0.003
+ 0.005	+ 5000	+ 0.6	+ 0.7	- 0.001
+ 0.010	+ 10000	+ 0.11	+ 1.4	+ 0.005
- 0.005	- 5000	- 0.06	- 0.7	+ 0.007
- 0.010	- 10000	- 0.11	- 1.4	+ 0.001
- 0.015	- 15000	- 0.17	- 2.1	+ 0.001

$Z'_\delta = +1.5 \times 10^{-4}$/deg. **

$Z'_\alpha = 42.0 \times 10^{-4}$/deg. **

* $Z'_B = Z_B / \frac{1}{2}\rho \ell V^2$

** Taken from Ref. 12.

Speed, Acceleration and Travel

The model response proved to be insensitive to variations in constant speed and "travel" but very sensitive to acceleration. The behavior of the model under these conditions is illustrated in Fig 5-b where neutral runs with constant velocity are compared to those with acceleration and different travel. Variations of these parameters arise from different launching conditions and performance of the model mechanism. Longitudinal acceleration has a marked effect upon the trajectory response of the model (see test run No. S-375). The nosing down for positive acceleration--a characteristic model response often observed in the launching tank-- is attributed to the increased flow from the propeller over the stern planes which are normally at 1.3 degree for dive. Conversely, negative acceleration has been observed to cause a nosing up response. Different constant velocity has no detectable effect upon the response as indicated by test run No. S-71 and 83. Also run No. S-375 shows no additional effects once constant velocity is attained, since a constant inclination and straight though inclined path results.

Variation of travel--the advance of the model per revolution of the propeller-- has no measurable effect upon the trajectory response for a neutral run at constant velocity as a comparison of runs in Fig. 5-6b illustrates. The divergence of the cam light positions indicates a different propeller speed, slip and subsequent travel for the same velocity response. While a variation in propeller slip and model travel is of little importance for neutral runs, the effect is of considerable concern when a program cam is used. The cam light location represents a given position on the program cam which advances at a fixed rate per propeller revolution. A change in travel (or propeller slip) at a constant velocity then causes an altered control program based on number of ship lengths traveled.

Alignment of Planes and Hull

While the requirements for test conditions relating to static trim, buoyancy and velocity are seen not to be critical, those concerning hydrodynamic forces and moments such as control surface and hull alignment proved to be severe. Figure 5-7 illustrates the limits of accuracy and consistecy allowable for setting and maintaining neutral control surface angles. The range of neutral angles shown is within the practical limits of accuracy

for the model linkage system (± 0.1 degree) and the agreement of the trajectories indicates this to be sufficient. Greater variation of neutral axes show a marked divergence of the trajectories.

The axial alignment of the hull is much more critical, as shown by Fig. 5-8. Test run S-321 was found to have an 0.1 degree misalignment between the forward and aft hull sections (see Fig. 2-14 for alignment technique) which required an 0.3 degree change in stern plane neutral angle to maintain straight flight. The curves shown for runs S-252 and S-253 illustrate the effect upon the trajectory response for a similar hull misalighment without changing the stern planes.

The ultimate accuracy of the control surface settings depended to a great extent upon the rigidity of the control system support, hull and appendages. The supports were made sufficiently rigid, as shown in Figs. 2-15 and 2-19, and the hull is inherently rigid due to its double convex curvature. However, the rigidity of the appendages presented a critical problem in achieving the necessary control accuracy and consistency. The thin-walled electro-formed horizontal and vertical stabilizer fins first used were sufficiently flexible to cause the noticeable difference in directional response of the model shown in Fig. 5-9. For a similar range of neutral angles (the shift in value is most likely due to hull alignment differences) the divergence of trajectories is very much greater than obtained with the machined fins as shown in Fig. 5-7. How much distortion is due to hydrodynamic forces or linkage spring load (used to overcome pivot friction and to take up slack) is not known, but the importance of rigid appendages is clearly shown. It is doubtful if effects of this sort would appear in the full scale submarine since the large size should permit adequate rigidity to be built in and the control surface actuating system would not exert forces of similar relative magnitude and distribution.

Normal wear and tear due to launching and handling of the model resulted in distortions and roughness of the hull on the order of ± 0.010 inch, usually of an axially symmetrical nature. Soldering of the deck, hull joint bridge fairwater and sealing of leaks with wax also contributed to roughness of the same order. In spite of these relatively large (but symmetrical) changes, no effects could be detected or measured. However, during preliminary test runs the addition of tape crosses (0.010 in. thick) to the

starboard side of the hull caused a definite turn to starboard, requiring additional rudder deflection to maintain a straight trajectory. Apparently this amount of roughness and longitudinal distribution was sufficient to disturb the flow outside the boundary layer, whereas the hull roughness (aft of the maximum section) was completely immersed in the boundary layer.

Effect of Yaw and Roll

Although the motion of the model was restricted to the vertical plane by proper neutral settings of the rudder and dorsal rudder, some slight amount of deviation was noted during the maneuvering tests. Figure 5-10 shows a comparison of neutral runs where the roll angle and the azimuth angle varied independently. The effect upon response in the vertical plane is seen to be within the normal scatter of successive trajectories. Deviations from the vertical plane were usually less than shown here.

This discussion has gone into considerable detail about some of the experimental aspects of the model test program for several reasons:

(1) To establish the reliability and consistency of the model performance;

(2) To establish experimental operating limits and indicate possible effects upon model behavior;

(3) To show the extreme accuracy required for consistent and reliable operation for small scale models;

(4) To show some interesting characteristics of behavior of the model and possibly of the full scale submarine.

After some experience with the Odax model, where one was never quite confident of its behavior from run to run, it is difficult not to praise the Albacore model performance. The consistency of trajectory response and the excellent directional stability bear evidence of the much better hydrodynamic design of the U.S.S. Albacore.

Phase 2: - Control Response - Original Configuration

Phases 2, 3 and 4 of the model test program were designed to explore the control response and maneuverability of the model with the original control surface configuration. In Phase 2, the full range of control available with the stern planes (18^{o} dive to 18^{o} climb) was investigated for entering

a turn in the vertical plane, the purpose being to determine final turning rates, angle of attack and transient behavior as a function of stern plane throw angle. This phase was divided into three portions, and is presented here in chronological order.

Neutral Family

The response of the model for changes in neutral angle of the stern planes is shown in Fig. 5-11a. The trajectories have been rotated to account for initial conditions of angular velocity but no adjustment of relative trajectory position was made since only final (equilibrium) conditions are of interest. The relative scatter to be expected for each curve has been shown in Figs. 5-3 and 5-4. The trajectories show an orderly divergence with change of stern plane angle within the ± 0.1 degree setting accuracy. The final curvature (see Fig. 5-11b) appears to be a linear function of stern plane angle over only a small range (from $+1^{\circ}$ to $+2^{\circ}$) with an average slope of 7.5×10^{-5} rad/ft/deg. denoted by the solid line. The intercept of this line verifies the value of the neutral angle determined previously from the trajectories (namely, $\pm 1.3^{\circ}$ for dive) and agrees well with predicted values given in Ref. 12. Whether this exact angle will be required for full-scale operation at 25 knots is subject to question because of several factors. First, the model speed is not scaled (it actually represents Froude-scaled 95 knots full-scale speed). Secondly, the flow in the vicinity of the stern planes may be somewhat different for very small angles because of the wake from the stabilizer fins. Thirdly, cross steering from the rudders may have been present. For these test runs, the torque reaction from the single propeller was accounted for by offsetting the rudders by two degrees each. The dorsal rudder was built into the bridge fairwater during this period of the test program and, therefore, could not be used to balance propeller torque. However, it is felt that small shifts of the neutral angle will not affect the response of the ship to large deflections from any such neutral angle.

Dive Family

The response of the model for entering a turn in the vertical plane with dive stern plane angles is shown in Fig. 5-12. The control program used was as follows: After a short neutral run (2 to 3 ship lengths) the stern planes were moved to the required dive angle at a constant rate

and held for the duration of the run. The range of stern plane deflection angles was nominally from 3 degrees to 18 degrees by 3-degree intervals at the 5-deg/sec prototype throw rate and an 18-degree throw at 10 deg/sec. The model had a metacentric height of 0.081 inch and a radius of gyration of 5.47 inches (0.68 feet and 45.6 feet, respectively, full scale). Bow planes were rigged out at zero degrees while the rudders were set + 2.2 degrees top and − 2.0 degrees bottom to account for propelier torque reaction. The curves shown here are selected from three test runs for each stern plane throw angle within the limits of initial conditions already discussed. About 400 feet of neutral run immediately prior to the stern plane action is included for comparison of the initial conditions.

This family of curves indicates a quick and positive response of the ship for intentional control surface deflections, particularly in inclination response. The depth response is much slower, however, which may be considered as indicative of large dynamic stability since an appreciable angle of attack is required to alter the trajectory. Steady turning, indicated when the inclination curves become straight lines, is reached quickly and smoothly. Some evidence of "hunting", i.e., oscillations of inclination about the curves shown on the order of $\pm 1/2$ degree, was noticed, although no consistent pattern could be determined and the amplitude was not much larger than the maximum limits of accuracy. It will be noted that at the higher plane angles additional increments of stern plane deflection have a smaller effect upon the final curvatures and trajectories of the model. The final portions of the trajectories exhibit an orderly progression and diminishing effectiveness of the stern planes with increasing angles, as do also the arrangement of the difference curves. The initial stages of turning, however, show a less orderly arrangement principally due to different initial conditions in angular velocity. (See Fig. 5-2 again for the effects of large initial angular velocity.) The differences in the curvature histories immediately after start of action illustrates this effect. The variation in linear velocity (V) curves are shown as percentages of the "approach" velocity (V_o) since the model velocity was not scaled. The reductions in velocity give an indication of the increased model drag during turning. The propeller speed (as determined by time between cam lights) remained essentially constant throughout each test run, although absolute velocity and

propeller speed varied from run to run. The time or distance required to reach steady turning is somewhat ambiguous since the angular velocity approaches its final value in an asymptotic manner and is further confused by the scatter and oscillations of the data. However, the general trend indicates that a minimum time is being approached with increasing stern plane angles. No cross steering effects between stern planes and rudder were noticeable or measurable beyond normal deviations in the lateral direction due to launching conditions. It is felt and, indeed, was observed in later model tests that some cross steering may be expected with the full scale ship where torque reaction of the propeller is accounted for by the dorsal rudder rather than by offsetting the top and bottom rudder planes as was done here. The appreciable deceleration shown and constant propeller speed would result in greater torque reaction than increased flow over the dorsal rudder while turning could overcome.

The small differences in stern plane throw rates (from 4.9 to 5.4 deg/sec) shown have very little effect upon the subsequent response. Even doubling the throw rate has relatively little effect upon the behavior as illustrated in Fig. 5-12c where two series of test runswith nominal 18 degrees stern plane deflection for 5 deg/sec and 10 deg/sec throw rates are compared. As would be expected, the final curvature is unaffected while the time required to reach steady turning is reduced. However, the gain is rather small. For instance, a 30-degree inclination is reached 55 feet (1.3 seconds) faster with a 10 deg/sec rate while distance traveled to reach 100 feet depth is reduced by 52 feet (1.2 seconds). This represents a gain of about 10 per cent in distance (and time) for the points given for a 100 per cent increase in throw rate. Whether such a gain would be of sufficient advantage in tactical maneuvers of the prototype to warrant increasing the plane rate cannot, of course, be evaluated here. However, because of the small difference shown, all of the remaining test runs were conducted using a 5 deg/sec rate.

Climb Family

The behavior of the model for entering a turn with climb stern plane angles under the same test conditions as for the dive family, is shown in Figs. 5-13a and 5-13b. The direction of stern plane movement was, of course, reversed.

The behavior of the model exhibits the same general characteristics for climb stern plane angles as it did for dive angles. The inclination response is quick and smooth, depth response lags behind inclination and velocity behavior indicates increasing drag. The orderly progression of trajectory arrangement and final curvatures illustrate the same decreasing effectiveness of the stern planes in producing accelerations with increasing angles. No large difference in initial response of heading after start of control action is immediately apparent, although a slightly faster climb response is noticeable. This effect is attributed to the asymmetry of the model in the vertical plane due to deck and bridge fairwater, which causes an inherent vertical lift and nose-up moment. (The 1.3-degree dive neutral stern plane is necessary in order to counteract this asymmetric force distribution.) It will be noted that the depth change is limited to about 150 feet in climb as compared to 300 feet maximum for the dives. This limitation was imposed to prevent any free surface effects upon the response in climb. The water level in the tank was maintained at least 250 feet (full scale) above the initial depth of the model. For the 18-degree throw angle curve, this places the bow 40 feet below the surface for a 150-foot depth of the center of gravity.

Equilibrium Conditions in Steady Turning

The steady state equilibrium condition in rise and dive are shown in Table 5-3 and in Fig. 14 as a function of the stern plane throw angle. The values of 1/R were determined from the slopes of the inclination curves of Figs. 5-12a and 5-13a, while the speed reduction was determined from the velocity change curves. The values of angle of attack, α, are the final values shown in Figs. 5-12b and 5-13b. These curves of equilibrium conditions show quite clearly the diminishing effectiveness of the stern planes at larger throw angles. An extrapolation of the 1/R curve yields maximum turning rate of 1.53×10^{-3} rad/ft in both rise and dive with a maximum angle of attack of about 9.0 degrees. This would correspond to a turning radius of about 3.3 ship lengths for a 25-degree stern plane throw angle with a final speed of 22 knots. It may be seen from Table 5-3 and Fig. 5-14 that the equilibrium turning in rise very closely matches the final turning in dive, within one percent for throw angles greater than 3 degrees. Even for 3-degree throw angles the response differs by only three percent however. The curvature

function in the region near zero exhibits an interesting nonlinearity which may or may not carry over to full scale. This nonlinearity, although previously reported to be much more pronounced due to an error in computation (Ref. 11), is, perhaps, due to the planes being shrouded in the wake from the stabilizer fins, thus having reduced effectiveness until deflected out of it. If a wake phenomena is involved, it is questionable whether this effect will carry over to full scale since Reynolds number is not scaled. Easier steering in the vertical plane will result, however, if it does because the ship will be less sensitive to small unintentional variations of the planes from the neutral angle. No indication of this behavior has been noted in the force and moment coefficient curves of Refs. 6 and 12. Whether this is an effect too minute to detect with the standard towing tank and water tunnel techniques, or whether it is a scaling effect of such a small-scale free body is not known. Perhaps critical comparisons between these model tests and the full-scale sea trials of the Albacore will throw some light upon this phenomena. The determination of angle of attack in this region is not precise enough for the free-running model data to resolve this question, hence no values are included.

Although an appreciable speed reduction is produced during these maneuvers (a maximum on the order of 10 percent), there is some question as to the magnitudes to be expected in full scale. The model operation, under essentially constant thrust and propeller speed, is based on geometric similarity of the trajectories and, therefore, independent of absolute velocity and time scale. However, geometric similarity for any corresponding portions of the trajectories also exists, and hence one would expect relative velocity to vary similarly, too. On the other hand, drag varies with Reynolds number and different deceleration may result as the ship progresses along the geometrically similar trajectory.

Some Maximum Transient Values

An additional curve which gives a measure of transient conditions is included in Fig. 5-14. The maximum angular acceleration produced, as measured from the slopes of angular velocity of Figs. 5-12b and 5-13b, shows the same general characteristics as final curvature, i.e., a reduced effect at larger stern plane angles. The acceleration response in dive is slightly greater than in rise, which may account for the shorter time

required to reach equilibrium conditions. These maximum angular accelerations are not considered very precise because the values represent averages of second differences of the data. They do show, however, the general trend in the transient behavior of the model.

Phase 3: Dive Incline Family - Original Configuration

The purpose of the third phase of the model test program was to determine the damping characteristics in response to 18-degree dive and return to neutral stern plane actions. The trajectory histories were also desired as a preliminary to Phase 4. The control program for these dive incline type of maneuvers was as follows: After a short neutral run, the stern planes were thrown for 18-degree dive, held for various times from 0.6 sec. to 7.6 sec., returned to neutral and held constant for the remainder of the run. The range of hold times was selected in an attempt to bracket a 30-degree final inclination angle since nothing was known of the damping characteristics of the model. The programs were designed from the response to 18-degrees dive action by assuming a reversible process in moving from 18-degrees dive to 0 degrees and using a sufficiently wide range of "hold" or delay times. The holding time designates the length of time that the planes are maintained at 18-degrees dive.

The behavior of the model for this type of program is shown in Figs. 5-15a through 5-15e. The initial portion of the trajectories, of course, repeats the 18-degree dive trajectory (shown by the dash lines for comparison) until removal of stern planes. No noticeable departure in inclination occurs until almost half of the stern plane deflection is removed and until considerably longer in depth. (The position along the trajectories at start of removal of stern planes is denoted by the small index marks.) The curves for successively larger holding periods "peel off" in an orderly manner clearly illustrated by the angular velocity curves. The damping time is quite lengthy; constant inclination is reached only for the 0.6 second curve for the length of trajectory possible in the tank. The generated angular velocity appears to decay in approximately an exponential manner. Although it is not a "deadbeat" or critically damped motion. Some oscillation is evident, and, even though the data is not sufficiently precise to yield accurate quantitative results, the trend is clearly established. Figure 5-15c illustrates data points for five test runs from which the 0.6 curve in Fig. 5-15b was derived. A measure of the damping may be obtained by

assuming an exponential function and measuring the distance required for a decay to (1/e)x the initial angular velocity. The "decay distance" curve in Fig. 5-15d shows the values obtained based on (1) the maximum angular velocity, and (2) the magnitude at the position the stern plane again reaches neutral (shown by crosses and circles, respectively). A minimum decay distance of 290 feet (1.45 ship lengths) is indicated. This corresponds to an exponent of $p = -0.69$ for a decay function of the form $\theta = \theta_o e^{-ps}$ where s is distance in ship lengths. This is admittedly a crude analysis and approximation but it does give a graphic picture of the damping characteristics of the submarine. More detailed analysis with much more precise data would, perhaps, yield a better measure of the damping function.

Because of this type of damping behavior, the control program used here is not well suited for attaining straight inclined trajectories in a reasonable length of travel or time. The 0.6 second curve requires almost 1200 feet after stern plane reversal to damp out to an inclination of 22.3 degrees, while it is estimated that the 7.2 sec. curve would require about 1300 feet to attain 55 degrees. Some estimated final values of inclination and damping distance are given in Fig. 5-15d as determined from the curve shown in Part e.

These curves are constructed by a simple graphical subtraction of each incline curve from the 18-degree dive curve of Fig. 5-15a and b.. The zero position of each difference curve was taken at the corresponding plane-removal index and shifted to a common zero for comparison. These curves then represent the departure or deviation of the incline trajectories from the dive trajectory for variation of holding time at 18-degree dive. These curves indicate the effect of initial angular acceleration upon the damping, for it will be noted that a common curve is approached with decreasing acceleration. The final inclination plot of Fig. 5-15d shows the same effect as it approaches a constant slope, as does the distance from zero, while the distance from reverse approaches a constant value of about 1300 feet.

This relatively long damping distance clearly shows the need for additional control for attaining a straight inclined path in a reasonably short time without exceeding inclination limits. It appears a "checking" rise angle of 18 degrees on the stern planes would easily reduce the angular velocity quickly enough to achieve inclined paths of 20 degrees or more. However, an 18-degree throw angle appears too severe for trajectory angles

smaller than 20 degrees since the time the planes are moving at a 5-deg/sec rate is relatively long and would necessitate reversing the planes before reaching 18 degrees dive. A higher rate of throw would be desirable in this case to reduce the plane deflection period and also to provide a more precise control program. The program would also be less sensitive to small variations of execution times.

Phase 4: Depth Changing Maneuvers - Original Configuration

The fourth phase of the model test program was concerned with determining an optimum depth changing maneuver and the corresponding stern plane program required to accomplish it. This maneuver has been aptly described elsewhere (Ref. 2) as a "limit" maneuver, i.e., one for which the maneuver is completed in a minimum time while pushing the maneuverability of the submarine to the maximum allowable limits of several operating conditions. The tests described herein were circumscribed by five limits, one of which proved to be unnecessary, however. They are:

(1) Depth change - 300 ft $\pm$ 10 ft
(2) Maximum inclination - $30^{\circ} \pm 1/2^{\circ}$
(3) Stern plane angle - $18^{\circ} \pm 0.1^{\circ}$ maximum
(4) Stern plane rate - 5 deg/sec $\pm$ 1/2 deg/sec
(5) Final inclination - $0^{\circ} \pm 2^{\circ}$.

Conditions (1) and (2) were prescribed by the contractor, while condition (3) was a limitation imposed by the model linkage and condition (4) resulted from the plane rate tests of Phase 2. Condition (5) in conjunction with the tolerance of (1) was settled upon as being within an easily controllable range by manual operation. Normal variations in operating conditions of the full scale, such as ballast changes, water temperature variations, static trim, etc., were neglected because of the high model speed for the reasons discussed under Phase 1.

The test technique was literally one of "cut and try" on the basis of the trajectory response for the previous control program. The control program was purposely limited to a single dive and hold, reversal to climb, hold and return to neutral in order to provide a precise, repeatable and easily executed control action. The initial estimate of the required program was synthesized from the dive, rise and incline maneuvers of Phases 2 and

3 by the technique illustrated in Fig. 5-16. The procedure consists of a simple graphical addition and subtraction with an appropriate shift of the zero index of the trajectories as shown. The inclination history was used as the primary index because it is more sensitive to control changes than the depth response. The process reduced to one of repeated plotting until first the maximum inclination condition was satisfied and then the depth change condition was met. Since nothing was known of the response for a full reversal of the stern planes from 18-degrees dive to 18-degrees rise, subsequent corrections were made from the response to this first trial by varying the holding times at dive and rise angles. Another factor not possible to evaluate was the variation in "travel" due to increase of drag during the maneuver.

In spite of these unknown quantities, the response of the model to the initial estimate of the stern plane program is in surprisingly close agreement with the synthesized trajectory as shown in Figure 5-17a by Curve No.1. The maximum inclination falls short by 5 degrees while the depth change is only 250 feet. This apparent increase in recovery over the sum of removal of dive and addition of rise angle response may perhaps be explained by the change in flow over the planes during the reversal. While turning at the maximum rate in dive, the local angle of attack of the stern plane itself is reduced by slightly more than the angle of attack of the hull (to about 10^{o}). When the stern plane is reversed to 18 degrees rise, its angle of attack is increased by the hull attack (to about 28 degrees assuming instantaneous plane deflections) giving rise to a much larger moment than for initially straight path for which the rise trajectory was determined. This condition exists only temporarily (until the angle of attack passes through zero) and does not accumulate to more than the 5-degree and 50-foot difference noted for this particular trajectory.

Two other successive trials are shown on Fig. 5-17 which approach fairly close to the desired depth change maneuver. Both trajectories were derived from the same program cam and illustrate the effect of travel variation upon the response of the model. Travel was one variable that could not be controlled precisely due to launching velocity variations and propeller condition. Provided that the initial velocity during the neutral portion of the trajectory was essentially constant, the trajectories are still valid although the resultant control program is different. In essence then, we have several

control programs with slight variations of holding times (small changes of throw rates are also included but have quite small effects) which give a measure of over- or under- shooting of the desired conditions for "errors" of execution. It is immediately apparent that small differences in the first portions of the trajectory have a profound effect upon the subsequent trajectory. However, no unstable divergence occurs, such as was observed for the Odax model during some zig-zag maneuvers in which it failed to recover from the dive with full reverse on the stern planes.

Only two depth-changing control programs were run before Phase 4 was terminated in order to change over the model to the "revised" control surfaces. Although the optimum maneuver was not obtained, the main features were approached rather closely. The complete control program requires only 30 seconds from start of action until planes return to neutral. In this time the trajectory has completed the major portion of the maneuver although beyond the tolerances of final depth and inclination desired. By way of comparison, the 18-degree dive alone requires about 22 seconds to reach 300 feet (with 63 degrees inclination and 0.0063 rad/sec angular velocity, in addition).

The trajectories of Fig. 5-17a indicate that the limiting condition (2) of 30-degree maximum inclination is an unnecessary restriction for an optimum 300-foot depth change maneuver with 18-degree stern plane angles. For with the control program used, the inclination cannot reach 30 degrees without exceeding the 300-foot depth change. The short time of the maneuver (30 sec. or 6.5 ship lengths) makes exact execution of the program imperative and reduces drastically the ability to anticipate required corrective measures. In fact, the anticipation requirements in this case approach the realm of "pre-science" wherein recovery action is necessary before the maneuver is one-third completed. Hence before one becomes aware of an error in depth, it is already too late to prevent overshooting. (The depth change is only 20 feet when recovery action is required.)

Figure 5-17c suggests a method of predicting the "execute" angles for a given depth change. The "execute" angle is defined here as the inclination angle at which a change in control action is initiated. For example, the first execute angle, θ_{e1}, (denoted by the index mark on the inclination history curve) is the inclination angle for which the stern planes are reversed from the 18-degree dive position. Since the maximum inclination angle restriction

is unnecessary, attention may be focused primarily on depth change and on final inclination secondarily. With only minor differences due to final execute angles, the depth is a function of the first execute angle. Thus one may select the desired depth change and read the execute angle directly. The final execute angle appears to be almost constant at about 13.5 degrees and should bring the maneuver sufficiently close to final depth for normal steering control. This method would require additional mapping in order to be completely reliable and accurate. However, the technique appears to hold promise. Application to an optimum 300-foot depth change maneuver indicates the following sequence of orders:

Execute Angle, θ_e deg.	Command	Approx. Time sec.	Approx. Dist. ft.
0	18° dive	0	0
15.4	18° rise	8.3	350
13.5	neutral	24.0	940
-1.0	steer *	-	-

* Helmsman begins required control to level off.

Further refinements with this simple type of control program could be made to obtain a true optimum maneuver, but the value of the gain is questionable. The major portion of the trajectory is rather well defined, while the final portion is subject to only minor improvement unless recourse to a more complex program is made. It appears that the inclusion of an additional reversal of, perhaps, 5 degrees dive and immediate return to neutral would suffice to elininate the residual angular velocity and bring the final inclination to within the desired limits.

Trajectory Elements

Another technique of optimum maneuver prediction has been developed in the process of synthesizing and correcting the depth changing control programs. The method is an extension of the graphical technique described in Fig. 5-16 using trajectory "elements" from all phases thus far tested. A trajectory "element", is defined, in this case, as the change or difference in response due to imposing a control action upon the existing

program. Thus the depth change maneuver consists of three elements; (1) a dive, (2) a reversal, and (3) a neutralizing action. Figure 5-18a gives the plots for each type element for the original configuration as determined from trajectories of Phases 2 and 3. The construction of a given trajectory prediction is a trial and error procedure which will have, of course, somewhat less accuracy than the element curves. The final conditions are not clearly defined by the experimental trajectories, so that any predicted trajectory will also be somewhat ambiguous although within control of the helmsman. Figure 5-18b illustrates the construction technique for the prediction of the optimum 300-foot depth change maneuver. At (1) the dive element is traced as shown. Beginning at (2), the reversal element is added to the dive trajectory resulting in curve (b), then at (3) the neutralizing element is added to curve (b), completing the trajectory at (4). The indices (2) and (3) are adjusted during construction until the desired depth and final inclination are achieved.

The method has one major limitation, however, which restricts its use to maneuvers involving depth changes of 200 feet or less. Each element was derived from portions of the trajectories with essentially state turning, for which the effect of initial angular accelerations cannot be assessed.

The accumulative effects are, however, indicated in Fig. 5-15e. Rather extensive experimental mapping would be necessary to enable prediction of a wide range of maneuvers reliably. The termination of Phase 3 with the "original" configuration in favor of more urgent work for the "revised" configuration prevented further investigation along this line.

Phase 6: Control Response - Revised Configuration

Part 2 of the model test program was concerned with the dynamic response of the model with the "revised" control surfaces. The test program for Phase 6 was not as extensive in the basic trajectory responses as for Part 1. This portion was restricted to a few comparisons with the response for the original controls and an exploration of the behavior of the model in the region near zero curvature for small control surface deflections. A rather complete investigation of depth changing maneuvers for several parameters was carried out in Phase 7.

Small Stern Plane Deflections

The response of the model to the stern plane throw angles in the range of ± 3 degrees is shown in Fig. 5-19. The purpose of these tests was to clarify the final curvature function near zero in the region of nonlinearity exhibited for the original configuration. Some question of the validity and magnitude of such nonlinearity existed for the original configuration since the values were determined with a limited range of neutral angle settings. The trajectories show a regular divergence with increasing throw angles typical of the control characteristics observed in Phase 2. The final turning rate as a function of stern plane throw angle, as shown in Fig. 5-19c, exhibits the same nonlinear behavior as did the original configuration but in a more definite manner. The response shows a linear range from about -2.7 degree (rise) to $+0.5$ degree with a slope of 1.05×10^{-4} rad/ft/deg. Above $+1.5$ degrees the slope becomes 1.94×10^{-4} rad/ft/deg., an almost two-fold increase. Since the neutral angle is $+1.3$ degrees, the amidship position of the stern planes falls in the middle of this linear range, as shown by the dashed line. This gives credence to the theory of a wake phenomenon discussed for the original configurations. One would expect the wake to be essentially symmetrical about the horizontal centerline (amidship position) with equal deflection of the planes to either side necessary to penetrate the wake. The question of whether this behavior will carry over to full-scale operation still remains. Also, an effect of this sort may be difficult to detect and assess in full scale or, perhaps, may be masked out by other effects such as sea currents, minor variations of control angles, etc. The angel of attack exhibits the same general characteristics but with less accuracy.

This nonlinear behavior for small plane angles raises interesting questions concerning coefficient measurements for this region. Is this nonlinearity actually present in the coefficient functions? If so, is it detectable and measurable or is it masked out by inherent inaccuracies and scatter of the data? A close examination of the moment coefficient data of Ref. 12, Fig. 13, for control arrangement "B" (which closely approximates the CIT model stern planes and stabilizers) reveals some indication of nonlinear variation. Whether the deviations are significant depends upon the accuracy and reliability of the data which cannot be assessed here. Since insufficient data points in the ± 3 degrees plane throw range exist to clearly define the coefficient function, further investigation of this region appears desirable to

clarify the behavior for small stern plane throw angles.

Rudder and Bow Plane Response

The behavior of the model for small deflections of the rudders and bow planes is shown in Figs. 5-20a and 520-b. These tests were made for various neutral settings (since no linkage was available for program control) over a limited range of angles (± 3 degrees for bow planes and 0 to + 1 degree for rudder). The stern planes were maintained at the normal neutral angle of +1.3 degrees dive. The accuracy of adjustment of the bow planes and rudder was ± 0.2 degree as compared to the usual ± 0.1 degreefor the stern planes. The two upper curves of Fig. 5-20a are for the bow plane response only, while the two lower curves are for rudder response.

These trajectories show a different initial response for bow plane than for stern plane angles in that inclination angular velocity is developed almost immediately. No particular significance can be attached to this, however, since the bow planes begin exerting lift during acceleration in the launcher and cause an angular acceleration before the model tail clears the guide rails. It would be necessary to provide bow plane control linkage to determine such effects, plus considerably more testing. The final turning rate as a function of bow plane angle appears to be nonlinear although not well defined, as shown in Fig. 5-20b. The bow plane effectiveness in dive is about one-half that in rise. This may possibly be attributable to the plane position (see Fig. 2-11) which has a smaller local angle of attack in dive than in rise. Another explanation may be found in a greater interference of the hull on the flow over the bow planes in dive than in rise. Reference 12 gives some support to this nonlinear response where Fig. 20 (with plane position corresponding to the "revised" configuration) shows smaller bow plane effectiveness in dive. On the other hand, Fig. 19 indicates just the reverse for bow planes corresponding to the original configuration. No equivalent comparison was made with the model using the original configuration and more precise and detailed tests would be necessary to clearly define the behavior in this region. The over-all bow plane effectiveness is approximately one-half that of the stern planes in rise, while about one-fifth in dive.

The response of the model to rudder angles indicates a much greater rudder effectiveness than stern plane effectiveness, as shown by

Figs. 5-20a and 5-20b. Although the data is less precise and reliable in the horizontal plane, the general response is fairly well determined and appears to be linear in the range tested. The lateral displacement curves are compared arbitrarily to the neutral run rather than rotated to a straight zero path, because the lateral play of the model in the launcher was not controlled sufficiently and mismatch of projector focus and magnification was not corrected. Some cross steering between rudders and stern planes is present and large roll change was observed. Since roll affects this behavior, modeling of metacentric moment is required and, therefore, these model tests would correspond to prototype behavior at about 90 knots. The response is still useful in indicating the rudder effectiveness compared to stern planes. No tests were made with the original configuration for comparison to these results.

Comparison of Response

Comparisons of the response of the model for the original and revised control configurations is shown in Fig. 5-21 for an 18-degree dive trajectory and in Fig. 5-22 for an 18-degree incline maneuver. The curves represent averaged points of the test runs listed.

The curves show essentially the same response in dive, although the revised configuration had a 0.3-degree larger stern plane throw angle. The same program cam was used for both series of runs, but the linkage ratio of cam elevation to stern plane angle was slightly greater for the revised controls resulting in the larger throw angle. The turning rate at 18 degrees for the revised controls thus appears slightly smaller than for the original configuration. Reference 11 originally reported a 25-foot lag in the response of the revised configuration, which proved to be a delay error in the cam lights as discussed in Phase 2 for dives. These curves show a response more consistent with the small differences between the original and revised control areas and arrangement. (See Table 2-1)

Figure 5-22 shows the same relative comparison in response for a dive incline program. An exact comparison was not possible, however, due to the slight difference in throw angle and model travel resulting in a changed program. The solid line represents a second curve for the original configuration for a relative comparison. Trajectories indicate the same smaller stern plane effectiveness noted for the dive comparison which appears

to mask out differences in damping characteristics. The angular velocity curve shows a similar decay with distance consistent with the difference of maximum angular velocity. The shapes of the inclination and angular velocity curves after return to neutral of the stern planes, being quite similar, would indicate little difference in view of the small changes in control configuration. Additional tests would be necessary (with identical control programs) in order to resolve the damping characteristics or the effects of changes in individual appendages.

Phase 7: Depth Changing Maneuvers - Revised Configuration

Phase 7 is divided into three sections dealing with different approaches to a 300-foot depth changing maneuver. Section (1) is concerned with determining the required control program for 18-degree throw angles with a 30-degree maximum inclination limit, while Section (2) deals with 12-degree throw angles and a 15-degree maximum inclination. Section (3) is concerned with a comparison computed and experimental depth changing trajectories and an indication of the effects of metacentric moment on maneuvers in the vertical plane for high model speeds.

Section (1) - 30-Degree Maximum Inclination

The purpose, scope and techniques used for the tests of this section are identical with those discussed in Phase 4. The two program cams of Phase 4 were rerun with the revised control surfaces for a comparison of response in addition to that obtained for the 18-degree dive and dive incline comparisons. Figure 5-23a shows a comparison of the response of the original and revised control surfaces for program cam No. 1. The programs could not be duplicated exactly because of slight differences in travel and throw angles, and these two test runs represent the best match obtained. The initial diving and recovery portions agree closely although the revised configuration requires a slightly larger (18.9^{o}) dive angle than the original (18.5^{o}) as was shown in Fig. 5-21. The recovery or leveling-out portion exhibits a greater difference than would be expected, however. The larger rise throw angle and longer holding time of the original configuration account for the increasing divergence of the trajectories.

Additional trajectory histories for program cams 1 and 2 are shown in Figs. 5-23b and 5-23c. The same general characteristics as

noted for the response of the original configuration to " "simple" program are evident. Although the required depth change is very closely approached by Cam No. 1a, an excessive final angular velocity is present. An additional reversal of the stern planes appears necessary to improve the final conditions. Here, too, as was seen in Phase 4, the limiting maximum inclination angle is not reached without exceeding the 300-foot depth change.

Successive attempts to "refine" the maneuver, that is, to more closely approach the optimum trajectory within the set limits, are shown in Figs. 64 and 65. The refinements include (1) an additional reversal of the stern planes to some nominal dive angles in order to accomplish a faster recovery and leveling off at the desired depth, (2) variation of holding times at dive and rise angles, and (3) adjustment of the throw angles in rise and dive to 18.0 degrees to account for linkage changes. Figure 5-24 compared to Fig. 5-23 shows the effect of the additional reversal or checking angle (7.2^{o}) in reducing the final angular velocity, while Fig. 5-25 shows the effect of a larger kick (10.5^{o}). The throw angles varied somewhat due to the linkage ratio changes and errors of elevation in the cams. The trajectories are still useful, however, in showing the influence of small variations (from 17.7^{o} to 18.8^{o}) of throw angles upon the response. The principal effect of the added reversal is to allow buildup of a larger maximum inclination angle and a closer approach to the desired depth before final recovery. It is apparent, still, that the initial "execute" angle is the primary parameter of the maneuver, while the second execute index affects only the final attitude.

The duration of the maneuver, although somewhat ambiguous, is roughly equivalent to the duration of the stern plane program. The final estimate of the optimum maneuver (Cam No. 6) achieves a maximum depth change of 292 feet in approximately 31 seconds, while the control action requires 34 seconds of which 4 seconds is expended for the final checking action. Additional checking control to correct the 0.4-degree per second nose-up angular velocity and 3.7-degrees nose-up inclination is necessary. While these terminal conditions represent a relaxation of the original limits ($\pm 2^{o}$), it appears that the submarine may be easily adjusted to a level path with little change in depth. It is felt that this curve (Cam No. 6) represents as close an approach to the optimum maneuver as is practical with the model, since improvement of the final conditions by variation of the final checking angle would have negligible effect on the over-all character of the maneuver.

Anticipation Requirements. Figure 5-26 illustrates the dependence of the maneuver upon the initial "execute" angle (the inclination angle for which a change of control action is begun) for the revised controls. The maximum inclination shows a definite relation to the first execute angle and to the dive throw angle parameter. The maximum (or final) depth is less definite, however, being influenced by the reversal and checking throw angles indicated. The effect of the checking angle is indicated by the differences in slope of the depth versus execute angle curves for each cam. The plot of depth at the first execute angle illustrates again the necessity of a preknowledge of the complete maneuver, since recovery control must be initiated before the depth has changed by 5 per cent of the maximum depth change.

Figure 5-26b shows a correlation of the response to the several control programs based on the relative throw angles. The values are "corrected" to a standard of 18 degrees throw angles as indicated on the figure. The maximum inclination angle shows good agreement when compared on the basis of the dive throw angle only. The scatter shown (within 1.0 degree) is probably the cumulative effect of the variation in stern plane throw rates, since maximum inclination is attained slightly before full stern plane reversal is reached. The correlation of depth at the second execute angle indicates a dependency upon throw angles, holding times and throw rates, while the comparison for maximum depth shows the effect of the final checking action. The depth difference curve ($D_m - D_{\theta 2}$) indicates, on the other hand, that the second execute angle is the more important parameter since no difference exists for cams 1 and 2 which have no checking action.

Application of these anticipation requirements for the revised configuration indicates a control program for the 300-foot depth change as shown in the following table:

Inclination Angle deg.	Command	Approx. Time sec.	Approx. Dist. ft.
0	18^{o} dive	0	0
15.2	18^{o} rise	6.8	395
9.0	10^{o} check	24.8	1050
0	steer	33.0	1385

Trajectory Elements. Figure 5-27 gives the trajectory elements for the revised configuration for the 300-foot depth change maneuver with 18-degree stern plane throw angles. The spread of the curves indicates the effect of the small variation in throw angles upon the response. The dashed curves represent the response corrected to 18-degree stern plane throw angles. The checking response curves are uncorrected, however, since no standard angle was decided upon. The technique of construction and use is as discussed in Phase 4 for the original configuration. Figure 5-27b shows several trajectories constructed from these elements for 200, 300 and 400-foot depth changes with no limiting maximum inclination prescribed. The dashed curves indicate the extension of successive element combinations. It is felt that trajectories may be predicted in this manner within a 10 per cent tolerance of depth such that final conditions are easily controlable by ordinary steering. This tolerance is necessary because these elements are determined from transient portions of the trajectories. A series of model test runs to map out such elements for a given stern plane throw angle might consist of the following maneuvering sequences:

1. Dive - throw stern plane for dive and hold.
2. Reversal - Dive, hold for various times and reverse to rise and hold.
3. Check - Rise throw plus reversal to dive, hold for various times and return to neutral.

Such a program would, of necessity, be quite extensive in order to evaluate all variables involved, but a few selected maneuvers should allow reasonable predictions by interpolation.

Section (2) - 15-Degree Maximum Inclination

The depth-changing maneuvers described in Section 1 were seen to be quite rapid, perhaps too rapid a maneuver to be attempted in full scale until considerable experience in handling the U.S.S. Albacore had been acquired. At the suggestion of the Bureau of Ships, a more "gentle" maneuver (15 degrees maximum inclination) for the 300-foot depth change was investigated.

It was found necessary to limit the plane throw to 12 degrees in order not to exceed the 15 degrees maximum inclination during the first stern plane movement. A similar, although more complex control program than for the 30-degree maximum inclination maneuver evolved in order to maintain a straight inclined path. As shown in Fig. 5-28, the required control program was as follows: after a short level run the stern planes were thrown for 12 degrees dive, held a short time, reversed to 12 degrees climb and almost immediately returned to neutral, held, then thrown to 12 degrees climb and later returned to neutral. Cam No. 1 was synthesized from 12-degrees dive and rise maneuvers only for the original configuration, while succeeding alterations were based on the response to Cam No. 1.

The response to three of the program estimates made is shown in Figs. 5-28a and 5-28b. The results of missing Cam No. 2 were uncertain since stern plane action began while the model was still in the launcher. The difference in the throw angles shown is due to a mistake in the computation of the elevation of Cam No. 1 giving throw angles too large in dive and too small in rise. The trajectory remained useful, however, to show the effect of a small variation (1 degree) of the stern plane angle upon the overall response.

The control program, although more complex, lends itself more readily to prediction than the control program for the 30-degree maximum inclination maneuver because two distinct regimes of the maneuver are present. The first regime is concerned only with attaining the 15-degree straight incline, which, once attained, has no effect upon the final depth. The second regime is concerned only with the checking action from the steady inclined path. The checking control for these tests was constant, i.e., constant hold time at 12 degrees rise. Hence different depths may be obtained by merely varying the holding time at neutral before beginning checking action.

The final conditions are not clearly defined for this maneuver since the length of run possible in the tank was not sufficient to provide such data. However, the over-all character of the maneuver is well described for depth change and inclination response. The response in inclination resulting from the first reversal of stern planes and subsequent return to neutral exhibits an interesting behavior. This "impulse" causes a highly damped oscillation in inclination as indicated by the angular velocity curve and to a smaller degree by the angle of attack and rate of depth charge curves. This behavior was noticed (although less pronounced) for the original configuration during "incline" maneuvers. As a result of this oscillation the inclined path is not quite straight, which makes extension to greater depth somewhat uncertain. Since so few control program estimates were necessary, insufficient data is available to provide adequate anticipation information for this type of maneuver. Although the 15-degree maximum inclination pullout was intended as a less rapid and more "gentle" maneuver than the 30-degree maximum inclination pullout, a comparison of elapsed times indicates that it is still fairly rapid. The 12-degree cam program requires 39 seconds to complete, while the maneuver is completed in 43 to 45 seconds as against 34 seconds and 31 seconds, respectively, for the 18-degree cam program. It is, of course, unquestionably more gentle since only one-half of the inclination and smaller angular accelerations are attained during the maneuver.

Section (3) - Comparison of Computed and Experimental Trajectories

The model tests thus far discussed were made with the assumption that metacentric moment has no effect on vertical maneuvers at high prototype speed. Therefore, model speed need not be scaled, and the arbitrary value of 16 fps was selected for convenience and to avoid complications that may arise from Reynolds number effects. If metacentric moment is significant, then model speed should be 4.2 fps to represent 25 knots full scale speed.

It was desired, nevertheless, to make some tests which may indicate the effect of metacentric moment on vertical maneuvers (if such an effect does exist) and to compare experimental model trajectories with those computed from theory. Several alternate ways of achieving this comparison suggest themselves:

1. Reduce model speed to 4.2 fps to model true full-scale conditions of metacentric height, z_B = 0.8 ft., and a velocity of 25 knots.

2. Increase the model's metacentric height by the ratio $(\frac{V_m}{4.2})^2$ where V_m is the actual model speed.

3. Run the model at 16 fps with its z_B unaltered, and compare the test results with prototype trajectories computed for either one of the following conditions:

   (a) Correct prototype speed of 25 knots but with a reduced metacentric height of 0.07 ft instead of 0.8 ft.

   (b) Correct metacentric height of 0.8 ft but running at the higher speed of 95 knots.

Alternate (1) would have required a major revision of the model. This was done later for modeling horizontal maneuvers after these tests were made. Alternate (2) is physically impossible to achieve because of the weight distribution required by the construction of the model. A metacentric height of 1.38 inches would be necessary for the 16 fps model speed. This would require that the C.G. be about 0.3 inch above the base line. Alternate (3) was selected and calculations by REAC were made under both conditions listed.

The computed trajectories are based on the hydrodynamic coefficients obtained from towed models at David Taylor Model Basin (Ref. 7) and Experimental Towing Tank (Ref. 6) and computed acceleration components. The metacentric moment effect is represented in the nondimensional equations by the term $\left[(2240\ \Delta\ z_B)/(\frac{1}{2}\rho \ell^3\ U^2)\right]\ \theta$ which includes displacement (Δ), metacentric height (z_B), length (ℓ), velocity (U) and inclination angle (θ). The computations were carried out on the REAC at David Taylor Model Basin in the manner described in Ref. (3). It may be pointed out here that the coefficients were measured for a model with a somewhat different tail assembly than configuration I of the free-running model.

A comparison of model experimental and computed trajectories for condition (a) is shown in Figure 5-29a. The envelope of three model trajectories from Phase 4 of the test program for program cam No. 1, are compared with the computed trajectories for z_B = 0.8 feet with and without "bias" of the stern plane angle and for z_B = 0.07 feet without bias. The

"bias" refers to the initial or neutral stern plane angle which is necessary to maintain the model on a straight, level path. A fourth "computed" curve has been added by applying the effect of the bias on the z_B = 0.8-foot curve to the z_B = 0.07-foot curve. The computed curves with bias show better agreement with the model curves than those without bias. However, such agreement is not consistent throughout the trajectory. The model turns more quickly initially, indicating a smaller metacentric moment but also recovers more quickly, indicating a larger metacentric moment than for the computed trajectories. The experimental scatter in the inclination history is seen to be less than the effect of change in z_B of the computed. This indicates that some other effect than metacentric moment is the cause of the discrepancy. Most likely the model damping is less than that used in the computations, although the manner in which the damping terms were obtained is not known The differences in tail configuration may account for the discrepancy. The coefficients were measured on the tail assembly "B" (Ref. 6) which had a total projected area of stabilizers and stern planes of 299 square feet, whereas the CIT model configuration I area was 334 square feet, for which one would expect greater damping.

A comparison of computed and model trajectories for condition (b) is shown in Fig. 5-29b. Here the model attempted to reproduce the computed control program in order to compare trajectory response. A prescribed control program may be duplicated exactly experimentally only when the "travel" of the model is exactly that for which the program cam was computed. The travel of the model changed sufficiently between computing and testing to give the different control programs shown. Successive test runs will repeat the program and trajectory response consistently and precisely as illustrated in Figs. 5-29c and 5-29d. However, the experimental curves bracket the computed curve and appear to match fairly well when interpolated according to the control programs. Of course, the smaller plane angles and slower plane rates reduce the differences also. It is felt that a more valid determination of the metacentric moment effect would result from comparing a computed trajectory for 95 knots having the same nondimensional cam program as the free-running model. The differences exhibited in Figs. 5-29a and 5-29-b do not appear to warrant consideration of the metacentric moment for these free-running model tests at high model speeds.

Summary and Conclusions

Whereas Chapter 4 has shown that full-scale behavior may be modeled by small, free-running models, the work discussed herein shows, in addition, that the model will yield precise, detailed and reliable information concerning stability, control and maneuverability.

Model Behavior

These tests have shown that consistent and repeatable data will result only if a high degree of precision is maintained in both building and maintaining the model and in making the measurements. It was found that:

1. Control surface positions must be known and controlled to within $\pm$ 0.1 degree.

2, Hull alignment must be maintained within $\pm$0.03 degree.

3. Hull and appendages must be made sufficiently rigid to prevent distortion or bending from either hydrodynamic or control linkage forces.

The model performance and trajectory response at the relatively high model velocity (15-16 fps) proved to be insensitive to:

(a) Small changes of buoyancy ($\pm$0.5%)

(b) Large changes of static longitudinal trim ($\pm 30^{o}$)

(c) Differences of constant velocity (10%)

(d) Variation of propeller slip (12%) providing constant velocity was maintained.

(e) Symmetrical hull surface roughness

but sensitive to:

(a) Longitudinal accelerations

(b) Assymetrical hull surface roughness of e/d = 0.003.

Full Scale Behavior

Prediction of full-scale stability and control characteristics from the model tests indicate that:

1. The vehicle possesses excellent dynamic stability. Small disturbances damp out within two shiplengths as a new straight course is assumed.

2. Providing model behavior carries over, the ship should be easy to steer in the vertical plane. That is, it should be insensitive to small unintentional plane angle deflections.

3. Control response for greater deflections ($\pm 3^{o}$) is quick and positive with a short transient phase. Minimum turning radius is about 3.25 ship lengths at 25 degrees plane angle.

4. The rudders are about twice as effective as the stern planes, while the bow planes are about one-half as effective for steering and turning equilibrium rates.

5. A plane throw rate of 5 deg/sec appears to be adequate. Transient response for a doubled plane rate of 10 deg/sec is reduced by only 10 per cent at 18 degrees plane angle.

6. Angular damping exhibits an approximate exponential decay with a decay distance of about 1.5 ship lengths (7 seconds at 25 knots). A highly damped oscillation was evident.

Comparison of the response for the original and revised control surface configurations showed that:

1. Control response is only slightly better for the original configuration than for the revised at 18 degrees plane angle. (The revised configuration requires 18.4 degrees to attain the same turning rate in dive.)

2. No significant difference in damping is detectable.

Investigation of optimum depth changing maneuvers for both configurations reveals that:

1. Specific maneuvering problems may be solved by means of the model to within narrow prescribed limits by successive approximations.

2. A high degree of prescience is required to operate along an optimum or "limit" trajectory.

3. The ship is at all times controllable, i.e., there is no tendency to "run away" such as was observed for the U.S.S. Odax.

4. With 18-degree plane angles (at 5 deg/sec rate), a 300-foot depth change may be achieved in about 30 seconds (6.5 shiplengths) at 25 knots with a maximum inclination angle of 29.5 degrees. The holding time at the first dive angle exerts predominant influence upon the maneuver.

5. With 12-degree plane angles, a 300-foot depth change requires about 44 seconds (9.3 shiplengths) with a maximum inclination of 15 degrees.

6. Preplanned maneuvers for various depth changes appear desirable for high-speed limit maneuvering.

Comparison of experimental with computed trajectories did not yield information significant enough to separate and evaluate metacentric moment and damping moment effects.

CHAPTER 6

TEST RESULTS AND DISCUSSION U.S.S. ALBACORE MODEL IN HORIZONTAL TURNING MANEUVERS

Purpose

The purpose of Part 3 of the investigation of dynamic control characteristics of submarines by means of free-running models was to determine the horizontal turning characteristics of the U.S.S. Albacore, SST Scheme IV, submarine with the revised configuration of the control surfaces. The characteristics include the equilibrium values as well as transient variations of lateral and vertical displacements, azimuth, inclination and roll (heel) response, velocity reduction, angles of attack and appropriate angular velocities in response to a full range of rudder throw angles. Adequacy of control of depth and roll by means of stern planes and dorsal rudder was investigated and the effects upon turning characteristics determined.

Model Test Program

The scope of the investigation with an outline of the model test program is given in Table 6-1. The study falls into five main categories according to the type of control program used, as listed below:

Phase 1 - Preliminary test runs to determine model sensitivity for velocity, buoyancy and static trim, and response to small control surface angles.

Phase 2 - Horizontal turning while allowing depth change - to determine trajectory response for a wide range of rudder deflections.

Phase 3 - Horizontal turning while maintaining constant depth - to determine the stern plane program required for limiting depth change to within ± 10 feet for a large range of rudder deflections.

Phase 4 - Horizontal turning while controlling roll-investigation of dorsal rudder control to reduce the transient roll response and limit the equilibrium roll angle while allowing depth change (no stern plane control).

Phase 5 - Horizontal turning while controlling roll and depth change - investigation of the stern plane program required to limit depth change to within ± 10 feet while controlling roll.

TABLE 6-1

MODEL TEST PROGRAM - PART 3

HORIZONTAL MANEUVERING WITH C.I.T. MODEL OF U.S.S. ALBACORE, SST SCHEME IV

Phase	Type of Control Program	Control Surface Programs				Characteristics Determined
		Rudder	Stern Plane		Dorsal Rudder	
			Rise	Dive		
1	Neutral	0-1°Stb. 0.5 " 0.5 "	- - -	- 0.3-1.3 -	- - 2.3-4.3 Port	Directional control and model sensitivity to launching conditions and static trim
2	Rudder only	2°Port to 35°Stb.	Neutral	Neutral	Neutral	Turning response allowing depth change
3	Rudder and stern planes	6°-35°Stb.	0.5-9.0	1.0-9.0	Neutral	Turning response for depth control
4	Rudder and dorsal rudder	18°Stb. 35°Stb.	Neutral Neutral	Neutral Neutral	22.5°Port 37.5°Port	Turning response for roll control only
5	Rudder, stern plane and dorsal rudder	18°Stb. 35°Stb.	1.5 3.0	3.0 3.0	22.5°Port 37.5°Port	Turning response for roll and depth control

Presentation of Trajectory Curves

The results are presented principally in three types of curves, expanded to full-scale dimensions, showing the dynamic response of the model to various stimuli. They are:

1. Trajectory Plot - Histories of velocity, azimuth, roll and inclination angles, and lateral and depth displacements of the C.G. as a function of distance along trajectory or horizontal distance for various control programs.

2. Curvature Plots - Histories of angles of attack, angular velocity in azimuth, roll and inclination, and rates of change of lateral distance and of depth versus distance along the trajectory for various control programs.

3. Equilibrium Conditions Plot - Variation of steady-state values of turning rates, angles of attack in vertical and horizontal planes, roll angle and velocity reduction as functions of control surface angles. Some transient conditions may also be shown on these curves.

Additional curves, as needed, are explained in the text. The method of data reduction from the film record to presentation in the above curves is described in Appendix C.

The technique of aligning and rotating individual trajectory plots to a common initial path is shown in Fig. 6-1 for the lateral curve of a typical 35-degree rudder throw test run. The plot of the trajectory data as computed and as it appeared in the launching tank due to position and angle of the launcher, is shown in Part (a), while the rotated plot is seen in Part (b). First, the plot of lateral displacement versus horizontal distance is rotated physically to make the tangent at beginning of rudder action parallel to the abscissa. Then the lateral displacement of each rotated point is plotted at the corresponding distance along the trajectory as shown for a typical point. The azimuth curve is shifted by the angle of rotation of the tangent line. The depth trajectory and inclination are rotated in a similar manner. The rate of change of lateral and depth curves are shifted by an amount corresponding to

the slopes of the respective tangents. The cam program is aligned with the trajectory by means of the cam light streak positions. Individual runs are then aligned on composite and family plots by means of the start of cam action.

Phase 1 - Preliminary Testing

Since the horizontal turning maneuvers were to be run at Froude scaled speed in order to model heel, other gravity and inertia forces, such as buoyancy and metacentric moment, also became of equal importance. The purpose of the preliminary testing was to determine model response and sensitivity to small variations in these quantities.

Acceleration: The trajectory response of the model was quite sensitive to linear acceleration, although small differences in constant velocity caused no measurable change in dynamic response. Figure 6-2a shows the characteristic nosing-up for deceleration and nosing-down for acceleration of the model, perhaps due to flow differences over the control surfaces that was observed previously for high model speeds. Initial disturbances due to the launcher were observed to continue longer than at the higher (16 fps) model speed, particularly acceleration effects. Angular velocities in azimuth and roll continued longer with greater effect on the trajectory after initiation of control action. The test results presented hereafter were selected for minimum deviations during the neutral portions of the trajectories.

Static Trim: The model proved to be insensitive to small buoyancy (0.005 lb) and static trim angles ($\pm$0.5 degree) changes, as shown in Fig. 6-2b. The deviation of the trajectories is well within that shown for the neutral trajectories where buoyancy and trim were controlled to $\pm$0.00025 lb and $\pm$0.1 degree, respectively. Normally, buoyancy and trim were adjusted to within $\pm$ 0.0005 lb and $\pm$0.2 degree prior to each test run.

Behavior near Free Surface: When, in the course of the horizontal turning maneuvers, the tank water level was lowered to repair the launcher support, the behavior of the model running near the free surface was determined. Figure 6-2c compares neutral trajectories in the vertical plane for submergences of 3.1 diameters (10 inches) and 9.2 diameters (30 inches) as they appeared in the tank, i.e., no rotation of the trajectories has been made.

At 3.1 diameters submergence an immediate nosing-down occurs and continues at about constant angular velocity. The slightly upturning trajectory at 9.2 diameters represents normal behavior due to variations in launching attitudes and neutral settings. All maneuvering test runs were made at this submergence (9.2 dia.) or greater. Reference 3 reports a repulsion in lift and a nose-down moment at 3 diameters submergence throughout the full speed range. The model behavior appears to verify this force and moment response in a qualitative sense.

Phase 2 - Horizontal Turning Allowing Depth Change

The dynamic behavior of the Albacore upon entering and maintaining a turn in the horizontal plane in response to rudder control only, was investigated in Phase 2 of the model test program. The specific response characteristics to be determined were:

(1) horizontal turning rate
(2) heel due to metacentric height
(3) cross steering due to heel
(4) velocity change

as functions of rudder throw angle. These quantities are equilibrium values in addition to and derived from the histories of azimuth, roll and inclination angles, lateral and depth trajectories and velocity variations.

The control program was as follows: After a short neutral run, the rudders were thrown to the desired angle at a 5 deg/sec rate (full scale) and held for the duration of the run. The range of rudder throw angles was (a) from 2 degrees port to 2 degrees starboard in 1-degree steps, (b) from 3 degrees to 18 degrees starboard in 3-degree steps, and (c) 35 degrees starboard. (A starboard rudder deflection causes the ship to turn to starboard.)

The test results for this phase are shown in Fig. 6-3 and Table 2. The horizontal and vertical projection of the trajectories (see Fig. 6-3a) present the paths of the C.G. in response to the various rudder deflections shown. The trajectories are seen to depart from the original path in an orderly manner with rudder throw angle, requiring between one to two ship-lengths to develop a noticeable deviation. The curves also become closer together with larger throw angles, indicating that the rudders are becoming less effective in producing additional turning. However, a high degree of

maneuverability is evident, particularly at a 35-degree throw angle where the ship executes a full half turn with a diameter of about 800 feet or four shiplengths. The depth trajectories indicate a rather pronounced cross-steering effect which increases rapidly with higher rudder throws. The increase in depth shown is a transient condition, however, since a final nosing-up angular velocity was observed for all control programs. The 35-degree rudder throw curve completed about a three-quarter turn (270°) in the tank before losing power, but disappeared from view of the cameras because of the large depth change (250 ft. maximum) after about a one-half turn (180°). (See Appendix B for optical coverage in the tank.) Visual observation showed that the model was climbing after the one-half turn during the test run.

The histories of the linear and angular positions and velocity variation as a function of the distance along the trajectory (see Fig. 6-3b) illustrate the degree of interaction of the cross steering which caused the depth changes noted above. The azimuth response is seen to be quick, requiring about one-half to one and one-half shiplengths of travel to develop a noticeable deviation in heading. Essentially steady turning, as denoted by the constant slope of the azimuth curves, is achieved fairly quickly (2 to 3 shiplengths) for all throw angles shown, but the attainment of steady-state conditions of roll, inclination, depth change and velocity change require much longer. A decreasing rudder effectiveness in producing additional turning is again indicated by the smaller increments of slope of the azimuth curves with equal increments of rudder deflection.

Considerable transient variation of roll (heel) angle, becoming almost a violent oscillation at a 35-degree rudder throw, is present. This roll oscillation is noticeable for rudder deflections above 3 degrees, reaching a maximum of between 35 - 40-degrees change in roll at the largest deflection. The initial conditions in roll (as well as azimuth and inclination) shown are representative of the ability of the launching mechanism to release the model. About two to three shiplengths of run were provided prior to control action to allow damping out of small initial disturbances. The roll oscillation, although highly damped, persisted for the full length of the trajectories possible in the tank for the 6 - 35-degree rudder deflection range.

The inclination response reflects this roll oscillation to a noticeable degree up to 18 degrees deflection, and to a considerable degree for a

35-degree throw. The curves exhibit a nosing-down proportional to the maximum roll variation (15° nose-down inclination for 35° roll), but all eventually show a nose-up angular velocity. Only the 35-degree curve continues to oscillate in pitch (about ± 2 degrees after 7 shiplengths) while the roll oscillates with about ±5 degrees amplitude.

The depth response, as was seen in Fig. 6-3a, shows the cumulative effects of the transient roll and inclination response. The transient depth change is moderate (35 ft maximum) except for the 35-degree rudder throw angle which reached an estimated 250-feet depth increase before recovering. No effect of the roll oscillation is evident in the lateral displacements, although the azimuth curves exhibit some oscillation at maximum roll.

The mechanism of this transient behavior may be visualized as follows: As the hull begins to yaw after rudder throw, the bridge fairwater develops a relatively large lift and a resulting roll moment. As roll develops, the downward component of the lift causes a nose-down moment and downward force which overpowers, temporarily, the equilibrium nose-up moment and upward force caused by the asymmetry of the hull and "down-wash" flow from the bridge fairwater. The rudders also contribute some nose-down moment due to roll angles. The small inertia and damping in roll allows an oscillation under the influence of the bridge fairwater lift and metacentric restoring moment.

The variation of model velocity during turning is shown also as a function of the initial velocity at start of control programming. Appreciable decelerations occur (56% for $\delta_r = 35^\circ$) for the model during the maneuver. Whether the same final velocity (or even rate of change) will occur with the full scale Albacore is questionable since the Reynolds number differs 1000-fold. (Model $R_e = 7 \times 10^5$; prototype $R_e = 7 \times 10^8$). However, the same general character of deceleration should follow.

The variations in curvature of azimuth, roll and inclination are shown in Fig. 6-3c for a few selected trajectories. These curves are faired in from the plots of the average values of successive differences of the tabular data because the experimental scatter was quite large. Data points for one 35-degree azimuth curvature only are shown for comparison. The maximum and final values were derived from the slopes of the angular curves of Fig. 6-3b. The curves are included to illustrate the characteristic oscillation of

the roll and to indicate the large angular accelerations involved as well as the phase relation between yaw, roll and inclination. It may be pointed out that the curvature scales are in rad/foot because the time scale varies considerably with distance traveled along the trajectory depending upon the model deceleration.

Estimated equilibrium conditions as well as transient values for these turning maneuvers as functions of rudder deflection angles are shown in Fig. 6-3d. The plotted points shown on the figure were measured or estimated from the trajectory histories shown in Fig. 6-3b, except for the angles of attack which were estimated from the tabular data and individual plots. The equilibrium conditions are denoted by the solid curves while the maximum transient values are given by the dashed curves. The transient curves of horizontal curvature (1/R) and roll showing minimum values reached during oscillations - not included for reasons of clarity - would lie approximately an equal distance on the opposite side of the steady-state curve. The curves again show the decreasing effectiveness of additional rudder deflections and indicate that a maximum turning rate of $1/R = 2.55 \times 10^{-3} ft^{-1}$ (R = 390 ft) is being approached for a rudder throw angle of between 40 - 45 degrees. Table 6-2 gives the corresponding numerical values of the equilibrium and transient conditions in turning for the nominal control angles tested.

It may be of interest to compare the correctly "banked" roll angles with the actual roll response of the model. The computed heel angle for correct banking, i.e., when the centrifugal moment is balanced by the metacentric moment, is about 10 degrees during the initial stages of turning (velocity = 25 knots) with a 35-degree rudder throw. After the speed reduction to about 15 knots, the computed heel angle becomes about 4 degrees for a turning radius of 400 feet. The roll angles recorded during the test run are seen to be over three times these computed values for both transient and equilibrium conditions.

The large cross-steering effects exhibited by the Albacore model clearly indicate that some measure of control over depth change or roll, or both, would be desirable in order to maintain a reasonably level horizontal turn. Safe operating limits of crew and ship were not included in these model tests, nor were they even known. However, even aside from these two very important considerations, the ability to maintain control over depth, particularly in shallow water and under emergency conditions in evasive

TABLE 6-2

C.I.T. MODEL - REVISED CONFIGURATION, U.S.S. ALBACORE, AGSS 569, SST SCHEME IV

PHASE 2 - EQUILIBRIUM AND TRANSIENT CONDITIONS IN SUBMERGED TURNING

			Equilibrium Conditions					Transient Conditions					
δ_r deg.	δ_s deg.	δ_d deg.	β_f deg.	Φ_f deg.	R_H ft	R_V ft	V_f -knots	Φ_m deg.	$(R_H)_{max}$ ft	Θ_{max} deg.	Advance ft	Depth ft	Offset ft
+2	0	0	-1.0	-2.0	-3880	111,000	24.7	-2.6	-	+0.2	-	+2	-
+1	0	0	-0.5	-1.0	-7680	500,000	24.9	-1.3	-	+0.1	-	+1	-
0	0	0	0	0	0	0	0	0	-	0	-	0	-
-1	0	0	+0.5	+1.0	+7680	500,000	24.9	1.3	-	+0.1	-	+1	-
-2	0	0	+1.0	+2.0	+3880	111,000	24.7	2.6	-	+0.2	-	+2	-
-3	0	0	+1.5	+3.0	2780	55,000	24.6	4.0	-	+0.3	-	3	-
-6	0	0	+2.9	+6.0	1430	15,600	24.2	7.8	-	0.5	-	6	-
-9	0	0	+4.3	+8.8	990	7,880	23.9	11.5	970	1.0	-	11	-
-12	0	0	+5.5	+11.7	783	5,620	23.1	15.2	752	1.3	1060	18	-
-15	0	0	+6.4	+14.2	667	4,450	21.9	18.7	625	2.0	983	25	-
-18	0	0	+7.2	+16.5	585	3,740	20.5	22.0	548	2.7	890	35	-
-35	0	0	+9.0	+22.5	403	2,080	14.0	+35.0	336	14.0	+671	+250	-790

CONFIDENTIAL

CONFIDENTIAL

maneuvering, becomes vital. The capabilities of the Albacore in this respect were investigated and are shown in the following sections of this chapter.

Phase 3 - Horizontal Turning with Depth Control

The purpose of this phase of the model test program was to investigate the control of depth during horizontal turning maneuvers by means of stern-plane control. More specifically, it was desired to determine the required stern-plane program for maintaining depth within ±10 feet. Force measurements in restrained turning (Ref. 3) gave a measure of the equilibrium values to be expected but gave no indication of the transient behavior which is shown in Phase 2 of this study. Because the major portion of a normal turn proves to be in the transient regime, the control of depth during this transient turning assumes primary importance.

The method of solution used here is identical to that used in Chapter 5 of this report for the depth changing maneuvers. In essence, (1) a control program is estimated from available trajectory data, (2) the model response determined for the estimated control program, (3) the program modified on the basis of (2), and (4) the model response again determined, and so on.

Figures 6-4a and 6-4b show four such trial stern-plane programs and resulting trajectories for a 35-degree rudder throw. The initial estimate of the required stern-plane program was made first by adding the trajectory for 3-degrees rise from the response of the model in the vertical plane at high speed (15 - 16 fps) to the inclination and depth trajectories, respectively, for horizontal turning in order to correct the transient diving response. Then a 3-degree diving trajectory was added to this "corrected" trajectory to control the rising equilibrium response. Cross-steering effects could not be taken into account for lack of information. The ±9 degrees stern-plane program was included to evaluate the effects of over-correction.

The trajectory histories of Fig. 6-4 show that sufficient control is available with relatively small stern-plane throw angles ($\pm 3^{o}$) while a ±9-degree deflection is seen to over-control in inclination and depth. Although the general roll response is little affected by addition of stern-plane control, a slight reduction in magnitude of maximum roll and amplitude of oscillation is evident, i.e., it appears that some damping is introduced. The inclination history exhibits the characteristic transient nosing down due to the large roll

indicating that a constant 3-degree rise angle is not sufficient.

A significant difference in azimuth and lateral response with stern-plane programs in the transient phase of turning is seen by the early deviation of the curves. The equilibrium turning rates appear to be affected also by this cross steering, as indicated by the slightly divergent slopes of the azimuth plots. This interaction between stern plane and rudder affects the initial or "entering-the-turn" phase sufficiently to cause an estimated 50 to 60 feet difference in "maximum lateral deviation" or tactical diameter of the turning maneuver. Figure 6-4a illustrates these differences to a somewhat exaggerated extent since part of the difference is due to the change in depth.

It will be seen that essentially constant inclination was attained eventually for all 3-degree rise and dive trajectories but that depth trajectories differ considerably in final slope and, consequently, in final depth. However, the final stern-plane program maintained the depth within 25 feet as compared to 250 feet maximum depth change without depth control. Although this is beyond the limits of $\pm$10 feet originally prescribed, it is felt to be adequate for the "simple" type program used here, and further refinement does not appear worthwhile. A more complex program may be devised that will counteract the effects of the large transient roll response but only at the expense of precise and easily repeatable control actions. Such a program might require an initial 2-degree rise angle plus an increasing rise angle to match the roll change during the first portion of the maneuver and a 3-degree dive angle to control the equilibrium condition.

The same cut-and-try procedure described for the 35-degree rudder depth-controlled trajectories of Fig. 6-4 was applied for rudder throws from 6 to 18 degrees also. The stern-plane program was restricted to the simple rise-hold-dive type with variation of the absolute and relative deflection angles. Three ratios (1:1, 1:2 , 2:3) of rise to dive angles were tested in combination with various "hold-at-rise" distances. The results of the best stern-plane program for each rudder throw from 9 to 35 degrees is shown in Fig. 6-5. The 6 and 3-degree curves are omitted because any of the control programs tested proved worse than those with no control. Each trajectory shown represents the closest approach (after from 3 to 5 estimates of the stern-plane program) to equilibrium turning conditions obtained. The principal criterion was attainment of a zero final curvature (i.e., constant

slope depth trajectory). It may be noted that in several cases the change of depth is actually greater for the length of run shown than was seen in Fig. 6-3 without depth control. However, as was shown in Fig. 6-4, the final depth trajectory condition (depth and slope) is primarily determined in the transient phase provided, of course, that the final stern-plane angle is correct. Further estimates and trials of stern-plane programs where only the holding time at rise angles would be varied, did not appear worthwhile. The same general effects of stern-plane control upon the turning characteristics, as shown in Fig. 6-4, were found in the dynamic response for all rudder throw angles although to a smaller degree.

From the curves shown in Fig. 6-5a and b plus the trajectories of trials not shown, the equilibrium and transient conditions were estimated. Figure 6-5c shows these estimated values as a function of rudder throw angles. Comparison with Fig. 6-3d reveals that the only significant differences in equilibrium values occur for 35 degrees rudder throw where the horizontal turning rate is about 8 per cent lower and roll angle is reduced by about 10 per cent. Angle of attack in the horizontal plane appears unchanged for all rudder throws. The two curves at the top of Fig. 6-5c give the estimated stern-plane rise angles and holding distance for controlling the transient response in depth due to roll. Table 6-3 lists the corresponding numerical values for the nominal rudder throw angles tested.

Thirty-five Degree (35°) Rudder Throw Maneuver Movie Film

A 16 mm movie film is available (Ref. 5) showing the dynamic behavior of the Albacore model in turning with 35-degree rudder deflection. Two maneuvers are shown; (a) a turn while allowing depth change, and (b) while controlling depth with the final stern-plane program tested.

The launcher position and cam timing were so adjusted that the full turn was made by the model in the field of view of one of the tank's five regular 35 mm cameras. That is, the entire maneuver is thus viewed from a single point of view. The 35 mm film was rephotographed frame by frame onto 16 mm film to make a projectionable movie. The picture-taking rate of the 35 mm original was so adjusted that the 16 mm copy, when projected at 24 frames per second, shows the model making the turn in the same time that the full size Albacore would make it when running at an initial speed of 25 knots.

TABLE 6-3

C.I.T. MODEL - REVISED CONFIGURATION, U.S.S. ALBACORE, AGSS 569, SST SCHEME IV

PHASE 3 - EQUILIBRIUM AND TRANSIENT CONDITIONS FOR DEPTH CONTROL

Equilibrium									Transient			
δ_r deg.	δ_s deg.	δ_d deg.	β_f deg.	Φ_f deg.	R_H ft.	a_f deg.	R_v ft	V_f knots	Φ_m deg,	R_H ft	Stern Plane Program	
											rise angle	hold distance
3	0	0	1.0	4	2850	-	0	24.6	5	2850	0	-
6	+0.5	0	2.4	7	1440	-0.5	0	24.2	9.5	1440	-0.5°	500 ft
9	+1.0	0	3.9	9	960	-1.3	0	23.5	13.6	960	-1.0°	570 ft
12	+2.2	0	5.2	11	757	-2.0	0	22.7	17.2	746	-1.4°	630 ft
15	+2.7	0	6.0	12	645	-2.4	0	22.1	20.3	617	-1.8°	680 ft
18	+3.0	0	6.8	13	577	-2.7	0	19.5	22.8	532	-2.2°	750 ft
35	+3.2	0	9.0	15	436	-3.0	0	16.0	34.5	364	-3.0°	900 ft

This film produces a vivid visual impression of the violence of the diving-while-turning in the absence of depth control, as well as of the flat turns that can be made with depth control.

During the runs from which the 16 mm film was produced, the other 35 mm cameras were also used so that stereoscopic analysis was possible, and the runs were also useful as data-taking tests.

Phase 4 - Horizontal Turning with Roll Control

The large transient roll response found in Phase 2 and the small effect upon the same of the stern plane depth control programs noted in Phase 3, make control of roll appear highly desirable. It appears that a reduction of the maximum transient roll would aid considerably in maintaining constant depth by reducing the corresponding transient diving response. The purpose of Phase 4 of the model test program was to investigate (a) the effect of bridge fairwater height on the roll response, (b) reduction of the transient roll response by application of dorsal rudder, and (c) limitation of the equilibrium roll angle to something nearer to the correctly banked value.

Reduced Height Bridge Fairwater: As a preliminary to the roll control test runs, (prior to revision of the model for dorsal rudder control) several launchings were made with a reduced height (1/3) of the bridge fairwater (see Fig. 2-27) in order to determine the effect of this appendage upon the roll and dive responses which accompany turning. The propeller torque reaction (normally balanced by the dorsal rudder) was accounted for by offsetting each bow plane by 1.5 degrees. A comparison of the response with the 1/3 height and the normal height appendage is given in Figure 6-6a and b for the 18 and 35-degree rudder throw angles. The curves indicate a radical difference in response both in the vertical and horizontal planes. The transient roll response is greatly reduced (from 35° to 11° at 35° rudder throw) and the final roll to almost zero (from 12.5°). The effect of this reduction in transient roll response is to reduce greatly the nosing-down and diving response noted for turning with the full height bridge fairwater while allowing depth change (Phase 2). The transient phase in the vertical plane is thus considerably shortened and the equilibrium nosing-up and climb response is attained more quickly. The climb rate is also higher than with the full height bridge fairwater. The transient horizontal turning rate is reduced considerably, as

shown by the divergence of the azimuth curves after one ship length, although the final turning rates differ but little. The velocity history shows no significant difference. These curves clearly indicate the role of the bridge fairwater in producing the large transient roll and vertical response during turning maneuvers and show that considerable differences in depth response may be expected to result from roll control by means of the dorsal rudder.

Dorsal Rudder Control: The behavior of the model with roll control was investigated for two rudder throw angles, 35 degrees and 18 degrees, and only one linkage ratio for dorsal rudder, providing 37.5 degrees and 22.5 degrees port throw angles, respectively. The control program used was as follows: After a short neutral run, the dorsal rudder was thrown simultaneously with the rudder (by the rudder cam) to port and held. (A "port" dorsal rudder throw angle causes the model to roll to port - analogous to a starboard rudder throw causing a turn to starboard.)

A comparison of the response of the model with and without dorsal rudder control for the two rudder angles tested is shown in Fig. 6-7a and b. The principal effect of the addition of dorsal rudder control is seen to be a delay of the transient roll response (by imparting an initial roll to port) and a reduction of the equilibrium roll angle. The total change in roll (from maximum port angle to maximum starboard angle) is essentially the same. This difference in roll response has a marked effect upon the inclination and depth response. The maximum transient inclination is reduced by about one-half at 35 degrees rudder throw and two-thirds at 18 degrees. The larger relative dorsal throw at 18 degrees may account for the greater reduction. The equilibrium nosing-up conditions is reached more quickly with dorsal rudder control (yet considerably later than with the one-third height bridge fairwater) and inclination angular velocities for both 18 degrees and 35 degrees rudder approach, a common value which appears to be slightly higher than that obtained without dorsal rudder control. The subsequent transient depth change is greatly reduced (about 1/10) as a result of the reduced inclination. The 30-foot maximum depth change (from 250 feet) for 35 degrees rudder throw is only slightly greater than was obtained with depth control by means of stern planes (25 feet) illustrating again the profound influence of transient roll behavior upon the response in the vertical plane.

Relatively little effect upon the response in the horizontal turning rate

is noted for a 35-degree rudder throw but quite a large difference occurs for the 18-degree rudder throw. The cause appears to be in the larger initial roll response to port which delayed the "entering-the-turn" portion of the maneuver.

Phase 5 - Horizontal Turning with Roll and Depth Control

Although control of roll response by means of dorsal rudder materially reduces the transient response in the vertical plane, some measure of control over depth remains desirable in the transient phase and is necessary in the final or equilibrium phase. The purpose of Phase 5 of the test program was to investigate briefly the stern-plane program necessary to maintain depth within ±10 feet.

Two stern-plane programs were tested for 35 degrees rudder throw while only one program was checked for 18 degrees rudder throw. (The actual cams used here were also used in Phase 3 of the test program.) Figure 6-8 shows a comparison of the model response with and without stern-plane control for 35-degree and 18-degree rudder throws and 37.5-degree and 22.5-degree dorsal rudder throws, respectively. The influence of the transient roll response upon transient inclination and depth response remains large. The same general type of depth correction program (by means of stern planes) is required as for uncontrolled roll (Phase 3) with some modifications. It appears that a smaller (about 1/3 less) initial rise angle, coupled with a longer hold time (about 700 feet) would be sufficient to control the transient vertical response. A larger (about 1/3 more) dive angle appears necessary to control the larger final nose-up angular velocity (due to reduction of roll by dorsal rudder - Phase 4).

The effect of cross steering due to stern planes in the initial or "windup" portion of the trajectory is clearly shown by the 35-degree rudder throw curves. The 3-degree rise stern-plane angle decreases the initial azimuth response considerably, while the 3-degree dive increases the response after about two and one-half shiplengths. The three curves become approximately parallel later, indicating negligible cross steering at equilibrium turning conditions. The roll response, too, is affected. Both initial rise and dive stern-plane angles are seen to increase the maximum roll angle as well as the final roll angle. The same behavior to a reduced extent is noticeable for

18 degrees rudder throw also.

As was noted previously (Phase 3), the simple rise-hold-dive type of stern-plane program tested here does not appear adequate to maintain depth within the prescribed limits of ±10 feet. Even so, the maximum transient depth change is only 25 feet (compared to 250 feet for rudder control alone). Since the transient inclination response is reduced greatly by the dorsal rudder control, a more complex program, in this case, might include a constant rise angle and a variable dive angle.

Equilibrium and Transient Conditions

Estimated equilibrium conditions in steady turning plus some transient values for Phases 4 and 5 are shown in Table 6-4. The values shown are estimated from the curves shown in Figures 6-7 and 6-8 and from the tabulated data, in comparison with the trajectory response determined in Phases 2 and 3. Since some of the trajectories tested in Phase 5 controlled the final angular velocity in the vertical plane, the equilibrium values given are somewhat uncertain, being rather an educated guess. However, on the basis of the consistent performance of the model, it is felt that the magnitudes are sufficiently close to provide adequate control of the submarine during such a maneuver.

Comparison of the Depth Control Techniques

A comparison of the relative response of the model for the various combinations of control actions for a 35-degree rudder throw angle is shown in Fig. 6-9 and in Table 6-5. Representative trajectories from Phases 3, 4 and 5 are compared to the trajectory response of the model for rudder control only (Phase 2). In general, these curves illustrate the pronounced cross-steering effects of the stern planes during the transient phase of the turning maneuver. The cumulative effects of such cross steering and control of depth is seen in the divergence of the lateral curves (Fig. 6-9a) in the horizontal plane. The azimuth curves of Part (b) are seen to be approximately parallel after about four shiplengths, which indicates only slight cross steering for equilibrium turning conditions.

It should be noted here that, in general, for the length of model run possible in the tank, none of the trajectories has reached a true equilibrium condition, although steady-state turning is closely approached. A small

TABLE 6-4

C.I.T. MODEL - REVISED CONFIGURATION, U.S.S. ALBACORE, AGSS 569, SST SCHEME IV

ESTIMATED EQUILIBRIUM AND TRANSIENT CONDITIONS IN SUBMERGED TURNING FOR ROLL CONTROL

Phase	Equilibrium								Transient				
												Stern Plane Program	
	δ_r deg.	δ_s deg.	δ_d deg.	β_f deg.	Φ_f deg.	R_H ft	α_f deg.	R_v deg.	V_f Knots	Φ_m deg.	R_H ft	Rise Angle	Hold Distance
4	-18	0	-22.5	+5.5	+6.5	640	-1.1	6230	19.7	20	553	-	-
	-35	0	-37.5	+7.5	+6.0	380	-4.5	2500	14.8	27	345	-	-
5	-18	+3.0	-22.5	+6.5	+5.5	651	-1.8	0	19.7	20	556	2°	700 ft
	-35	+3.0	-37.5	+8.5	+7.5	403	-3.3	0	14.8	33	358	2°	800 ft

oscillation in roll is always found to persist throughout the full length of recorded trajectory. The influence of this roll oscillation is essentially damped out after about 6 shiplengths, however, so that the final portions of the curves shown describe the equilibrium condition very closely. Table 6-5 lists the estimated equilibrium conditions for 35 degrees rudder throw for each test, which indicate the effectiveness of the three combinations of stern plane and dorsal rudder programs for controlling depth and roll response. These values indicate that the use of the dorsal rudder contributes materially toward increasing the equilibrium turning rate whether with or without stern-plane control. The three right-hand columns of Table 4 give, perhaps, a better picture of the over-all effect on the trajectory. These figures again indicate that control solely with the dorsal rudder is more effective in limiting transient depth change while achieving the most compact turning maneuver. It is of interest, too, that the maximum lateral offsets are smaller than the diameter of the constant turning circle given by corresponding values of R_H in each case except for Phase 4, indicating the effect of the transient phase upon the subsequent history of the trajectory.

One general observation may bear repetition and emphasis, i.e., for turning maneuvers within a normal range of operation (a 180-degree change of direction) steady-state equilibrium conditions are closely approached but never attained. It is estimated that in order to achieve a 180-degree change in direction without over-shooting,the rudder should be returned to neutral after about 150 to 160-degree change in heading. The ship has barely approached equilibrium in this space when it is again thrown into a transient phase of the maneuver.

The large transient response in depth may be of some tactical advantage for evasive maneuvering, however. Use of stern plane and dorsal rudder for controlling depth is seen to increase the maneuvering space required (increased advance and offset). If transient depth changes on the order of 50 feet are permissible, depth control by means of the dorsal rudder only is more effective from the standpoint of a "tighter" maneuver in the horizontal plane. But, on the other hand, if an evasive type of maneuver is considered, turning with rudder control alone appears to have a distinct advantage, for, in this case, a 250-foot increase in depth is achieved without the necessity of stern-plane programming while reversing direction of travel in the minimum horizontal space with only a 50-foot increase in distance traveled.

TABLE 6-5

U.S.S. ALBACORE, AGSS 569, SST SCHEME IV

ESTIMATED EQUILIBRIUM AND TRANSIENT CONDITIONS IN SUBMERGED TURNING FOR VARIOUS COMBINATIONS OF CONTROL ACTIONS FOR 35° RUDDER DEFLECTIONS

Test Phase	δ_r Deg.	δ_s Deg.	δ_d Deg.	$\beta_{o\,o}$ Deg.	Φ Deg.	a Deg.	R_H Feet	R_v Feet	V_f Knots	Maximum Lateral Offset Feet	Maximum Advance Feet	Maximum Transient Depth Feet
2	-35	0	0	+9.0	+12.5	-	417	3800	15.7	-790	+673	+250
3	-35	+3.0	0	+9.0	+12.5	-4.0	437	0	15.4	-840	+700	+20
4	-35	0	-37.5	+7.5	+6.0	-	380	2500	14.8	-798	+678	+37
5	-35	+3.0	-37.5	+8.5	+7.5	-3.3	403	0	14.8	-805	+720	-

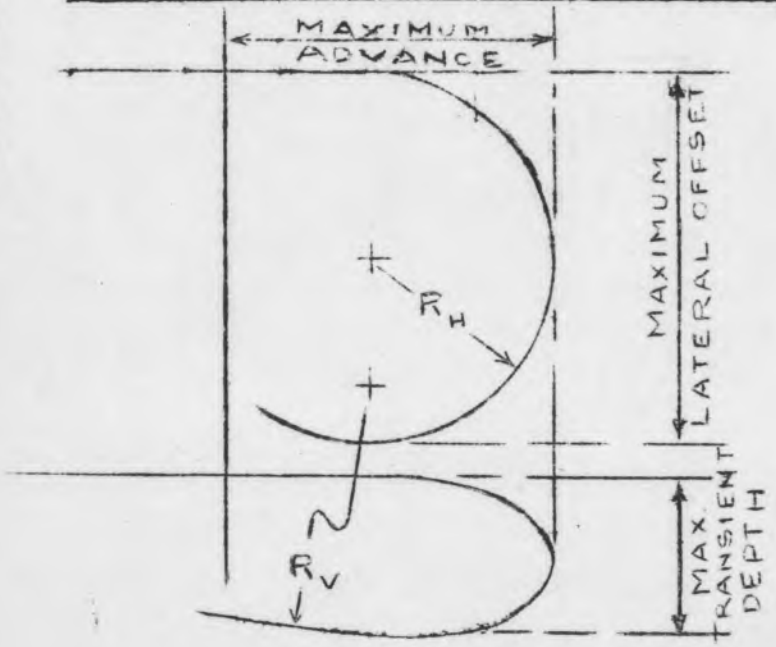

CONFIDENTIAL

CONFIDENTIAL

Comparison of Free-Flight and Captive Model Data

Extensive testing with captive models of the U.S.S. Albacore, Scheme IV, submarine has been done with the standard force-measuring techniques (Refs. 3, 6, 12) or extensions thereof (Ref. 4) to six degrees of freedom. Only Ref. 4 has reported determination of equilibrium turning conditions while the others reported force and moment data. The results obtained with the free-flying model (see Table 6-2) afford an excellent opportunity for comparison of two diametrically opposed techniques for determining such equilibrium turning conditions.

TABLE 6-6

COMPARISON OF EQUILIBRIUM TURNING CONDITIONS

Item Model	δ_r	δ_s	β_o	r'_o	R_H	θ	ϕ	V_f	δ_d	Model Configuration	Test Phase
ETT*	35	+3.6	+7.8	0.42	476	-1.0	+12.9	15.7	0	II	I
CIT	35	+3.2	+9.0	0.46	436	-3.0	+15.0	16.0	0	Revised	2
ETT	35	+3.0	8.6	0.40	500	0	+ 8.3	15.5	40	II	II
CIT	35	+3.0	8.5	0.495	403	-3.3	+ 7.5	14.8	37.5	Revised	5

*The sign convention has been changed where necessary to correspond to that used throughout this report.

Table 6-6, above, shows a comparison of equilibrium turning conditions, (1) as computed from forced turning tests at ETT (Ref. 4) and (2) as estimated from free turning tests at CIT (part 3 of this report).

Table 6-7, below, shows relative areas of appendages and control surfaces for the models tested at ETT and CIT. Unfortunately, the configurations are not identical so that an exact comparison of results is impossible. The CIT model, however, represents the prototype configuration as tested in full scale trials off the coast of Florida in 1955. Also it is understood that full scale trials will be made with another configuration that was tested at ETT (Configuration I). Thus a direct comparison with full scale data for the CIT model results reported herein will be possible while a similar comparison will be available for the ETT tests.

TABLE 6-7

CONTROL SURFACE DIFFERENCES

Projected Areas sq. ft.	ETT Conf. II	CIT Revised
Fin and rudder (2)	288.6	159
Rudder	101.0	107
Bridge fairwater	239*	277
Dorsal rudder	27.0	24.0
Bow planes	27.0	32.0

*Assumed equivalent to CIT "original" configuration.

In spite of the differences between models, the agreement in equilibrium turning conditions is quite good except for (1) turning radius, and (2) inclination angle. The other quantities are all within the experimental error quoted for both types of testing. The free-turning model shows an appreciably smaller turning radius and larger nose-up inclination angle. The reasons for these differences may, perhaps, be found in the following factors:

(a) The model appendage configurations tested are not identical (Table 6-7);

(b) The accuracy of model test results;

(c) The inherent differences in test techniques, that is, captive versus free-flying models;

(d) Validity of scaling laws.

The purpose of the present discussions is only to point out the agreement or disagreement between results by the two modeling techniques and to suggest some possible reasons for such differences. Since detailed discussions of each factor are found elsewhere in this report, and in Ref. 4, it is felt sufficient to summarize the primary difference in modeling technique only.

1) Captive models provide information on certain force and moment functions under steady-state conditions only. Assumptions regarding additional functions required and application of such measured and assumed functions to existing theory of motion must be made. Force

data is measured directly while accelerations, rates of change and position-time data must be computed.

2) Free models require only one assumption, although a large one. The flow around the model is assumed to be similar to the flow around the prototype. Position-time data may be measured directly, while rates of change and accelerations must be derived by differentiation of measured values.

How closely either modeling technique predicts full-scale behavior must necessarily await comparison with prototype tests provided, of course, that such full-scale information is as reproducible as that obtainable with models.

Summary and Conclusions

The experimental work described in Chapter 6 of this report represents the first time that the Controlled Atmosphere Launching Tank has been generalized to six degrees of freedom. As such, this generalization is an important extension of the usefulness of the facility for determining motions of free bodies under truly similar force systems (within certain limitations, of course).

This work also represents the generalization of a self-propelled, free-body to six degrees of freedom under the influence of multiple and complex control programming. The feasibility of operating a small scale (100:1) model at a Froude-scaled speed of 4.25 fps and determining position-angle-time data with adequate precision has been demonstrated.

Model Behavior: It was found necessary to control physical factors of alignment, rigidity, etc., as closely for Froude-scaled velocities as for high model speeds (Part 2). The model performance and trajectory response at the relatively low model velocity (4.25 fps) was found to be:

A. insensitive to:
   (a) small changes of buoyancy (0.1%)
   (b) small changes of static longitudinal trim ($\pm 0.5^{\circ}$)
   (c) differences of constant velocity ($\pm 15\%$),

but B. sensitive to:
   (a) longitudinal accelerations
   (b) initial conditions - disturbances from the launching mechanism continued after initiation of control action

(c) proximity of the free surface when the submergence was reduced to 3 diameters. (The model was normally run at 9.2 dia. submergence.)

Full Scale Behavior: Prediction of full scale dynamic control characteristics from the model tests indicates that for rudder control only:

(1) Control response in the horizontal plane is quick and positive for all rudder throw angles tested (2^{o} port to 35^{o} starboard). Essentially steady turning is reached in 2 to 3 shiplengths. Minimum turning radius is about 1.95 shiplengths (390 ft) at 40^{o} - 45^{o} rudder throw angle.

(2) A large transient roll response exists due to lift on the bridge fairwater as yaw develops. A damped oscillation in roll persists for a relatively large portion of the turning trajectory.

(3) Pronounced nose-down cross steering due to (2) occurs in the transient phase which overpowers temporarily the equilibrium nosing-up condition.

(4) Appreciable longitudinal deceleration occurs at higher rudder throw angles (46% at 35^{o}).

Investigation of control of depth change by means of stern-plane programming showed that:

(1) Adequate control is available with stern-plane deflection angles not exceeding ± 3 degrees for all rudder throw angles tested. The simple rise-hold-dive type program maintains depth within reasonable limits.

(2) The roll response, both transient and equilibrium, is little affected by application of stern-plane control.

(3) Cross-steering due to stern planes was small and limited to the early stages of turning.

Investigation of the mechanism of roll response by means of a reduced height bridge fairwater indicated that:

(1) The bridge fairwater is primarily responsible for the large transient roll response, subsequent transient depth change and magnitude of the final roll angle.

(2) The bridge fairwater contributes materially to the horizontal turning rate.

Investigation of control of transient roll response and reduction of equilibrium roll angle by means of dorsal rudder control showed that:

(1) Duration of transient roll response may be reduced, although total change of roll angle (from initial to maximum value) is little changed. Final roll angle is reduced appreciably.

(2) Transient depth response is greatly reduced while equilibrium nosing-up rate is unchanged.

(3) Horizontal turning is delayed slightly due to initial roll to port but final turning rates appear to be increased.

(4) Dorsal rudder control appears more effective than stern-plane control in limiting depth change during the transient stages of turning.

(5) A measure of depth control by means of stern planes remains necessary in the equlibrium phase of the maneuver.

Investigation of control of depth change by means of stern planes with roll control shows that:

(1) The simple type of rise-hold-dive stern-plane program is adequate for controlling depth change. Smaller rise angles and larger dive angles than for stern-plane control alone are indicated.

(2) Maximum and final roll angles are increased slightly by application of stern planes.

(3) Horizontal turning is retarded slightly for rise stern-plane angles and increased for dive angles during the transient phase, and unaffected at equilibrium.

Some General Conclusions

(1) A comparison of depth control techniques shows that control solely with the dorsal rudder is more effective in limiting transient depth change while achieving the most compact maneuver.

(2) For turning maneuvers within a normal range of operation (a 180° change in direction), steady-state equilibrium conditions are

closely approached but never attained. That is, the normal mode of turning is transient.

(3) Under certain conditions, the large transient vertical response may be useful in evasive type of maneuvers. Large changes in depth simultaneous with turning are obtained without necessity of stern-plane control.

(4) Comparison of free-running model results with forced turning results (for a slightly different control surface configuration) agree within experimental accuracy for horizontal angle of attack, roll angle, final velocity and stern-plane angle. Horizontal turning radius and inclination angle differ significantly.

CHAPTER 7

SUMMARY OF STUDY

Summary

A rather detailed discussion of the various aspects of this study of the stability and control of submarines by means of self-powered, self-controlled, free-flying models has been presented. The usefulness of free-flying models depends largely on the experimental techniques which, in this case, are quite demanding, and also on an understanding of the relatively simple theory of modeling the dynamics of submerged bodies. Therefore, it was felt necessary to discuss the theory of modeling, to describe the experimental techniques in detail, and to examine the test results critically in order to evaluate the technique and to prescribe areas of validity and limits of usefulness.

Self-powered, controlled, free-running models of two submarines - the U.S.S. Odax and U.S.S. Albacore - have been developed which are capable of consistent and reliable performance in response to prescribed control programs. Techniques of construction for unusual shapes were developed to provide precise external dimensions with a maximum usable internal volume at a reasonable cost. A power plant using gas-water accumulator and terry-type turbine geared to the scaled propellers was built to fit into the model hulls which provides an essentially constant power output for propulsion and control mechanisms. The control system yielded very accurate and consistent programming of the control surfaces. The need for precise model dimensions, careful construction and maintenance in order to maintain extremely close tolerances has been pointed out.

Parallel developments of experimental techniques and auxiliary equipment for use in the Controlled Atmosphere Launching Tank have been described. A new linear launching mechanism was built and operated successfully for accelerating the self-powered models up to speeds of 16 fps. Although this was the maximum speed required in this study, the launcher was designed with the capacity to accelerate a 4.5-pound model to 250 fps. A second launcher was designed for the lower speed range of 3 to 5 fps.

Part of the study represents the first generalization of the launching tank to stereoscopic observation of motion having six degrees of freedom. A precise alignment of the optical systems of the tank and analyzer for

stereo-optic analysis was quite satisfactorily accomplished. Measuring accuracy, sources of possible error, and effects upon test results have been discussed. This represents an important extension of the usefulness of the launching tank for the study of free-body dynamics.

Test results of the dynamic behavior of the U.S. S. Odax model have been presented. These results show that the small-scale model can duplicate full-scale behavior for prescribed control programs within certain limitations. The model exhibited known stability and control characteristics of the prototype vessel. Consistency of behavior of the model in repeated test runs was rather good for such an unstable shape.

The test results for the U.S.S. Albacore model, on the other hand, are presented as a prediction of the dynamic behavior of the prototype vehicle in vertical and horizontal maneuvering. This model exhibited much better directional stability and control response characteristics, and indicates a superior hydrodynamic design to that of the U.S.S. Odax model. Specific maneuvering problems have been solved by the process of successive approximation. A comparison between trajectories computed from theory and experimental trajectories with the model was made, but the differences could not be resolved. The use of the model in the study of horizontal turning characteristics represents an important extension of the free-running model to six degrees of freedom and multiple control programming, in addition to scaling of static as well as dynamic forces.

In general, it has been shown that the small-scale, free-running models can yield precise and detailed information regarding stability, control and maneuverability of powered and submerged bodies. From the foregoing, one may draw perhaps a single conclusion to sum up the study: The free-running model is a useful and powerful research and design tool for the study of the dynamic control and behavior of fully submerged bodies.

Suggestions for Future Research

Since one purpose of this study was to develop a modeling technique for predicting prototype behavior, it is felt that additional applications of the technique should be pointed out and future avenues of investigation of a general nature should be suggested.

The tests with the Odax model have demonstrated the ability of a small

scale model to duplicate prototype behavior under specific conditions. The Albacore model tests, on the other hand, have extended the range of conditions to such an extent that extrapolation to full scale is no longer obviously valid. Therefore, the next most logical step would be a critical comparison of the behavior predicted from these model tests with the actual behavior of the full scale vehicle. The full scale sea trials of the U.S.S. Albacore with the controls and appendages corresponding to the "revised" configuration of the model which were made off the Florida coast in the fall of 1955 offer an excellent opportunity for such a comparison. It is understood that the tests were quite extensive within the limitations of safety for crew and vessel. A direct comparison of trajectories under identical conditions of control program, initial conditions, etc., should be possible in a good many cases. Comparable full-scale tests are available for only some of the model tests. This is due to the fact that some of the model tests were intentionally designed to determine the ultimate maneuvering capacity of this new submarine. At the present stage of experience with this new vehicle and with its higher speeds it is still considered unsafe to follow to the limit on the basis of model predictions. However, the comparisons that can be made will provide a good measure of the reliability of model predictions, and, if this proves to be good, it will establish the usefulness of the free-flying model for investigating limit maneuvers.

A number of other problems of submarine control and stability would be amenable to solution by means of self-powered, free-flying models also. The problems of operation near a free surface are manifold, particularly at higher speeds, due to the large forces and moments of varying magnitude and direction with changing speed and submergence. One example is the approach from depth to a straight and level flight at periscope depth, where such forces are encountered with no previous warning. The investigation of the effect upon the maneuver and the prescience necessary to successfully accomplish the maneuver appears desirable. A crash dive from the surface is another example which has added complications due to piercing the free surface. Acceleration and deceleration characteristics and attendant control problems may be attacked by means of free models. Maneuvering at "zero" speed, i.e., from a hovering attitude to very small forward or reverse speed, is an example at the extreme limit of the velocity scale.

Perhaps the most valuable and important contribution the free-running

controlled model technique can make is to the general theory of motion of a submerged body. It should be possible at last to settle the form of the equations of motion by a coordinated program using data from both free and captive models. Such a study would be free of the handicap of scale effects by virtue of identical size of the captive and the free model. Therefore, the one assumption involved in the free model - that of similitude of flow between model and prototype - is eliminated. One has, thus, at hand an automatic computing machine with built-in equations of motion limited only by the accuracies of the input functions and the data read-out (i.e., the analyzing technique). The question of what pertinent data should enter the equations for any given formulation could be answered. In addition, since the model is free, an evaluation of the interference effects of struts and walls in the tunnel upon the force measurements should be possible.

One specific problem that comes to mind is the effect of fin size and shape upon the stability and control of the submerged vehicle. A systematic variation of such appendages and location on suitable body shapes would yield valuable design information as well as provide an insight into the basic theoretical problem of the origin of the force system acting on fin-stabilized bodies of revolution.

Another valuable contribution would be an evaluation of scale effects by a definite measure of the differences between the behavior of model and prototype. This would require the development of full-scale test techniques which would yield information as reproducible as that obtainable with the model, and a demonstration of reproducibility of full-scale test results.

In conclusion, it is felt that the investigation reported herein represents only the initial development of the self-powered, self-controlled, free-running model. As useful and powerful a tool as it is in its present state, continued development of this modeling technique can make a significant contribution to and advance in the state of the art of free body dynamics.

APPENDIX A

LIST OF REFERENCES

1. "Submarine", Film No. 2, Contract N6onr-24428, California Institute of Technology, Hydrodynamics Laboratory, Unclassified.

2. Williamson, R.R. and Peters, B.H., "Trajectory Analysis of the Relationship of Stability to Maneuverability in the Manual Control of Submarines", Stevens Institute of Technology, Confidential Report No. 389, December 1949.

3. Church, J.W., "Theoretical Study of the Effect of Stern Plane Deflection Rate on the Dive Maneuver of the Experimental Submarine Albacore (AGSS 569) with Tail Surfaces Aft of the Propeller", David Taylor Model Basin Report No. C-525, January 1953.

4. TMB Confidential Ltr. C-S1/2/Albacore, C-NC1/C.I.T. (543:L.P:mb) No. 0165 to Calif. Institute of Technology, Mr. Joseph Levy, dated 17 Feb. 1953.

5. TMB Confidential Ltr. C-S1/2/Albacore (543:JWC:mb) No. 0607 to Calif. Institute of Technology, Mr. Joseph Levy, dated 29 May 1953.

6. Strumpf, A., "Model Tests of the Scheme IV Submarine (Configuration II) in Rise and Dive", Stevens Institute of Technology, Confidential Report No. 432, March 1952.

7. DTMB Confidential Ltr. C-SS/1 C-NS 715-084 No. 0874 to Calif. Institute of Technology, Mr. Joseph Levy, dated 30 July 1952.

8. Hoyt, E. D., and Imlay, F.H., "The Influence of Metacentric Stability of the Dynamic Longitudinal Stability of a Submarine", DTMB Confidential Report C-158, Oct. 1948.

9. Knapp, R. T., Levy, J., O'Neill, J.P. and Brown, F.B., "The Hydrodynamics Laboratory of the California Institute of Technology", Trans. ASME, Vol. 70, No. 5 , July 1948.

10. Knapp, R. T., "Special Cameras and Flash Lamps for High-Speed Underwater Photography", Journal of the Society of Motion Picture Engineers, Vol. 49, No. 1 (July 1947).

11. Progress Reports (25 issues) Office of Naval Research, Contract N6onr 24428, Project NR 063-087, HDL-CIT, June 1949 through Oct. 1955.

12. Niederer, O. C., "Model Investigation of the Dynamic Stability and Control Characteristics of U.S.S. Albacore (AGSS 569), DTMB Confidential Report C-531, Feb. 1953.

13. Landweber, L. and Gertler, M., "Mathematical Formulation of Bodies of Revolution, DTMB Report No. 719, Sept. 1950.

LIST OF REFERENCES
(cont'd)

14. Gertler, M., "Resistance Experiments on a Systematic Series of Streamlined Bodies of Revolution - for Application to the Design of High-Speed Submarines", DTMB Report No. C-297, April 1950.

15. Strumpf, A., "Equilibrium Attitudes of Three SST Scheme IV Designs of the USS Albacore (AGSS 569) in Submerged Turns of Small Diameter Evaluated from Forced-Turning Model Experiments, and An Investigation of Three Methods for Reducing the Roll Angle in Turn," ETT Confidential Report No. 503, January 1954.

16. Film No. 3, Contract N6onr-24428, California Institute of Technology, Hydrodynamics Laboratory, Confidential.

17. Hoyt, E. D., Imlay, F. H., Hawkins, F., and Fisher, D. "Pullout and Zig-Zag Test Data from Trials of U.S.S. Odax, March 1949," DTMB Confidential Report No. C-239, July 1949.

18. Bruce, V. G., "An Analysis of Free-Running Trajectories of an Experimental Submarine SST-E-27.1, Dec. 1953, Confidential.

19. Levy, Joseph, "An Experimental Study of Control and Maneuverability of Submarines", Proceedings, Joint Admiralty-U. S. Navy Meeting on Hydroballistics, Sept. 1954, Confidential.

ACKNOWLEDGMENTS

In a project as long and comprehensive as reported herein, a large number of persons contribute valuable help and suggestions in many ways. An attempt to list the specific contribution of each individual and to give due credit is almost impossible. Rather, the authors wish to express their appreciation to the staff of the Hydrodynamics Laboratory in general and merely to list those who have worked directly on the project. The study was brought to the Laboratory through the efforts of Dr. R. T. Knapp, and was under the supervision of Mr. Joseph Levy since its inception. The models were designed by John T. McGraw and George Hotz. Karl Pinsak built and maintained the models. The experimental tests were directly supervised successively by Roger Chambers, Robert C. Jackson and Donald Price, while Vaughan V. Smith and Lester M. Carey conducted the model tests. The film analysis, data reduction and curve plotting were done by Miss Genevieve Wilcox (now Mrs. J. A. Stubstad), Mrs. Laura Gaard and Mrs. Grace Iten. The report curves were prepared by Mrs. Laura Gaard and Miss Donna Snyder, while Mrs. Rose Grant, Miss Ann Rankin and Mr. Edison Hoge prepared the text and figures for publication.

APPENDIX B

DESCRIPTION OF CONTROLLED ATMOSPHERE LAUNCHING TANK

The model tests were performed in the Controlled Atmosphere Launching Tank (Fig. B-1), which was designed and built primarily for the study of water entry of free-flying bodies. The facility is of such construction that it is well suited for a number of other types of studies involving hydrodynamic phenomena. This study on control and maneuverability of submarines represents the first such extension of the usefulness of the launching tank. The third portion of the study, horizontal maneuvers, represents a further extension, e.g., a generalization of the tank (and models) to six degrees of freedom.

The launching tank and its associated equipment have been very completely described previously in Refs. 9 and 10, and will be described only briefly here. Rather detailed attention will be given to the additional equipment and improvements required for the free-running model control and maneuverability study.

The Tank

The tank consists of a large horizontal cylinder 13 feet in diameter and 29 feet long, to one side of which is attached a section of a smaller cylinder 6 feet in diameter and 23 feet long. A battery of five 35 mm high-speed movie cameras are mounted on the horizontal centerline of this "bulge". The flash lamps which illuminate the interior of the tank are installed in the six lucite tubes which pass through the bulge above and below the cameras. Additional cameras and flash lamps are mounted near the top of the tank to record the air flight of bodies launched with the centrifugal launcher which is mounted on the underside of the large hatch on top of the tank. The tank is filled to about 2-1/2 feet above the centerline (total depth 9 ft.) with about 25,000 gallons of distilled water which is continuously filtered through sand and alum filters and exposed to ultraviolet lamp radiation at the surface in order to maintain maximum optical clarity. A 3/32-inch thick lining of a poly-vinyl chloride plastic ("Koroseal") prevents corrosion of the tank shell and consequent contamination of the water, provides a dark background and protects models from abrasion damage. Figure B-2a shows the interior of the tank when drained of water, indicating the location of the lucite tubes and

camera windows in the bulge. Part (b) shows the protective net which was installed to prevent damage to the free-running models by collision with the tank walls. It consists of 1-inch mesh cotton netting in the form of a rectangular box with one end open and a detachable top flap. The net is stretched between square frames at the ends of the tank by means of lines and pulleys for easy removal and installation. This cotton net was later replaced with a smaller gauge thread, one-inch mesh nylon net.

Model Launcher

Vertical Maneuvers: An additional launcher mechanism was added to the tank for the submarine study. Its function was to accelerate the model up to its running speed in as short a stroke as possible in order to leave a maximum of the tank's length for the constant speed run. This "linear" launcher, mounted on the horizontal centerline of the tank below the centrifugal launcher, consists of two major components; (1) the actuating mechanism and (2) the interchangeable guide rails. The actuating mechanism (see Fig. B-3) consists of a 3-inch ID cylinder and a one piece piston-and-rod, mounted externally with the rod extending into the tank through an O-ring seal. The air flask holds the compressed air for driving the piston, while an air cushion ahead of the piston in the cylinder stops the piston and rod at the end of its stroke. In its starting position, as shown, the piston covers the air inlet port and thus acts as a quick opening valve to start the launching

The interchangeable brass guide rails are mounted inside the tank coaxial with the cylinder (see Fig. B-4). Four brass rails guide the model hull as it is ejected by the piston rod. A model pusher supports the end of the piston rod and cradles the tail of the model during acceleration. A trigger wheel on the rails depresses the turbine starter button in the deck of the model at the beginning of the stroke. The guide rails for the Odax model were fixed to the mounting flange, while the Albacore model cradle was pivoted for easier installation of the model. A guide tube for the bridge fairwater of the Albacore model was also added.

In operation, the sequence is as follows: The piston is retracted, the model installed in the guide rails, and the air flask charged to the desired pressure. When the firing control circuit is closed, the actuating cylinder opens the main valve and, at the end of its stroke, closes the circuit of the 3-way solenoid valve. This by-pass valve admits air behind the piston and

moves it enough to uncover the port from the main valve. Thus the full pressure is applied to the piston almost immediately. The full triggering sequence requires about 0.3 second, while at 24 psi initial flash pressure, the launcher accelerates the model to 15 fps in 0.4 second. A set of electrical contacts near the end of the launcher rails , which are wiped by a contact on the model pusher, gives a measure of the model velocity.

Horizontal Maneuvers: In order to achieve the longest possible trajectory in the available space for horizontal maneuvering, it was desired to have the launcher guide rails easily adjustable in position and angle. Since the air-operated launcher was fixed in space and direction, and in addition was not sufficiently accurate and consistent at speed below 5 fps, it was decided to use a spring-operated mechanism within the existing cradle. The mechanism and mounting arrangement in the tank are shown in Fig. B-5. The location with respect to the trajectory recording system is seen in Fig. B-6.

The accelerating mechanism consists of a 50-lb spring and piston-damper unit mounted coaxially with the same guide rail cradle as used for the vertical maneuvers. The cocked spring is visible at the center of the rails in Fig. B-5b, while the damping cylinder, plenum chamber and exhaust line to the adjustable orifice are seen at the right end. As much excess material was removed from the cradle as possible to better establish the flow around the model. The launching velocity is adjusted by varying the orifice opening seen in Part (a), and the shield deflects the orifice exhaust away from the model as it emerges from the rails. The launcher is cocked by closing off the orifice and opening the port with a sliding gate between the two plates of the valve. Water is pumped back through the exhaust line into the cylinder, forcing the piston back and compressing and latching the spring. The crank and pull chain at the center of the cradle depresses the model turbine starter button,while the pull rod at the right releases the spring to launch the model. The electric contacts at the ends of the guide rails are actuated by the model tail to indicate the launching velocity of the model.

The cradle assembly is mounted on a horizontal tube in the tank, as shown in Fig. B-5c. The cradle may be positioned from 12 inches to 45 inches horizontally from the tank centerline and rotated ± 45 degrees in the horizontal plane and ± 1 degree in the vertical plane. Two actuating solenoids

are suspended from the net frame bar at the top of the picture, one for triggering the model turbine and the second for triggering the launcher mechanism when the model machinery is up to speed. A time delay in the launcher flash-lamp circuit triggers the launcher at the proper place on the movie camera film.

Trajectory Recording System

The model trajectory is recorded by a battery of high-speed motion-picture cameras using standard 35 mm film in conjunction with a large battery of synchronized high-intensity flash lamps. The maneuvering space and the optical coverage of the cameras is shown in Fig. B-6, along with launcher positioning and typical model trajectories for vertical and horizontal maneuvers. Almost complete stereoscopic coverage of the maneuvering volume is available from the tank centerline to the rear, while toward the cameras only saw-tooth shaped volumes are covered. However, the model may be seen in any position by at least one camera. This multiple coverage makes it possible to use stereoscopic techniques for analysis of the recorded data to obtain six components of motion, longitudinal, lateral and vertical movements, and rotation in the horizontal and both vertical planes, provided sufficiently sharp and detailed images are obtained.

Cameras: Figure B-7 shows details of the underwater cameras (Ref. 10) which consist of a lens and guide roller assembly permanently mounted on the tank with a detachable film magazine containing a 32-foot continuous film belt. The lens is a 1-inch f/2.3 Bausch and Lomb Baltar mounted at the center of a spherical correcting window which eliminates distortion due to refraction at the water-glass interface. The lens has a field of view of 53 degrees which provides a 50 per cent overlap of coverage of adjacent cameras at the centerline of the tank. The film, guided through the focal plane by a series of rollers (Fig. B-7b) to reduce friction to a minimum, is driven by a common drive shaft at constant speed and the exposure is made by intermittent illumination of the tank interior with the high speed flash lamps. Each film belt is measured and spliced to exactly the same length (by counting sprocket holes) so that it may be brought up to speed gradually, exposed and then slowed down gradually and yet utilize the full length for recording the trajectory. An indexing device on the camera drive allows initiation of the model run at any of twelve positions along the film loop.

Tank Illumination: The model trajectory is lighted (intermittently) by high-intensity, short-duration gas discharge flash lamps (see Ref. 10). Because of the lower speeds of the maneuvering models (15 fps vs 120 fps for air-launched models), the flash rate, i.e., the picturing-taking rate, was reduced to 100 and 200 cps which, due to the design of the power pulse units, also reduced the light intensity. To overcome this, a number of flash lamps and reflectors were removed from the lucite tubes and sealed into submersible lucite cans (Fig. B-7a) which may be located underwater to illuminate the trajectory to the best advantage. The parabolic reflector covers a 2 x 5-foot oval area 6 feet from the lamp to spotlight the trajectory, while the remaining lamps in the bulge tubes provide general lighting. On the back wall of the tank directly opposite each camera are mounted reference and framing flash lamps. These "cross lights", sealed in brass boxes with an inverted "L"-shaped cut-out, flash simultaneously with the illumination lamp providing alignment references for each frame in the trajectory analyzer.

Power for each flash lamp is provided through an individual pulse generator mounted in racks behind the tank and a 100 kva transformer primary power supply. All units are triggered by a single frequency generator and controlled in number of flashes by a timer.

Increased illumination of the trajectory became available for the horizontal maneuvering tests with the design and construction of twenty-four new flash lamp power units. These units, as developed by the electronics section of the Laboratory, provide about a five-fold increase of light output over the original units while providing more reliable operation at a reduced frequency of 50 cps and an increased duration of 10 sec. Six auxiliary submersible lamps incorporating a new coaxial flash tube of higher intensity and short duration (one microsecond) were used inside the tank for spotlighting purposes. The remaining eighteen flash lamps were installed in the lucite tubes near the camera. This light output increase was sufficient to allow reduction of camera lens apertures and an appreciable decrease of the film development time. Figure B-7c shows one of the twenty-four new power pulse units.

Film Emulsions: An important factor in the accuracy of the data measured from the photographic record is the quality of the projected model images which is directly related to the sensitivity of the film emulsion to

the spectrum of the flash lamps. (The lamps are especially rich in the blues.) Three emulsions were used in the course of the study-- Eastman Kodak (1) Panchromatic Background X, (2) Linograph Ortho, and (3) Tri-X Panchromatic. Figure B-9 shows a comparison of model images with the various emulsions in chronological order, and indicate improvements of image quality with additional illumination and sensitivity. The Background X, although fine-grained, was far less sensitive than the Linograph Ortho. The Tri-X, by comparison with the Linograph Ortho, has a more stable emulsion with twice the speed, smaller grain size and wider latitude of exposure.

Trajectory Analyzing System

The data analyzing or trajectory mapping system is essentially a one-half scale reproduction of the trajectory recording system of the launching tank plus an image tracking device. A general view of the analyzer room and a schematic diagram of the system is seen in Fig. B-10. The projectors replace the cameras and an exploring screen or target replaces the model.

Projectors: The lens of each projector, Fig. B-11a, is matched to the corresponding camera lens on the tank and the film is held flat in the focal plane by two optically flat glass plates (replacing the rollers in the camera). Because of the spherical window in the tank, the images are projected in the analyzer room geometrically correct except for a slight increase in magnification due to the deletion of the water. The difference in magnification affects only the lateral dimensions in projection. The film is advanced frame by frame simultaneously in all projectors by a hand-operated, common drive shaft. The frame is located behind the lens by aligning the projected images of the reference cross lights with corresponding reference crosses on the back wall of the analyzer room. The light source consists of an incandescent bulb and condensing lens with a water cell and forced air cooling to maintain a low film temperature.

Mechanism: The image-tracking device consists of a moving bridge and carriage arrangement with three degrees of linear motion and two degrees of angular motion. These motions are motor driven and controlled by push buttons from the control console (Fig. B-11b). The motions are followed and indicated by selsyn repeater units which drive indicating counters on the console showing positions to 0.01 inch and angles to 0.1 degree. The third

angular motion (roll) was incorporated into the Albacore model targets.

Targets: The model targets for the maneuvering studies are shown in Fig. B-12. The target for the Odax model consisted simply of a silhouette outline attached to the existing exploring screen. The first target for the Albacore model (Part b) consisted of a half-size reproduction of the body of revolution of the model hull, sectioned along the vertical plane of symmetry and mounted on the screen with the scaled center of gravity located at the center of rotation. The thread crosses reproduce the cross center lines on the model. A roll-measuring attachment (c) was added later in the test program. The half model target is mounted on a rectangular screen which in turn is fastened to the movable frame of the attachment. A small hand screw on the left moves the target while the scale at the right end indicates the roll angle. This geometrically similar target using three crosses allows alignment with the projected image in all six dimensions with a single projector as well as with stereoprojection.

A new target was necessary for adequate analysis of the horizontal turning maneuvers. The half-model target used in the vertical maneuvers was not suitable for determining the position of the model when it is heading toward the camera or when it turns around to present its other side.

The new target, seen in Figure B-13, consists of a full model of the basic body of revolution with forward deck and bridge fairwater only. The deck is built up with a synthetic metal putty and contoured from the model hull on the pantograph milling machine, while the bridge fairwater is machined to the given contours and mounted on top of the deck. The model cross centerlines are scribed into the target, duplicating the cross arrangement on the model (to half scale).

The target is mounted clear of the analyzer carriage in the assembly shown and is pivoted about a transverse axis through the scaled center of gravity position. The inclination is positioned with the small hand wheel at the stern and is measured with the scale and vernier on the target frame. The carriage mechanism has been rotated 90 degrees in the horizontal plane, and what used to be the inclination mechanism is used to position and measure roll. A correction for the displacement of the target c.g. with rotation in the horizontal plane is made in the computations. (The indicating counters give the position of the center of rotation of the carriage.).

Optical System Alignment

For the vertical maneuvers a single projector type of analysis was used wherein the lateral position of the target (distance from the projector) was determined by matching the magnification or size of the image with the target. With the Odax model, appreciable departures of the trajectory from the vertical plane (in azimuth, roll or lateral) were unacceptable and those test runs were not used. Minor deviations with the Albacore model were allowed(and measured) within narrow limits. The existing alignment of the recording and analyzing system (for which the projector lenses were set for best focus in the maneuvering plane) provided adequate information of the model behavior in the vertical plane.

However, for the horizontal maneuvers where behavior of the model in the horizontal plane is of prime importance, it was necessary to align the tank and analyzer optical systems very precisely for stereoscopic reprojection. Although stereoscopic analysis would yield more precise data of trajectories restricted to the vertical plane as well, several factors have delayed the use of this technique. The principal factors have been the lack of adequate illumination, coupled with less sensitive film emulsion available up to the time of this study. The improvements made in tank illumination have been described, while new, highly sensitive emulsions (Fig. B-9) have become commercially available. The limitation of trajectories to the vertical plane and the simplicity of analysis of the record by means of single projectors have had some influence also. Since each camera lens is mounted at the center of a spherical window constituting the air-water interface, a fixed magnification results and the focus is adjusted by varying the film position behind the lens. The spherical correcting window acts as a negative lens which reduces the apparent object distance sufficiently for the lens to cover a depth of field six to sixteen feet from the lens in the tank. The Baltar lenses were matched in pairs between camera and projector according to focal length but the focal lengths of the camera lenses were found to vary over a 1-1/2 per cent range which, although small, was sufficient to cause considerable variation of depth of field and point of best focus in the tank when coupled with the spherical window. Five lenses were selected for the underwater cameras on the basis of depth of field at a constant film-lens distance. A typical image of a 6-inch square grid at 45 degrees to the camera axis is shown in Fig. B-14a where the near end is 6 feet and the "L"-

shaped references are 16 feet from the lens. For the purpose of tying the cameras together optically, four targets of known dimensions were placed on the tank centerline in view of adjacent cameras and photographed simultaneously with all cameras. The resulting image from one camera is shown in Fig. B-14b.

The analyzer optical system was aligned in a similar manner using the aligning target images. The projector lenses were selected and matched to the corresponding camera lenses on the basis of focus and magnification. Since the film position is fixed and the lens movable on the projector, the depth of field coverage and magnification are adjustable within narrow limits. The focus and magnification were adjusted successively from projector to projector using the target images from adjacent cameras. The analyzer references crosses were then adjusted to the correct distance from the projectors based on the mutually compatible magnification of the image references. A reduction of distance from the lens to the image occurs due to reprojection in air in place of water, and in the absence of the spherical window. This shrinkage is accounted for during expansion of the data to full scale.

The precise alignment of the optical system revealed a discrepancy in film positioning hitherto undetectable. The camera gate (consisting of a series of rollers) did not hold the film in the same position as the projector film gate (consisting of two flat glass plates). Also, the film emulsion caused a transverse curvature of the film which cannot be eliminated by the rollers, whereas the projector gate clamps the film flat. This difference in film position and curvature, although small, (0.001-0.002 in.) was sufficient to upset triangulation in the horizontal plane with variations of ± 0.10 inch in lateral position and ± 2 degrees in angular positioning of the image. This film "buckle" was corrected by inserting appropriate shims between the film and glass plates in the projector on the basis of images such as shown in Fig. B-14c. The four aligning targets were hung in a vertical plane near the rear wall of the tank and photographed by three adjacent cameras. The film curvature in each projector was then adjusted to match images from adjacent projectors to a common vertical plane while magnification is held constant by the previously adjusted reference crosses. Variations of curvature from frame to frame during analysis of a model test run are accounted for by adjustment of magnification with the projector lens to match the reference crosses.

APPENDIX C

DATA REDUCTION PROCEDURE

The procedure for reduction of the data on the film record to a usable form may be divided into three steps: (a) analysis of the film record (read-off), (b) computations, and (c) curve plotting. Essentially the same procedures were used throughout this study except for variations required for either single projector or stereo analysis.

Analysis of the Film Record

A frame-by-frame technique is used in mapping the trajectory of the model. The films for one test run are placed in the corresponding projectors and synchronized so that corresponding frames taken at the same time will be projected at the same time. (A "sync" frame is placed on all films before each test run by short burst of the flash lamps.) The frame to be analyzed is positioned behind the lens with the common drive shaft. The wall cross-images are then aligned on the reference crosses on the back wall by adjusting the lens vertically and horizontally, and by rotating the film. The target is then aligned to the projected image of the model by matching the thread crosses to the image crosses with either stereo- or single-projection technique. The counter readings are recorded, the film moved to the next frame to be read and the procedure repeated for the length of run recorded. Transfer from one pair of projectors to the next is accomplished by analyzing several mutually overlapping frames. Cam light positions are determined by measuring the streak position relative to the adjacent image frames. Figure C-1 shows a plot of the tabulated data (to an exaggerated scale) for a typical vertical maneuver of the Albacore model, illustrating normal reading scatter, effect of slight magnification differences and region of overlapping analysis. Each point represents the position of the model at five frame intervals for a 200-frame per second picture-taking rate.

The quality of the images greatly affects the ease and speed with which the record is analyzed. Some typical examples of images in various parts of the tank are shown in Fig. C-2 for a typical vertical maneuver. The skilled operators analyze even the less distinct images with a high degree of precision, although requiring more time and effort. For the quality of images shown, accuracy of measurement of the order shown in Table C-1 are

obtained in the analyzer. These figures represent the over-all reading accuracy due to alignment of the film in the projector, positioning of the target and ability of the operator to see the projected images.

With excellent images, an individual frame may be measured consistently to within ±0.01 inch in longitudinal and vertical, ±0.02 inch in lateral, ±0.1 degree in inclination, and ±0.2 degree in azimuth and roll once the film is aligned to the reference marks. These figures represent minimum accuracy possible if the film curvature in the projector exactly matches that in the camera for the particular frame being measured. Variation of the curvature of the film from frame-to-frame and subsequent magnification adjustment introduce errors in triangulation in the horizontal plane such as shown (greatly exaggerated) in Fig. C-3 where one film has incorrect curvature. This condition forces a compromise in aligning the target crosses with the images for, when setting the lateral by the center cross, the fore and aft crosses will not match the intersection of the projected image crosses. Splitting the difference (i.e., one image large, one small) reduces the angular misalignment but the lateral discrepancy remains. These effects are negligible when analyzing vertical maneuvers. The magnitude of the errors depends upon the position and heading of the model realtive to the projector and quality of the images (contrast, focus, etc.) making a rigorous determination of probable error extremely difficult and of doubtful worth. The values shown in Table C-1 represent an estimate of average errors in stereoscopic analysis for two positions and headings of the model in the tank. Values for those regions where only single projector analysis (nonstereoscopic) is possible are included also. Table C-2 shows the best accuracy of the full-scale data estimated on the basis of the foregoing discussion attempting to account for image quality and film positioning. The worst accuracy is evident in the scatter of the data points shown on the curves.

Computations

The raw data, as received from the trajectory analyzer, consists of tabulated data showing positions and attitudes of the tracking mechanism and target as indicated by the counters and scales for each frame analyzed. For the vertical maneuvers of the Odax and Albacore, this tubular data gives the positions of the center of gravity of the model directly. However, for the horizontal maneuvers, a correction is necessary for the 6-inch displacement

TABLE C-1

READING AND POSITIONING ACCURACY IN TRAJECTORY ANALYZER

Dimension	Vertical Maneuvers		Horizontal Maneuvers		
	Odax	Albacore	Model Heading		Single Projector(2)
			0^{o}	90^{o}	
Longitudinal - in.	$\pm$0.02	$\pm$0.01	$\pm$0.02	$\pm$0.07	$\pm$0.02
Vertical - in.	$\pm$0.02	$\pm$0.01	$\pm$0.02	$\pm$0.03	$\pm$0.02
Lateral - in.	N.M.(1)	$\pm$0.10	$\pm$0.05	$\pm$0.07	$\pm$0.10
Inclination - deg.	$\pm$0.2	$\pm0.1^{o}$	$\pm$0.2	$\pm$0.4	$\pm$0.2
Azimuth - deg.	N.M.	$\pm0.3^{o}$	$\pm$0.5	$\pm$1.0	$\pm$1.0
Roll - deg.	N.M.	$\pm0.3^{o}$	$\pm$1.0	$\pm$1.5	$\pm$2.0

(1) Not measured.

(2) Zero deg. heading only.

TABLE C-2

"BEST" ACCURACY OF FULL SCALE DATA

Dimension	Vertical Maneuvers		Horizontal Maneuvers		
	Odax	Albacore	Model Heading		Single Projector
			0°	90°	
Distances:					
Horizontal - ft	±1.0	±0.2	±0.3	±0.5	±0.3
Depth - ft	±1.0	±0.2	±0.3	±0.5	±0.3
Lateral - ft	N.M.	±1.7	±1.0	±1.2	±1.7
Along trajectory-ft	-	±1.0	±1.3	±1.5	±2.0
Angles:					
Inclination - deg.	±0.5	±0.1	±0.2	±0.4	±0.2
Azimuth - deg.	N.M.	±0.3	±0.5	±1.0	±1.0
Roll - deg.	N.M.	±0.5	±1.0	±1.5	±2.0
Velocity-fps(model)	±0.3	±0.2	±0.1	±0.5	±0.5
Rates of Change:					
Inclination-rad/sec	N.C.	±0.0002	±0.0001	±0.0002	±0.0001
Azimuth - rad/ft	N.C.	N.C.	±0.0002	±0.0005	±0.0005
Roll - rad/ft	N.C.	N.C.	±0.0005	±0.0008	±0.0010
Depth - ft/ft	N.C.	±0.003	±0.010	±0.020	±0.010
Lateral - ft/ft	N.C.	N.C.	±0.020	±0.040	±0.050
Angles of Attack:					
Vertical - deg.	N.C.	±0.3	±0.2	±0.5	±0.2
Horizontal - deg.	N.C.	N.M.	±1.0	±1.0	±1.0

N.M. = not measured

N.C. = not computed

TABLE C-3

COMPUTATION FORMULAS FOR EXPANDING DATA TO FULL SCALE

Dimensions	Description	Formulae		
		Odax	Albacore (vertical maneuvers)	Albacore (horizontal maneuvers)
L	Horizontal distance-ft	$= \lambda(\frac{2}{12})\ \Sigma\Delta L$	$= \lambda\ (\frac{2}{12})\Sigma\ \Delta L$	$= \lambda\ (\frac{2}{12})\Sigma\ \Delta L$
D	Vertical distance-ft	$= \lambda(\frac{2}{12})\Sigma\ \Delta D$	$= \lambda\ (\frac{2}{12})\Sigma\ \Delta D$	$= \lambda\ (\frac{2}{12})\Sigma\ \Delta D$
Z	Lateral distance-ft	—	$= \lambda\ (\frac{2}{12})\Sigma\ \Delta Z$	$= \lambda\ (\frac{2}{12})\Sigma\ K\ \Delta Z$
S	Distance along trajectory-ft	—	$\lambda(\frac{2}{12})\ \Sigma\ \sqrt{(\Delta L)^2+(\Delta D)^2+(\Delta Z)^2}$	$\lambda\ (\frac{2}{12})\ \sqrt{(\Delta L)^2+(\Delta D)^2+(K\Delta Z)^2}$
T	Time - sec.	$= \Sigma\ \frac{\Delta L}{\Delta T}$	$=$ S/42.25	$(\lambda)^{1/2}\ \Sigma(N/F)$
θ	Inclination angle-deg.	$= \theta_M = \theta_T$	$= \theta_M = \theta_T$	$= \theta_M = \theta_T$
ψ	Azimuth angle-deg.	—	$= \psi_M = \psi_T$	$= \psi_M =$ arc tan $(K \tan \psi_T)$
ϕ	Roll angle-deg.	—	$= \phi_M = \phi_T$	$= \phi_M = \phi_T$
β	Trajectory angle in vertical plane-deg.	—	$=$ arc sin $\Delta V/\Delta S$	arc tan $(\Delta V/\Delta L)$
η	Trajectory angle in horizontal plane-deg.	—	—	arc tan $(K\Delta Z/\Delta S)$
α	Angle of attack in vertical plane-deg.	—	$= \theta - \beta$	$= \theta - \beta$
γ	Angle of attack in horizontal plane-deg.	—	$= \psi - \eta$	$= \psi - \eta$
V	Velocity - fps	$= (\frac{2}{12})\ \Delta L/\Delta T$	$= (\frac{2}{12})$ F $\Delta S/M$ (model only)	$= (\lambda)^{1/2}(\frac{2}{12})(F\ \Delta S/M)$
$\dot{\theta}, \dot{\psi}, \dot{\phi}$	Angular Velocities-rad/sec or rad/ft	—	$= \frac{1}{\lambda}(\frac{12}{2})(\frac{\pi}{180})(\frac{\Delta\theta}{\Delta S})\ 42.25$	$= (\frac{1}{\lambda})(\frac{12}{2})(\frac{\pi}{180})(\frac{\Delta\theta}{\Delta S}, \frac{\Delta\psi}{\Delta S}, \frac{\Delta\phi}{\Delta S})$
$\dot{D}, \dot{Z}$	Rates of change of depth and lateral-ft/ft.	—	$\Delta D/DS$, $K\Delta Z/\Delta S$	$= \Delta D/\Delta S$, $K\Delta Z/\Delta S$

CONFIDENTIAL

CONFIDENTIAL

of the target c.g. from the center of rotation. The true position of the target is given by

$$L_T = L_C + 6 \cos \psi_c$$

$$Z_T = Z_C + 6 \sin \psi_c$$

where the subscripts refer to target and carriage positions. The dimensions are defined in the list of symbols in Table C-4.

The correction for the "shrinkage" in the lateral dimension due to deletion of the spherical window and projection in air (for the horizontal maneuvers only) consists of a linear expansion of the lateral distance and the tangent of the azimuth angle. The corrected lateral and azimuth angle then become

$$Z = K Z_T$$

$$\psi = \arctan (K \tan \psi_T)$$

where K is the ratio of the focal plane distance in the projector to that in the camera. For the alignment of the optical system made here K = 1.065.

The tabular data is first reduced by a successive differencing scheme from which rates of change of angles and displacements, and angles of attack are obtained. A numerical integration and expansion to full scale is then performed simultaneously on the differenced data. The formulae used for each part of the study, along with a description of the symbols used, are shown in Table C-3. The differenced quantities, as denoted by the operator, Δ, represent the analyzer dimensions, i.e., one-half model size. The rates of change or velocities represent values averaged over three successive data points (1, 2 and 3) in the following manner:

$$\text{Ave.} \frac{\Delta\theta}{\Delta S} = \frac{1}{2}\left(\frac{\theta_3 - \theta_2}{S_3 - S_2} + \frac{\theta_2 - \theta_1}{S_2 - S_1}\right)$$

The expansion of the model data to full scale is seen to be a linear "blowup" of the model positions. The intervals between data points are selected so that no appreciable error is introduced in constructing the distance traveled (or time) from the chord segments rather than the true arc lengths. Due to the large number of trajectories analyzed and the corresponding larger number of data points, a special "square root" table was constructed

which greatly facilitated computations of

$$\Delta S = \sqrt{(\Delta L)^2 + (\Delta D)^2 + (K\Delta Z)^2}$$

$$= \Delta L \sqrt{1 + (\Delta D/\Delta L)^2 + (K\Delta Z/\Delta L)^2}.$$

The table gives values of the $\sqrt{1 + (\Delta D/\Delta L)^2 + (K\Delta Z/\Delta L)^2}$ multiplier for a wide range of values of $\Delta D/\Delta L$ and $K\Delta Z/\Delta L$ with a high degree of precision.

Sign Convention: The sign convention followed for this study agrees with the established arrangement of the tank and analyzer system. Table C-4 lists the positive direction for each quality listed. The convention is seen to follow the right-hand rule, except for the control surface angles which are considered positive when causing a positive displacement of the primary quantities. Rates of change and angular velocity are positive for positively increasing values of the primary dimensions.

TABLE C-4

LIST OF SYMBOLS AND SIGN CONVENTION

Symbol	Definition	Positive Direction
L	Horizontal distance	Along axis parallel to tank centerline from launcher.
D	Depth or change of depth	Down from tank horizontal centerline.
Z	Lateral	From tank centerline to back wall.
S	Distance along trajectory	Along direction of forward motion.
T	Time	From first frame analyzed or start of control program.
θ	Inclination of model axis with respect to horizontal	For bow down.
ψ	Azimuth angle of model axis with respect to tank centerline	For bow to starboard.
ϕ	Roll angle of model vertical plane of symmetry	For heel to starboard.
α	Angle of attack in model vertical plane (inclination)	For bow down with respect to tangent to trajectory.
γ	Angle of attack in horizontal plane (azimuth)	For bow to starboard with with respect to tangent to trajectory.
β	Angle of tangent to trajectory with respect to horizontal.	For increasing depth.
η	Angle of tangent to trajectory with respect to tank centerline	For increasing lateral.
δ_s	Stern plane angle	For causing model to dive.

TABLE C-4
(Cont'd)

Symbol	Definition	Positive Direction
δ_r	Rudder angle	For causing model to turn to port.
δ_b	Bow plane angle	For causing model to dive.
δ_d	Dorsal rudder angle	For causing model to roll to starboard.
R	Turning radius	For turn to starboard.
V	Velocity of C.G. of model along trajectory	—
λ	Linear scale factor of model of prototype size	—
F	Flash rate of tank high-speed lamps or picture frame data	—
N	Number of frames on film record between data points or frames analyzed	—
K	Correction factor for lateral dimensions in analyzer.	—

INITIAL DISTRIBUTION
Contract N6onr-24428

No. of Copies	
10	Chief, BuShips, Attn: Project Records (Code 324) for additional distribution to: Research Division (Code 330) Ship Design (Code 410) Preliminary Design (Code 420) Hull Scientific (Code 442) Submarines (Code 515) Technical Library (Code 327)
30	Commanding Officer and Director, David Taylor Model Basin, Washington 7, D.C., Attn: Contract Research Division (Code 580), for additional distribution to: Commanding Officer and Director (Code 100) Submarine Program Officer (Code 101) Technical Information Division (Code 140) Chief Naval Architect (Code 500) Hydrodynamics Division (Code 540) Stability and Steering (Code 541) Submarine Motion Analysis (Code 543) Submarine and Torpedo Hydrodynamics (Code 545) British Joint Services Mission
2	Assistant Naval Attache for Research, U.S. Embassy, London, England, Navy 100, F.P.O., New York, N.Y.
1	Commander, Submarine Development, Group TWO, Box 70, U.S. Naval Submarine Base, New London, Connecticut.
1	Commander, Naval Ordnance Test Station, Inyokern, China Lake, California.
1	Officer-in-Charge, Pasadena Annex, Naval Ordnance Test Station, 3202 East Foothill Blvd., Pasadena, California.
3	Chief, Office of Naval Research, Washington 25, D. C., Attn: Mechanics Branch (Code 438), for additional distribution to: Undersea Warfare (Code 466) Naval Sciences Division (Code 460)
1	Commanding Officer, Office of Naval Research Branch Office, 1030 E. Green Street, Pasadena 1, California.
2	Director, Experimental Towing Tank, Stevens Institute of Technology, 711 Hudson St., Hoboken, N.J., via Office of Naval Research Branch Office, 346 Broadway, New York 13, N. Y.

INITIAL DISTRIBUTION
(cont'd)
Contract N6onr-24428

No. of Copies	
2	Supervisor of Shipbuilding, Groton, Connecticut, one copy of which to be forwarded to Electric Boat Co.
2	Commandant, Portsmouth Naval Shipyard, Portsmouth, New Hampshire.
2	Commandant, Mare Island Naval Shipyard, Vallejo, California.